

# The Analysis of Tool Wear Mechanisms in Dry Machining of Pre-Sintered Zirconia Dental Crowns

David Robert Irvine

A thesis submitted in partial fulfilment of the requirements of the University of the West of  
England, Bristol for the degree of Doctor of Philosophy in Engineering

This research programme was carried out in collaboration with Prima Dental

Department of Engineering Design and Mathematics, University of the West of England,  
Bristol May 2024

## **Abstract**

The research presented in this thesis investigates wear mechanisms in pre-sintered zirconia machining. Zirconia is being used for restorations in the dentistry field due to its favourable mechanical properties. Although, machining such a material in its much softer pre-sintered form poses issues to operational life and integrity for any tools used. This work aimed to address several areas of study within the machining of such dental restorations made from pre-sintered zirconia. Specifically to answer how carbide ball nose end mills can resist the wear that occurs during the machining process.

Due to limited literature on the machining conditions of materials similar to pre-sintered zirconia and how the tool parameters affect the material during cutting. This work bridges this gap in understanding by developing an optimal method of machining pre-sintered zirconia using carbide tooling with proprietary geometries. In pursuing this optimisation, other minor knowledge gaps were addressed. The path to optimisation consisted of investigating the tool wear and tool-workpiece interactions during and after the machining process. A design of experiments was developed to investigate the machining of pre-sintered zirconia under differing cut conditions with carbide tooling.

An optimal set of operating conditions have been determined along with a framework to aid in machining condition selection. The selection criteria for this optimisation and assistive tools are based on time, tool wear and surface finish. This work also considered and explained how the tool wear affects surface integrity. Here it was found that the wear mechanism was a third body abrasion and causes trans-granular rupture along the worn surfaces of the carbide end mill. It was also found that the workpiece is not subjected to enough heat to harden the zirconia during the machining process.

## **Contents**

Abstract .....	i
List of Figures .....	vi
List of Tables .....	ix
Nomenclature .....	x
Acknowledgement .....	xii
1- Introduction.....	1
1.1- Background.....	1
1.2- Aim of Thesis .....	4
1.3- Thesis Scope .....	5
Chapter 2 Literature Review .....	6
Chapter 3 Research Methodology .....	6
Chapter 4 Tool Wear Testing .....	6
Chapter 5 Pre-Sintered Zirconia Work Piece Testing.....	7
Chapter 6 Tool Life and Optimisation .....	7
Chapter 7 Conclusion.....	7
2- Literature Review .....	8
2.1- Pre-sintered zirconia in dentistry .....	8
2.2- Tooling Design .....	12
2.2.1- Tool Materials .....	12

2.2.2-	Coated and Uncoated Tools .....	14
2.2.3-	Tooling geometry .....	16
2.3-	Tool Life/wear .....	21
2.3.1-	Wear Forms .....	21
2.3.2-	Wear Progression and Wear Testing.....	24
2.3.3-	Tool Life .....	24
2.4-	Product Properties .....	27
2.5-	Dental CAD-CAM.....	30
2.6-	Modelling.....	33
2.7-	Discussion.....	35
2.8-	Chapter summary .....	39
3-	Research Methodology .....	40
3.1-	Introduction.....	40
3.2-	Research Design .....	42
3.3-	Limitations .....	46
3.4-	Conclusion .....	46
4-	Tool Wear Testing .....	47
4.1-	Introduction.....	47
4.2-	Tool Wear Pattern.....	49
4.2.1-	Method .....	49
4.2.2-	Observations and Results .....	49

4.2.3-	Discussion .....	52
4.3-	Tool Material Changes .....	53
4.3.1-	Introduction.....	53
4.3.2-	Tool life.....	55
4.3.3-	Test Method .....	55
4.3.4-	Results and Analysis .....	57
4.3.5-	Discussion .....	61
4.4-	Machining Condition Manipulation .....	64
4.4.1-	Method .....	64
4.4.2-	Results and Analysis .....	69
4.4.3-	Discussion .....	74
4.5-	Chapter Summary .....	75
5-	Pre-Sintered Zirconia Work Piece Testing.....	77
5.1-	Introduction.....	77
5.2-	Thermal Effects .....	79
5.2.1-	Methods.....	79
5.2.2-	Results and Discussion .....	81
5.2.3-	Discussion .....	83
5.3-	Pre-sintered Zirconia Surface Analysis .....	84
5.3.1-	Introduction.....	84
5.3.2-	Method of Analysis.....	85

5.3.3- Results.....	88
5.3.4- Discussion.....	91
5.4- Chapter Summary.....	92
6- Tool Life and Optimisation.....	93
6.1- Introduction.....	93
6.2- Tool Life Equation.....	93
6.2.1- Introduction.....	94
6.2.2- Adaption and Machining Constant.....	96
6.3- Optimisation Assist.....	101
6.3.1- Introduction.....	101
6.3.2- General theory.....	101
6.3.3- Tool creation.....	105
6.3.4- Implementation.....	107
6.4- Chapter Summary.....	110
7- Conclusion.....	112
7.1- Impact.....	114
7.2- Limitations and Future Work.....	115
8- Bibliography.....	116

## **List of Figures**

Figure 1-1: Examples of a Dental Crowns (Your Dentistry Guide, 2020) .....	1
Figure 1-2: Thesis Structure.....	5
Figure 2-1: A Machined Zirconia Crown (A-Underside, B-top) (Photos Taken by D.R.Irvine) .....	9
Figure 2-2: Typical Ball Nose End Mills Used in Machining Dental Restoration .....	12
Figure 2-3: Left to Right Sharp, T-landed and Honed Edge Preparations.....	17
Figure 2-4: Cutting Edge Geometry and the Tool Faces .....	19
Figure 2-5: Forms of Tool Wear (International Standard Organisation, 1989) .....	22
Figure 3-1: Examples of Images Captured Under Optical Microscope (left to right tip,face, relief).....	43
Figure 4-1: Results for 2 Point Bending Test of 2mm Ball Nose End Mills .....	48
Figure 4-2: Example of Wear Occurring on Secondary Relief of Tool After Machining Pre- Sintered Zirconia.....	50
Figure 4-3: SEM Image of the concentrated wear that occurred from machining pre-sintered zirconia.....	51
Figure 4-4: Example of Surface Welding on Relief Surface of Tool Highlighted in the Circle .....	52
Figure 4-5: Machined Zirconia Dental Crowns from a 100mm Disc A) Under/Fitting Side B) Top/Visible surface .....	54
Figure 4-6: Pre-Sintered Zirconia 100mm Disc Inside the CNC Router .....	57
Figure 4-7: Tool Wear Progression on a Ball Nose End Mill After 15 Minute (left) and 310 Minutes (right) at X8 Magnification.....	57
Figure 4-8: Tool Wear Curves .....	58
Figure 4-9: Unworn Carbide Grades Left to Right A, B & C.....	59

Figure 4-10: QBSD Images of Carbide a Worn Edges at 10 kX Magnification.....	59
Figure 4-11: QBSD Images of Carbide B Worn Tool Edges at 10 kX Magnification .....	60
Figure 4-12: QBSD Images of Carbide C Worn Edges 10 kX Magnification .....	61
Figure 4-13: Chipping on Tool Edge of Carbide C .....	62
Figure 4-14: Ball Nose Tool Geometry for Tip (A) and Face (B) Along with Data .....	65
Figure 4-15: Examples of Rake Face Microscope Image Capture A-4x Full Edge, B-11x Focus Wear .....	69
Figure 4-16: Examples of Relief Face Microscope Image Capture A-4x Full Edge, B-11x Focus Wear .....	70
Figure 4-17: Examples of Tool tip Microscope Image Capture at 4x .....	71
Figure 4-18: Mean of the means of tool wear for each machining condition .....	73
Figure 5-1: Thermal Couple Set up for Subsurface Thermal Testing.....	80
Figure 5-2: Set up of Slots for Condition and Thermal Forces Testing.....	81
Figure 5-3: Sub-surface temperature readings across time .....	81
Figure 5-4: Demonstrating Rzo Stylus Set Up.....	86
Figure 5-5: The RZo Stylus on Machined Zirconia Surface.....	87
Figure 5-6: Surface Roughness Against Tool Wear .....	88
Figure 5-7: Mean of Means for Machining Conditions Against Surface Roughness in Line with the Direction of Cut .....	89
Figure 5-8: Mean of Means for Machining Conditions Against Surface Roughness Across the Direction of Cut .....	90
Figure 6-1: Demonstration of Determining n for Taylor’s Tool Life Formula .....	96
Figure 6-2: Log Plot of Tool Life Against Feed Rate.....	97
Figure 6-3: Log Plot tool Life Against Cutting Depth.....	97
Figure 6-4: Log Plot Tool Life Against Spindle Speed .....	98



Figure 6-5: Machining Conditions Against Time .....	102
Figure 6-6: Machining Conditions Against Tool Wear .....	103
Figure 6-7: Machining Conditions Against Surface Roughness in Line with the Cut Direction .....	104
Figure 6-8: Machining Conditions Against Surface Roughness Across the Direction of the Cut .....	104
Figure 6-9: Decision Flow Chart for Optimisation Assist .....	109
Figure 1: Machined zirconia dental crowns A) underside or fitting edge B) top side or visible surface.....	128
Figure 2: Pre-sintered zirconia disc inside the CNC router.....	130
Figure 3: Tool wear progression on a ball nose end mill after 15 minute (left) and 310 minutes (right) at X8 magnification .....	131
Figure 4: Tool wear curve .....	132
Figure 5: Unworn Carbide grades left to right A, B & C .....	132
Figure 6: QBSD images of Carbide A worn edges at 10 kX magnification .....	133
Figure 7: QBSD images of Carbide B worn tool edges at 10 kX magnification .....	133
Figure 8: QBSD images of carbide C worn edges 10 kX magnification.....	134
Figure 9: Chipping on tool edge of carbide C .....	135

## **List of Tables**

Table 3-1: Machining Conditions of Both Testing Methods .....	41
Table 3-2: Taguchi Design of Experiment for Pre-Sintered Zirconia Machining Condition Testing.....	45
Table 4-1: Machining Conditions for Wear Pattern Testing.....	49
Table 4-2: The Material Properties of Carbide Grades .....	56
Table 4-3: Cutting Conditions.....	56
Table 4-4: Average Tool Life for Carbide Grades and Material Properties of Carbide Grades .....	58
Table 4-5: Machining Condition Test Levels .....	65
Table 4-6: Taguchi Design of Experiment for Condition Manipulation Testing .....	68
Table 4-7: Measure of Flank Wear for All 36 Test Runs .....	72
Table 4-8: Machining Conditions for Minimal Tool Wear.....	74
Table 5-1: Physical Properties of YTZP .....	78
Table 5-2: Speeds and Feeds for Slot Milling of Temperature Tests .....	80
Table 5-3: Peak Temperatures for Probe Height .....	82
Table 5-4: Machining Conditions for Ideal Surface Finish .....	91
Table 6-1: Three Sets of Conditions and Their Corresponding Theoretical Tool Life.....	99
Table 6-2: Advised Machining Conditions for Finishing Operations.....	107
Table 6-3: Range of Advisable Machining Conditions for Machining Pre-Sintered Zirconia .....	108
Table 6-4: Machining Conditions for Differing Operations .....	110

## **Nomenclature**

Abbreviation	Meaning
ae	Radial Depth of Cut
ap	Axial Depth of Cut
C	tool life Constant
CAD	Computer Aided Design
CAD-CAM	Computer Aided Design & Computer Aided Manufacture
CAM	Computer Aided Manufacture
CIP	Cold Isostatic Pressing
CFRP	Carbon Fibre Reinforced Polymer
CNC	Computer numerical control
d	Depth of cut
f	Feed rate
FEA	Finite Element Analysis
ISO	International Standards Organisation
MMPT	Millimetres per Tooth
MRR	Material Removal Rate
n	Machining exponent
PCD	Poly-Crystalline Diamond
RPM	Revolutions per Minute
SEM	Scanning Electron Microscope
SMM	Surface Metres per Minute
T	Tool life

V	Spindle Speed
WC	Tungsten Carbide
Y-TZP	Yttria Tetragonal Stabilized Zirconia poly-crystal

## **Acknowledgement**

I would like to thank my supervisors Jason Matthews and Marilyn Goh for helping me through my PhD guiding me in academic writing, and Prima Dental for funding my research. I would also like to mention how immensely grateful I am towards the workshop technical team: Chris Hart, Mark Allonby, Lucy Corfield, Doug Nash, Gary Slocombe and Nigel Cliff who for months put up with endless extraction running as I tested the various machining conditions needed to complete this work. Special thanks to Mark Allonby for helping me setup the CNC router and CAM package. Finally, I would like to thank my family and fiancée without whom my sanity would have been lost.

## **1- Introduction**

This chapter provides a brief overview on dental crowns' materials and machining, outlines the aims of the work and details the structure of the thesis and of each chapter.

### **1.1- Background**

Dental crowns are a forms of dental prosthesis, which is the practice of adding an artificial replacement of one or more teeth and/or associated structures (Almas, 2018). Replacing a tooth is a multi-stage process going from the patient side to a dental lab where the prosthesis is designed and manufactured, then back to the patient side. The manufacturing of the prosthetic is the primary focus of this research, primarily concerned with the machining step of the manufacturing.

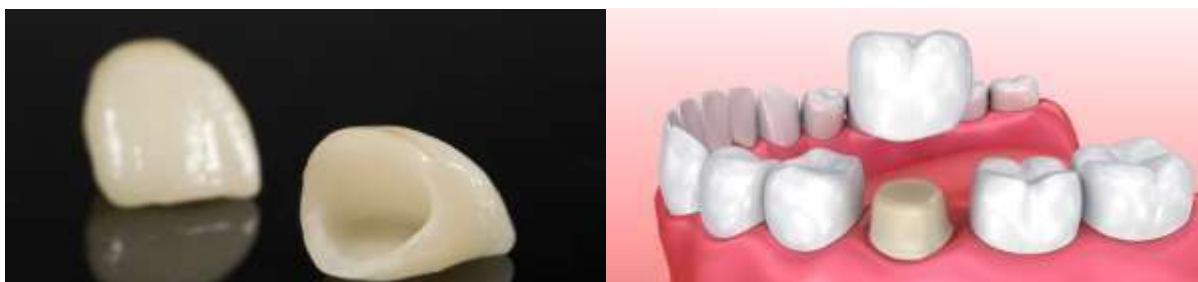


*Figure 1-1: Examples of a Dental Crowns (Your Dentistry Guide, 2020)*

Machinability refers to how easy a material is cut to shape; the higher the machinability, the higher the material removal rate (MRR) which leads to faster production times (Gale, 2003). This is preferable as restorations are bespoke and designs start from measurements of the patient, so keeping stock of things such as crowns is ill advised. Failure mode is slightly more obscure; this criterion involves how a specific part fails, not when or for what reason but how.

Yttria-stabilised zirconia is being used more and more in dental prosthesis due to its very high wear resistance and biocompatibility (Chew *et al.*, 2014; Anand, Arunachalam and Vijayaraghavan, 2018). The addition of yttrium oxide stabilises the –normally high-temperature– cubic phase of zirconia which has improved thermal, mechanical, and electrical

properties. The sintering process condenses the grain giving it its desired mechanical properties. Some Zirconia is impregnated with hydroxyapatite, the main Component in human bone, to increase its biocompatibility.

This material is generally machined in a pre-sintered state; that is very soft in comparison to the sintered version, which allows the material to be machined with end mills instead of grinding burrs. This leap to pre-sintered blocks of zirconia has allowed the crowns and coping to be made quickly enough to meet demand. Grinding down sintered zirconia or other such hard materials would take far too much machining time. Therefore, the preferred method of dental prosthesis creation is to machine pre-sintered zirconia and then sinter it.

Tool wear is the study of how machining tools fail through their working life. Much of this wear presents as a form of edge deterioration. Studies of tool wear generally involve performing mock manufacturing procedures, such as cutting slots or drilling repeated holes, or in the case of end mills machining pockets out of a specific material (International Standard Organisation, 1989b, 1989a). Studying the tool wear for the machining pre-sintered zirconia dental crowns involves several specific considerations. Firstly, the tools are of the ball nose type in order to allow more organic shapes to be formed. The second major factor is pre-sintered zirconia itself as by all accounts, it should take a very long time for the tungsten carbide tools to wear out machining a material as soft as pre-sintered zirconia is. Tool wear does however propagate rapidly, in most cases causing the tools to reach end life before 90 parts can be made (Irvine, 2017). It is this very unusual tool wear that is the focus of this study. This demand comes from wanting to understand the material more as many of the tools used to machine it are simple metal cutting ball noses end mills (Miyazaki *et al.*, 2009). The machining conditions are mostly inspired by similar processes and former procedures of hand tooling porcelain parts. Pre-

sintered zirconia has also been machined in the dental sector long enough to understand *in general terms* how the tools fail and what effect that has on the product (Boitelle *et al.*, 2018). A preliminary study (Irvine, 2017) was done as a Master's research project at the University of the West of England focusing on the tool geometry and design to increase tool life. Other studies on machining zirconia , include research into Zirconia's indentation mechanics to identify machining mechanics (Alao and Yin, 2016) and research that focuses on the marginal fit by analysing different methods of measurement in the practice (Boitelle *et al.*, 2018). These works and others are explored in depth in the later chapters of this thesis. Most of the works directly linked to zirconia are concerned with the fine details of either the material or the development of medical side of the procedure via *in vitro* studies.



## **1.2- Aim of Thesis**

The aim of this research is to analyse carbide tool wear in machining pre-sintered zirconia. To address the problems set forward in this project and analyse the machining of pre-sintered zirconia the following objectives should be met:

- To analyse how the cemented carbide tool is affected by the machining of pre-sintered zirconia.
- To understand the tool wear pattern and propagation along with the mechanism of this wear, and how these are affected by mechanical, chemical, and thermal properties of the workpiece and the tool and process.
- To understand the effect the material removal process has on the workpiece mechanically, topographically, and thermodynamically and how these factors influence further machining and final products.
- To develop the basis of a tool life equation for the machining of pre-sintered zirconia and other materials that share the same waste material properties.
- To create a tool to assist the operators in optimising the machining efficiency, by increasing tool life and decreasing damage to the workpiece in order to supply consistent dental restoration.

### 1.3- Thesis Scope

This section outlines the thesis structure and details the purpose of each chapter. The thesis is structured as shown in Figure 1-2.

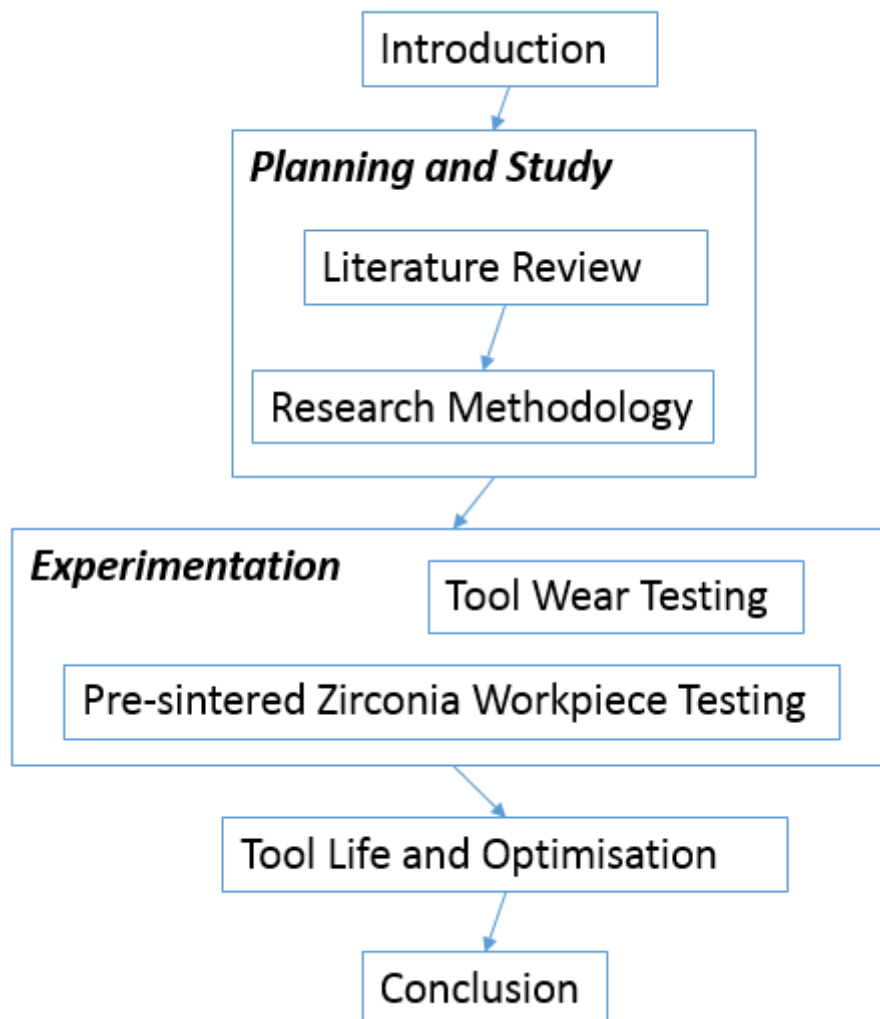


Figure 1-2: Thesis Structure

## **Chapter 2 Literature Review**

This chapter is a review of the current literature in and around the areas of study for this research. This review was conducted throughout the entirety of the doctoral study in order to ensure that knowledge was up to date. The information is collected into a comprehensive literature review and broken down into subchapters for each key area of the research. The first key area specifically deals with tool design, which is dependent on material, geometry and treatments or coating considerations. The second key area concerns tool wear, how different types of wear presents, progresses and methods of prediction. The next key areas cover the desired properties of the final product, the history and development of dental CAD-CAM and finally related modelling approaches.

## **Chapter 3 Research Methodology**

This chapter details the path and purpose the work takes, including why certain methods were used and why some aspects were not investigated. This chapter also includes the testing standard adapted for use during this work from metal cutting tests. This chapter is key to outlining the direction and focus of the research. Lastly, it details the limitations that this approach and experiment had and how in some cases these were mitigated.

## **Chapter 4 Tool Wear Testing**

This chapter covers all the wear testing done inside of the machining process. The propagation of the tool wear pattern is covered, first outlining how the tool wears and what areas are affected. This was to clarify the primary form of wear that occurs so that it can be better resisted. The tool condition manipulation testing method and results are also recorded at the end of this chapter. This testing involved over 100 blocks of pre-sintered zirconia and months of machining time. But the outputs from this test were used to evaluate other parts of the process.

## **Chapter 5 Pre-Sintered Zirconia Work Piece Testing**

This chapter includes the analysis of how the machining process affects the pre-sintered zirconia work piece. Following the tool testing all the zirconia blanks are saved for various investigations such as: surface roughness, damage induction and so on. This involves a series of specific testing such as surface roughness and temperature. The studies outlined here gave insight into how the material breaks down through the machining process.

## **Chapter 6 Tool Life and Optimisation**

This chapter contains analysis and model building. It details the process of constructing the tool life equation from the machining condition testing and tool wear analysis. This is done in an explanative method instead of a classic mathematical proof. The base for the tool life equation is the Taylor's tool life (Agapiou and Stephenson, 2016b) which has an in-depth proof and decades of use and modification. The second half of this chapter is concerned with optimisation. The optimisation refers to the efforts of fine tuning the machining conditions for surface finish, tool wear and lead time. This is done from data from the condition testing and other observations from testing done through the entirety of this research project. These sections are directed at the final two aims of the thesis.

## **Chapter 7 Conclusion**

This chapter holds closing remarks from this thesis summarising the work there in, and rounding up the overall work of each chapter in one comprehensive place. It also contains the suggestions for directions that this research can go in future works. It lastly contains the impact of this research and the work generated from it.

## **2- Literature Review**

This chapter covers the literature in and around the area of machining pre-sintered zirconia and tool wear forms, especially focusing on the manufacturing of dental prosthesis. This part of the research is intended to highlight the gaps in these fields and lead forward into the research that needs to be done.

The first section introduces the principles of machining pre-sintered zirconia in a dentistry context. The second section discusses how the tool's design affects the machining of zirconia, from the materials to the geometry used to resist the various types of wear. In the third section, the fundamentals of tool wear are presented. The fourth section shows that several product properties and requirements are affected by the machining parameters, chiefly the properties of zirconia, whether a specific finish is desired, and the impact of imperfections on the longevity of the finished part. The fifth section considers several aspects of CAD-CAM specific to the dental industry. Finally, in the sixth section the modelling and simulation of how pre-sintered zirconia reacts to cutting forces is investigated to find the current state of predicting the formation of the swarf.

These research areas are the building blocks of further work into the wear forms and what affects them.

### **2.1- Pre-sintered zirconia in dentistry**

For decades dental prosthesis has been a common method of restoration, but like many other medical sectors the methods, materials and technologies used to create these restorations have evolved throughout the application of these procedures. One such recent evolution is the shift in material towards using zirconia for structural parts of restorations such as crowns and copings. This is due to its high strength, excellent wear properties and biocompatibility. To manufacture

dental restorations, the generally implemented method is Computer Numerically Controlled (CNC) milling of zirconia in a pre-sintered state as this allows repeatable accuracy precision and high quality control (Buhrer Samra *et al.*, 2016). Pre-sintered zirconia is machined instead of its sintered counterpart due to the latter having high hardness and poor thermal properties, leading to low machinability. The mechanical property differences between sintered zirconia and pre-sintered zirconia are considerable. Pre-sintered zirconia has a hardness around 66 Vickers hardness and once the same block is sintered it increases to near diamond levels being above 1600 Vickers hardness. This increased hardness derives from the consolidation of grains. However, that is not the only property that increases the machinability of zirconia; the pre-sintered zirconia also can sustain greater amounts of mechanical damage and absorb more energy (A.-R. Alao and Yin, 2014). This allows it to resist the cracking induced damage sustained from machining.

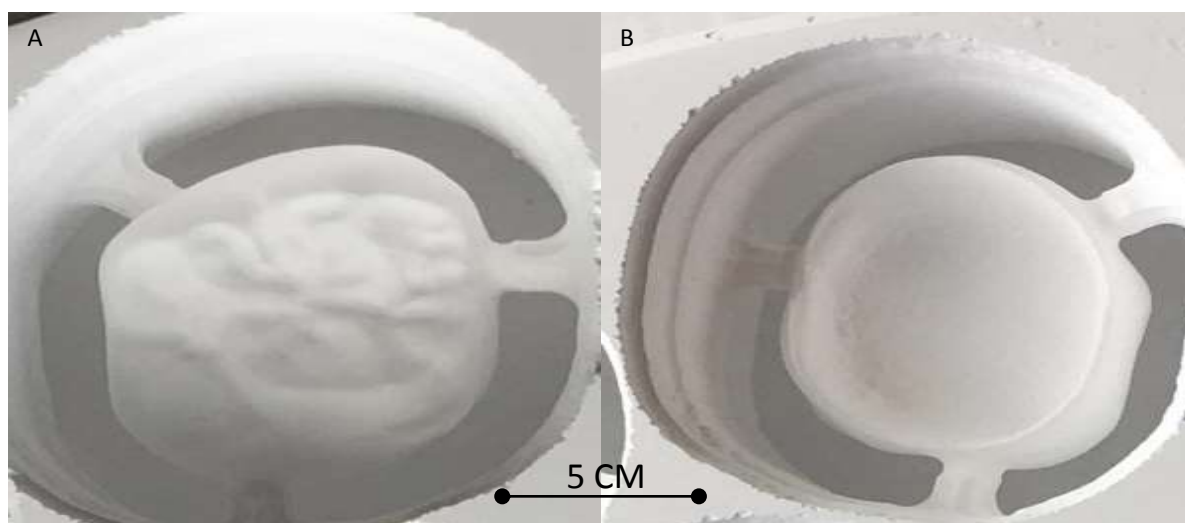


*Figure 2-1: A Machined Zirconia Crown (A-Underside, B-top) (Photos Taken by D.R.Irvine)*

Copings, crowns (like those seen in Figure 2-1) and other restorations have the main purpose of repairing damaged teeth to a state where they can again be used for mastication. In the cases of copings and crowns, they also have to protect the damaged tooth beneath them. These parts together give the need for well-fitted, hard and hardwearing parts. The ability to resist wear and impact comes from material, as the design of crowns cannot change on the exterior, so crowns

stay unnoticeable. The need for aesthetic matching of the surrounding teeth leads to other parts of material choice; the material should be able to blend in with the natural colour of teeth or be semi-translucent. This has caused the shift to zirconia with the development of yttria-stabilized zirconia. The high tolerance of the fit is what has led to the shift away from the classic hand tooling towards computer-aided manufacturing (CAM). The geometry for the machining is taken directly from the patient's mouth with the internal surface being fitted to the cut away enamel. These pieces need to be able to withstand a constant and wide variation of forces from differing directions. Because of these harsh loading conditions and the life span of the parts, the surface integrity of the part needs to remain intact; therefore any imperfections such as cracks introduced during the manufacturing need to be avoided as much as possible.

The machining process in dental labs typically used a small 4-axis CNC router; these machines are usually specifically set up for machining disc of pre-sintered zirconia (Kirsch *et al.*, 2017). The process also uses extraction and air blasts to control the waste material. The normal method of controlling swarf is the usage of coolant, but this cannot be used due to the porous nature of zirconia. However even with air blasts and extraction, the waste material is still uncontrolled with some staying in the flutes of tool and some moving out past relief edges causing abrasion on the way. This dust-like swarf is where most of the issues of machining pre-sintered zirconia come from because it causes abrasive wear. The manufacturing of such parts as stated previously is predominately done by machining the pre-sintered form of zirconia. The pre-sintered zirconia discs that are used in the manufacture of restorations are formed by cold isostatically pressing (CIP) them together (Demarbaix *et al.*, 2018), or what is referred to as green state zirconia together. If done correctly this results in a uniform density, however if the pressing is done poorly – say from only one direction – then the non-uniform density could lead to non-uniform shrinkage at the sintering step. The density controls the variance in shrinkage during sintering, the lower the density the higher the shrinkage. Sintering involves heating the machined parts at 1500°C for 2

hours, raising the temperature 8°C/min (Amat *et al.*, 2019), before the part is slowly cooled. If the cooling and heating are not properly controlled, they can accentuate any imperfections such as cracks induced during machining causing the part to immediately or eventually fail.



## **2.2- Tooling Design**

The milling process for fabricating dental restorations uses a series of ball nose end mills, like those seen in Figure 2-2. These tools are used as an organic shape has to be obtained in a suitable time frame. A series of different sized rounded cutting tools are the most effective way to accomplish this.



*Figure 2-2: Typical Ball Nose End Mills Used in Machining Dental Restoration*

Improving tooling in the majority of cases is an iterative method of fine tuning the geometry, tool material and coating. The design of ball nose end mills involves the same key elements, and understanding these elements separately allows for them to be put together.

### **2.2.1- Tool Materials**

In the machining of pre-sintered zirconia in the dental sector, tools are generally made of cemented tungsten carbide. This is due to tungsten carbides (WC) desirable mechanical properties like its

high hardness and transverse rupture toughness. However, these are general trends and different grades of carbide have varying properties. Cemented tungsten carbide, like any material, has many grades from small composition changes. While these can seem like minor changes, they can have huge impacts, allowing tungsten carbide to gain specialised properties for its designed task. For example, lowering the binder agents and encouraging fine WC grains improves erosion resistance (Katiyar *et al.*, 2016), or reducing carbide fraction increases impact resistance even on micro scale like that found in three body abrasion (Katsich and Badisch, 2011). This specialisation combined with its inherent mechanical properties is what makes tungsten carbide a prime choice for many tooling solutions.

Some studies such as that conducted by Wang *et al.* (2016) show the importance of the treating processes involved in creating carbide grades (Wang, Chen and Ding, 2009). That work focuses on shot peening; a process used to improve fatigue life by impacting a workpiece with particles with sufficient force to plastically deform the surface impact. This induces residual stresses to the outer layers work hardening them. This is generally avoided for treating carbide, as any force capable of deforming cemented carbide at room temperature will cause cracks instead of the desired plastic deformation due to how brittle it is.

Sintering can also have differing effects on materials as it consolidates the grain size which, in ceramics and composite cermet such as cemented tungsten carbide, is inversely proportional to hardness (Upadhyaya, 1998; Fang *et al.*, 2009; Katiyar *et al.*, 2016) which is then in turn inversely proportional to fracture toughness. However, Fang *et al.* (2009) showed that this relationship changes when the grain structure reaches the nanostructured scale; in both ceramics and metals, the fracture toughness and hardness both increase with reduction in grain size. This shift in mechanism was attributed to a highly increased volume fraction of grain boundaries and as deformation is dependent on the sliding interactions of grain boundaries. The paper also covers

the fabrication of nanoscale-cemented carbide and how the finished tool performs, however it does not do this in relation to materials like pre-sintered zirconia.

These studies are very tooling focused, however; it is unclear how increased fracture toughness aids the abrasive resistance of a carbide tool. A study by Katiyar *et al.* points out that lowering the binder content, which is typically cobalt or nickel, and making the grain structure finer assists the substrate of tungsten carbide to resist abrasive wear and erosion (Katiyar *et al.*, 2016). That study was centred on optimising the tool life of carbide mining drills and while based on a larger scale with different material and geometries, it does run into some of the same problems that are faced with machining pre-sintered zirconia.

Almost all of the works covered here use some form of scanning electron microscope (SEM) analysis, whether it is used for detection of surface imperfections or grain size analyse. However, when wear occurs during machining is there any change in the microstructure? Scanning electron microscopes could be used to observe changes in the microstructure after the machining process.

Approaching abrasive tool wear forms is rare due to the specific environments that cause them to be less common in metal machining. They do occur in composite and ceramics and with these materials being used more and more, abrasive tool wear has become prevalent. With composites being used heavily in aerospace industry, drill designs have been created to deal directly with the issues of finish and tool life that occur when using conventional drill designs, much like issues faced when machining pre-sintered zirconia. However, the literature concerning the development of these tools concentrates almost exclusively on the tool coatings, geometry and cutting conditions and almost completely neglects the carbide substrate chosen.

### **2.2.2- Coated and Uncoated Tools**

To increase the working life of a tool, the general approach is to coat it in a compatible material with the desired resistances. From the extensive selection of coatings currently available, most

assist the tool in resisting common forms of wear by lessening the thermal impact that machining has on the core material (Dearnley and Trent, 1982; Hedenqvist, Olsson and Söderberg, 1989; Wayne and Buljan, 1990). It was noted by Agapiou and Stephenson (Agapiou and Stephenson, 2016a, 2016c) that coatings are usually less resistant to three body hard particle abrasion. This form of abrasion is what occurs when multiple particles freely impact and slide across surface. This information brings forward a problem as the abrasion present in machining pre-sintered zirconia is three body hard particle abrasion and not sliding abrasion like that in machining composites. This restricts the list of coatings and makes selecting coatings difficult and would require validating which coating works and if it is cost effective. When considering the testing of coatings, there are a few methods available. One consists in using micro abrasive as was done by Fallqvist, Olsson and Rупpi (Fallqvist, Olsson and Rупpi, 2007) to test multilayer coatings; however this lacks the temperature element that comes with many machining operations. It is unclear the affect temperature has in the machining of pre-sintered zirconia.

Currently in the area of milling tools coatings, a commonly used one is titanium nitride (TiN) based and some are uncoated. TiN coatings are very effective and studies have shown that they outlast other coatings for cracking (Ghani, Choudhury and Masjuki, 2004). This cracking resistance is due to the thermal properties that TiN based coatings provide. These studies are usually done with steel as a work piece material, which has a different cutting mechanism and causes different wear patterns to when pre-sintered zirconia is machined. Part of the TiN based coatings is TiAlN: this coating is widely used and is even applied in the machine of crowns due to its exemplary wear resistance in high speed and dry conditions (PalDey and Deevi, 2003). It is said that the choice of TiN coatings is very dependent on the complexity of the wear mechanism. If the coating is selected poorly, it leads to the tool having what is called two-stage wear, because the coating wears first then the carbide wears (Dearnley and Trent, 1982). This can lead to the coating being rather counterproductive, as it simply falls away protecting the tool for only a

handful of parts. With this and the highly abrasive nature of zirconia affective coatings resist the wear become rare. The obvious choice for such an environment would be diamond coating (Montoya *et al.*, 2013; Gaugel *et al.*, 2016), due to its high abrasive resistance. This form of coating is expensive though and experimentation into its cost effectiveness for the form of wear that comes with machining pre-sintered zirconia has not been done. There are other more abstract solutions like WC-12Co, which was found to have a decent abrasive resistance when applied with HVOF spray (Wang, Chen and Ding, 2009). The abrasive wear was again sliding wear so a cost analysis for machining pre-sintered zirconia would be needed.

### **2.2.3- Tooling geometry**

Tool geometry can have massive impacts on the usability of a tool in certain situations. If a workpiece material is harder, then the response is to give the tool a negative rake face or lower clearance to put more material behind the cutting edge. However, pre-sintered zirconia is not a hard material as it has a Vickers hardness in the range of plastics. So to design the geometry of ball nose end mills for machining pre-sintered zirconia, the relevant mode of failure of cutting such materials needs to be understood.

In the design of ball nose end mills numerous changes can be made. As with all cutting tools, there is the issue of the geometries of the cutting edge or edge preparation; within this there is the general angles and land lengths of the different types. The main forms of edge preparation are: sharp, T-landed and honed, as shown in Figure 2-3.

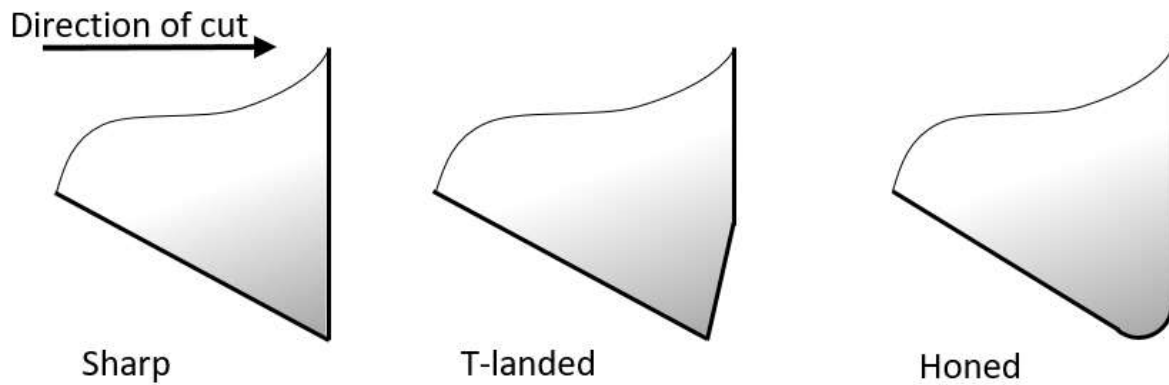


Figure 2-3: Left to Right Sharp, T-landed and Honed Edge Preparations

Each have their own strengths and weaknesses that make them more tailored towards certain purposes. The sharp preparation for example is for cutting softer materials such as wood, aluminium or plastic. This is the most commonly thought of edge as cutting makes most people think of kitchen knives. Kitchen knives are commonly made of steel and in a similar manner most tools that have a sharp edge preparation are high-speed steel tools and not ceramic tools. This is due to the brittle nature of ceramics causing the sharp edge to break away under sudden impact, especially when machining hardened surfaces or when dealing with fluctuating temperatures.

T-land refers to a small chamfer across the cutting edge shorter than the cutting depth. This new land adds some strength to the cutting edge without affecting the main rake face or relief. This makes a tool excellent for machining harder materials and pairs very well with ceramic tools and inserts. If the T-land is larger than necessary for the conditions, it can have a negative impact on the life of the tool as it effectively pre-wears the tool.

Honed edges are rounded across the cutting edge somewhat like T-landed tools. This form of edge preparation does reduce the clearance directly by the cutting edge. This can cause build up on soft materials and chipping in work hardening materials. As with T-land, the cutting conditions are balanced with the radius of the honing. Honed edges can be seen on drills used for composite drilling. It is remarked in some works (Bouzakis *et al.*, 2004; Yussefian *et al.*, 2010) that

increasing edge preparation decreases a tool's abrasive wear resistance which is one of the major forms of wear when machining pre-sintered zirconia. Beyond the cutting edge itself, the relief and rake faces can be modified; together they define the wedge angle, as shown in Figure 2-4. As with the edge preparations, adjusting these angles affects the strength of the edge as well as wear resistance. Increasing the relief reduces the contact that non-cutting surfaces have with the work piece, which reduces the wear on those surfaces, but doing so weakens the leading edge and again the geometries have to be balanced to match the purpose. Macro geometries such as the helix and shank can also be important. The shank is the holding of the tool and is designed more around the machine and the holding desired. The helix's main purpose is to evacuate waste material on ball nose end mills, and it is also used as a secondary cutting edge for end milling. Both of these functions are not needed in the milling of pre-sintered zirconia for dental restorations as end milling is used only on the round of the nose. This is due to the geometry of the part and due to the dust-like nature of the waste material the helix does little to control it.

In the dental industry currently, the tools are designed similarly to ball nose end mills used in metal cutting apart from a few slight changes. The first of these changes is the flute: while most of the geometry stays the same in the flute, some designs use longer and deeper flutes. This geometry change is typically seen on drills and tapered ball nose end mills used for machining soft material. With the soft nature of pre-sintered and the versatility that is demanded from the tools, it could be seen why this design choice was made. It may be necessary to apply some alternative tool geometries not usually used in conventional machining; take for instance the work done by Zhu *et al.*, (Zhu *et al.*, 2012) using a heat pipe up through the tool to draw heat away from the work surface. Something like this could be very effective in dry condition machining.

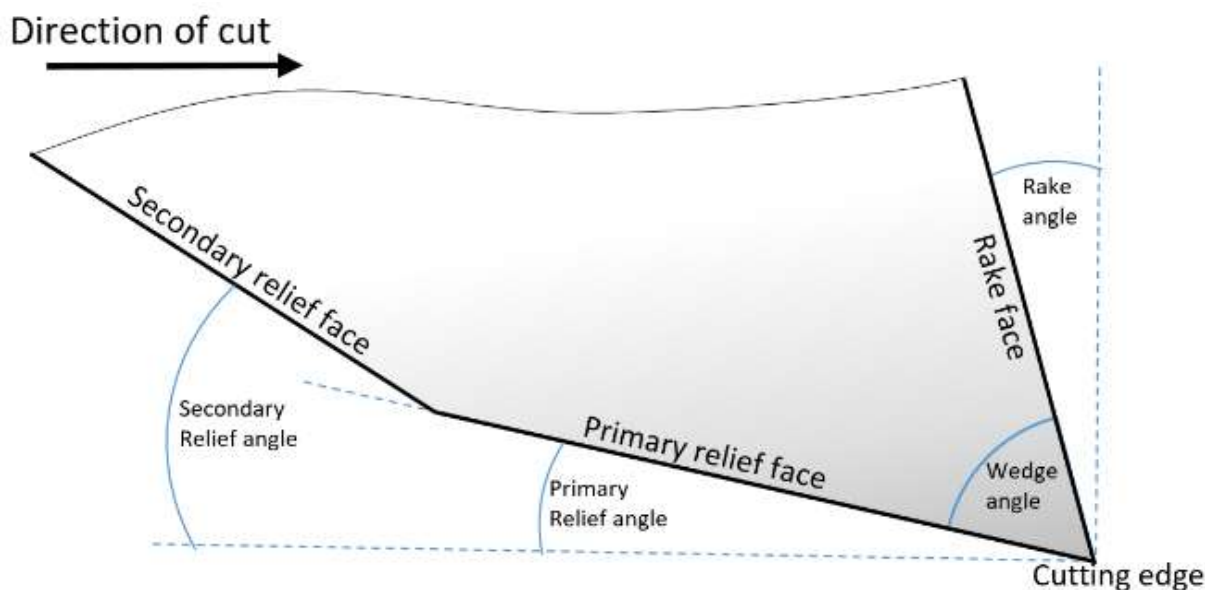


Figure 2-4: Cutting Edge Geometry and the Tool Faces

It would be beneficial if a heat pipe could be properly applied to the ball nose end mills used to machine pre-sintered Zirconia, because coolant cannot be used due to the porous nature of the workpiece (Cassie and Baxter, 1971). Other considerations include additional cutting faces and chip breaking, or the removal of flutes increasing the number of cutting faces. None of these have yet been done with no literature to explain why.

A type of analysis involving a series of accelerometers and dynamometers allowing for the analysis of the cutting across a time frame is available. This form of tool testing is excellent if the wear form and propagation are fully understood as it uses these initial force readings to predict how the tool will deteriorate. This method has been used by Ramesh and Siong (Ramesh and Siong, 2011) on ball nose end mills for machining titanium and found a T-landed ball nose end mill to resist the thermal and physical challenges that come with machining titanium. However, with pre-sintered zirconia the wear pattern is not as well documented as it is with titanium, which makes this method less applicable. Another method consists in measuring the wear as it progresses until it reaches a predetermined failure criterion; this is very time consuming but over time can build up an enough data to enable the earlier method.



Due to how recent the process of machining pre-sintered zirconia is, few papers have been published covering its machining. However, some studies approach problems similar to those faced in the machining of pre-sintered zirconia. One such study was conducted by Ohbuchi and Obikawa (Ohbuchi and Obikawa, 2003) which modelled the chip formation when using negative rake angles. This model incorporates a stagnant region by the tool tip to act as a stable edge then uses the stress flow to model how the chip forms and moves over the uncut material. This study showed the harsh forces that are introduced when machining with a negative rake angle. Applying this model to pre-sintered zirconia however might be difficult as it uses plastic deformation that happens only very briefly with pre-sintered zirconia. A similar simulation was done using varying rake angles from  $+15^{\circ}$  to  $-30^{\circ}$  to analyse the residual stress that these geometries introduce into the work piece material (Kundrák *et al.*, 2017) It also used hardened steel as a work piece, which has different properties to titanium, and found much the same as other studies that negative rake angles introduce higher residual stress. The use of negative rake may not even be necessary for such a soft material; many of the tools used in the industry have a neutral rake.

## **2.3- Tool Life/wear**

Tool life is the measure of how long a tool can be used until it can no longer achieve its specified purpose. Many works have shown the direct effect that tool wear has on the surface finish of the machined surface and the stresses induced during the machining process (Diniz and Filho, 1999; Ghani, Choudhury and Masjuki, 2004; Tamizharasan, Selvaraj and Noorul Haq, 2006). Both of these affect the end product of dental restorations especially at the high tolerance areas such as the marginal fitting edge, which is where failures occur the most (Nasrin *et al.*, 2016). It is therefore important to understand the propagation of wear and the affect it has on both the tool and work surface.

### **2.3.1- Wear Forms**

Tool wear covers many specific classifications that have been set by ISO 8688:1989 (International Standard Organisation, 1989a, 1989b) these are: flank wear, face wear, chipping, cracking and catastrophic failure, and are shown in Figure 2-5. Flank wear is the gradual loss of tool material from the tool's flank or edge during cutting, which leads to the progressive development of flank wear land. This flank wear land is a newly formed surface created from the worn away edge. Face wear is a gradual loss of material from the cutting tool's leading face, or rake face, during cutting. This can result in one of two differing forms known as crater wear and stair formed wear, which form craters or a sloping land respectively on the face.

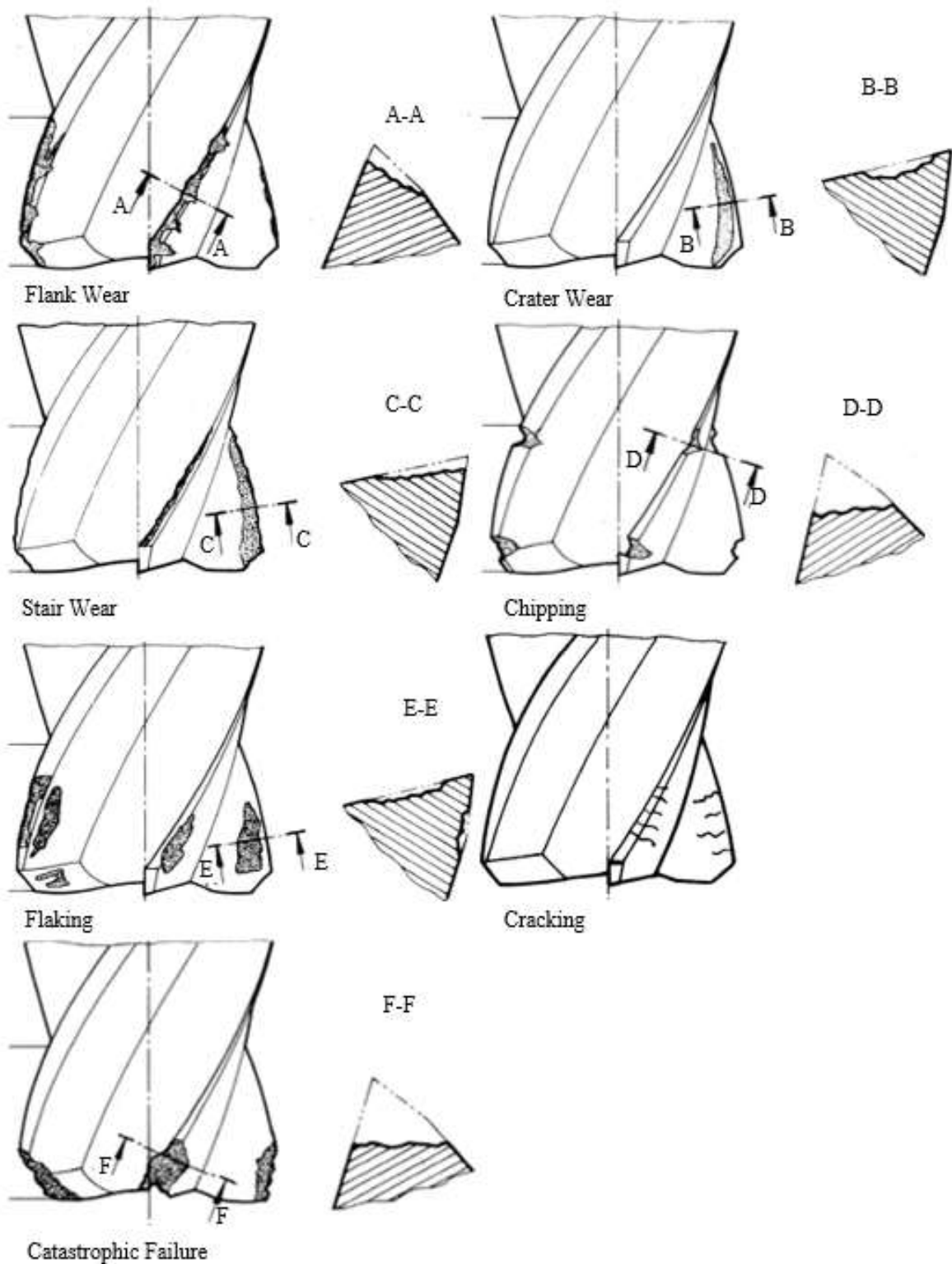


Figure 2-5: Forms of Tool Wear (International Standard Organisation, 1989)

Chipping is a form of brittle edge deterioration where parts of the edge break away unlike flank wear, though this tends to brittle. It is further classified, like flank wear, to be uniform, non-

uniform or localised. Cracking is a fracture in the tool material that does not lead to immediate loss of tool material. It can be parallel or perpendicular to the tool edge or, in some cases, randomly orientated irregular patterns. Flaking is the breaking away of material from the surface of the tool in a flake form. This also tends to be brittle and is more likely to occur on any face unlike other wear forms. The final form of tool wear is catastrophic failure. This is when the cutting part of the tool rapidly and completely fails. This results in the tool not being able to function.

Most of these wear forms occur due to incorrect cutting conditions, thermal circumstances or the material properties being too hard or abrasive in nature. Zirconia has been shown in previous work to be abrasive (Suh, Chae and Kim, 2008); this work evaluated the sliding wear behaviour between zirconia and series of structural ceramics including itself. It found that the coefficient of friction stays somewhat constant between all the ceramics. The controlling factor of this is zirconia, as it is a 'smooth' material. That study did also show that the wear on all of the ceramics is abrasive in nature. While this run of experimentation did not use tungsten carbide it does back up earlier work done that found that tool wear, when machining pre-sintered zirconia, is abrasive in nature. Jia & Fischer showed in their work that carbide's resistance to slide wear is dependent on grain size and cobalt content and not hardness. That paper also identified the wear as very thin shearing not plastic deformation or fractures (Jia and Fischer, 1997).

With cutting at speeds such as the ones used in the creation of crowns, it is understandable why tool wear may occur at a high rate. But it has been shown in several works that the conditions being used are perfectly acceptable. Tool wear in many advanced materials is affected by feed rate instead of spindle speed (Dolinšek and Kopač, 2006). It has also been shown that reducing the feed rate while machining brittle materials increases the quality surface finish (Liu *et al.*, 2013).

### **2.3.2- Wear Progression and Wear Testing**

In a work by Muthuraja and Senthilvelan, the abrasive wear on carbide was analysed with the aim of reducing it. The method uses carbide blanks and abrasive sheets and moves one across the other, measuring physical wear and temperature (Muthuraja and Senthilvelan, 2015). The solution found to counteract abrasion uses what is referred to as solid lubrication in the form of calcium fluoride, which acts as a form of sacrificial coating instead of protection. This solution however still uses some liquid during the cutting process, which is unfavourable during pre-sintered zirconia machining. Montoya analysed tool wear during carbon fibre reinforced polymer (CFRP) aluminium stack drilling (Montoya *et al.*, 2013). This is much more relevant than it first appears as CFRP causes abrasive wear and aluminium causes work piece build up on the tool, two things that occur during the machining of pre-sintered zirconia. That study highlighted the need for adjustments in tool micro-geometry. Continuing from CFRP machining, it has been shown that cutting edge rounding and secondary face wear are both characteristic of abrasive tool wear (Gaugel *et al.*, 2016). The work that showed this mechanism used cutting edge rounding to measure and track abrasive tool wear. These studies lay out very thorough tool wear tests. Most studies into end mills use straight line cutting as it is more controllable (John *et al.*, 2021). These tests and numerous others also use ISO 8688:1989 as a basis for experimental design but changing out the base material to match circumstances (International Standard Organisation, 1989b); this practice was followed within this work.

### **2.3.3- Tool Life**

Tool life is the measure of how long a tool can be used until it can no longer achieve its specified purpose. Many works have shown the direct effect that tool wear has on the surface finish of the machined surface and the stresses induced during the machining process (Diniz and Filho, 1999; Ghani, Choudhury and Masjuki, 2004; Tamizharasan, Selvaraj and Noorul Haq, 2006). Both of these affect the end product of dental restorations especially at the high tolerance areas such as

the marginal fitting edge, which is where failures occur the most (Nasrin *et al.*, 2016). It is therefore important to understand the propagation of wear and the affect it has on both the tool and work surface.

Usually to predict tool wear a model would have to be built to extract the flank wear growth, like that done by Ramesh and Siong (Ramesh and Siong, 2011). That study used ball nose end mills much like those used to machine pre-sintered zirconia in dentistry to machine titanium and monitor it with accelerometers, dynamometer and acoustic emissions sensors. The increase in cutting force was measured and used to track the progression of tool wear. This study was conducted with titanium as the work piece material, which has drastically different properties to pre-sintered zirconia along with the wear mechanism being primarily abrasive.

The prediction of tool wear and tool life based on cutting condition developed by Taylor, called Taylor's Tool Life has been modified and built upon over the decades (Taylor, 1907). All of these methods use a constant called Taylor's Tool constant and is indicative of the tool workpiece interaction. This constant does not currently exist for the interaction between carbide tools and pre-sintered zirconia.

Another method of predicting the tool life is to measure it in operation. One such way of doing this is to measure the vibrations within the tool as the tool wears (Bhuiyan and Choudhury, 2015). This involves installing sensors in the form of a tri-axial accelerometer in the tool holding. While the experiment run in this study was conducted with a lathe, the sensor could be adapted to be held inside or as part of a milling collet. With this method the vibration will start to peak before the tool breaks, and then the vibrations will fade to a negligible reading.

With the drastic shift in cutting mechanism that pre-sintered zirconia brings, it is likely there would also be a corresponding shift in tool wear patterns. A similar instance was investigated in a study (Zhou *et al.*, 2006) with glass as the work piece material. Cutting tests were carried out

using ultrasonic vibrations within the tool and were found to reduce the occurrence of brittle fracturing and reduced tool wear. The study also stated that further work was needed from a practical application standing as the tool mounting was specialised. While this study does not concern zirconia in any form it does bring up an abnormal solution for the machining of brittle materials, as vibrations are usually connected to increased tool wear.

## **2.4- Product Properties**

In dentistry zirconia is used primarily for crowns and other restorations including implants (Miyazaki *et al.*, 2009; Bona, Pecho and Alessandretti, 2015), due to zirconia's advantageous mechanical and chemical properties. The geometry of these restorations is taken directly from the patient allowing for bespoke design, with very tight tolerances that are even finer on certain edges where the fit is critical. On crowns and copings, these are referred to as marginal fitting edges and are located at the meeting point between the restoration and the remaining tooth, or in some cases gum.

This area is especially critical because it directly affects the survivability and comfort of the crown. A poor marginal edge would cause irritation of the gum (Abduo, Lyons and Swain, 2010). It has been shown in industry that an ideal fit not only reduces the irritation but also enhances the mechanical properties of the restorations. This greatly helps the pieces to be able to withstand the constant and wide variation of forces from differing directions the restorations have to resist. Many works have been done into the failure modes of zirconia crowns in both single piece systems and layered make ups, where porcelain or a similar ceramic is layered on top of the sintered zirconia part (Groesser *et al.*, 2014; Spintzyk *et al.*, 2016). These works show that the wall and marginal edge are the area's most likely to fail. Because of these harsh loading conditions and the life span of the parts, the integrity of these areas is essential. Therefore, any imperfections such as cracks introduced during the manufacturing need to be avoided as much as possible. For these reasons, if the marginal fitting edge of a crown is chipped or cracked it is discarded and the restoration is machined again with fresh tools. These works however do not cover how this damage can be reduced or how it is induced.

It has been shown that when grinding sintered zirconia it is possible to reduce machining induced damage by reducing grinding forces (Yin *et al.*, 2006). Certain manufacturers will look to finish



critical areas of a zirconia product with grinding to improve the surface integrity. This is however not cost effective, as this requires added machining, tooling and time. This reduction in grinding force increasing surface finish does match findings from studies done with cutting conditions and surface finish with a variety of materials (Chen, 2000; Lalwani, Mehta and Jain, 2008; Rao, Rao and Srihari, 2013; Polishetty *et al.*, 2017). These works found a varying range of these relations between cutting force and machining induced damaged that appears to be dependent on the material. None of these works cover pre-sintered zirconia however, and reduction of machining induced damaged on pre-sintered zirconia has not been studied significantly. In practice, it is assumed that the damage induced in the machined surface is much the same when machining metals, but with little to no supporting evidence.

Once the pre-sintered zirconia part is machined it has to be sintered. Sintering is a process of heating the part in an oven that causes the grain to consolidate. This increases toughness and hardness but has the side effect of causing the zirconia part to shrink (Camposilvan *et al.*, 2015). This shrinkage can cause surface imperfections to propagate into cracks or chips, which will cause the part to fail either at inspection or later in use. Understanding the way in which surface integrity decays is crucial to understand how these parts fail due to machining. Poor surface integrity causes residual stresses in the machined surface, and these residual stresses would cause chipping in brittle materials like zirconia and other ceramics. It was noted by that work that there was a drop in quantity of works for optimising cutting parameters for tool life and residual stress and an insufficient amount of work to draw a connection between surface roughness and residual stress. There are of course ways to improve surface finish after sintering using sand blasting and laser irradiation (Kirmali, Akin and Kapdan, 2014) however, in industry sandblasting is usually used alone as it is far more cost effective.

When the failure of the crown is researched, it is usually looked into from a design framework or clinical implementation standing (Sawada *et al.*, 2016; Spintzyk *et al.*, 2016). These studies and others collectively state that failure usually occurs in the adhesive join between crown and tooth or the layers between them depending on the design of the restoration. However the location where the main body of the restoration fails is usually at the marginal fitting edge or abutment of the restoration (Basílio *et al.*, 2016; Sawada *et al.*, 2016). Another study (Nasrin *et al.*, 2016) concludes that flexural stress concentrated over small areas caused failure within crowns during their life spans due to design errors. This study used Finite Element Analysis (FEA) to simulate an assembled crown being subjected to a single cycle indentation load. These papers and many others tend to disregard or forget the machining stage as a point of failure in the process and neglect how design and manufacture go hand in hand.

When the failure of the crown is researched it is usually looked into from a design framework or clinical implementation standing; the root cause has not been traced back, but failure has been noted to occur irregularly, which would coincide with manufacturing issues instead of a lifetime issue. It was also remarked that the failure rate of zirconia crowns and implants is still lower than their counter parts (Abdulmajeed *et al.*, 2017).

## **2.5- Dental CAD-CAM**

Computer Aided Design – Computer Aided Manufacture (CAD-CAM) is the digitising of design and manufacture. This is very useful for high precision parts such as those needed in modern dental restoration. Many labs use 4 axis CNC routers, like those made by Roland, to machine the restorations. These machines are built with dental restorations in mind including: seal and extraction to contain waste material, special nesting for dental materials, micro collets and tool racks for flexibility of process.

The implementation of CAD and CAM in dental labs is a relatively new addition changing from the hand tooling. Development of this shift started in the 1980s and is now widely employed across the dental sector. It was not until Dr Mörmann's work that it became recognised as a way of delivering ceramic crowns with measurements straight from patient's mouth, with much less time and higher accuracy than hand tooling (Mormann *et al.*, 1990). Mormann's work involved assessing the CAD-CAM at the time highlighting its many advantages over conventional methods. It also highlighted that the cost and time investment for implementing these processes was high. These have since decreased due to the increase in knowledge and emergence of expertise.

Another study (Zucuni *et al.*, 2017) concluded that the mechanical behaviour of zirconia used in dental restoration needs proper understanding before accurate simulation of the machining can be done. While this statement seems trivial, that work did highlight how little is understood about how pre-sintered zirconia reacts to being machined. That study also covered the best way to achieve a good surface finish and supported the milling of softer pre-sintered zirconia and then sintering. This conclusion is also reached by numerous other academic studies and industrial observations. Miyazaki and Hotta's work aimed to outline and review available fabrication techniques for restorative dentistry at the time (Miyazaki and Hotta, 2011). It did this very well,

highlighting the major methods as well as the use of Zirconia, which was not as widely used in 2011 as it is today. The paper outlines the areas in which research in this field should be undertaken, encouraging a shift to “digital dentistry” which is currently where the industry is heading. It also highlighted the importance of fully understanding pre-sintered and sintered zirconia from both an engineering and medical point of view to correctly serve the patient.

The development of more accurate contouring allowing dentistry to apply CAM technology (Lu *et al.*, 2011) has led to the use of CNC grinding in some cases (Anderson, Warkentin and Bauer, 2008; Anand, Arunachalam and Vijayaraghavan, 2018). While effective at producing high tolerance parts, grinding is time consuming and tooling is costly. The alternative, as previously stated, is to cut a softer material then treat it to become harder like with pre-sintered zirconia. Because of this divide, many ways of machining in dentistry have been investigated. A study was conducted (Zucuni *et al.*, 2017) that compared two systems of dental CAD-CAM the Cerec system and using grinding burrs for milling. The study was mostly concerned with topographical scans of the post machine surface. It also highlights the important impact that surface finish has on mechanical properties, finding that poor surface finish leads to failings of the restoration. It also found that a fine burr produced the closest to the surface finish of the milling method used in the Cerec system.

Very few studies have investigated the machining conditions, but one study has covered the spindle speed and feed rate (Demarbaix *et al.*, 2018). It found that pre-sintered material follows the same pattern as ductile materials when it comes to machining parameters selection. That study only covered spindle speed, feed rate and cutter depth; however this work is an excellent start for future testing and optimizations on this subject.

There are numerous studies from earlier research giving an overview of dental CAD-CAM: two stand out papers are (Yin *et al.*, 2006; Miyazaki *et al.*, 2009). Miyazaki *et al.* covers the process from chair side data collection to dental lab and back to patient, whereas Yin *et al.* is a

review of the emergence of new ceramics as the field started to adopt new tooling. Both are fairly outdated at this point with Yin *et al.* being more concerned with hand finishing. However, the processes are still very similar to the present system. Another overview is (Uzun, 2008) which covers the networking and digital functions of production systems and developing towards a future of patient side CAD-CAM.

## **2.6- Modelling**

This section covers the many methods modelling the cutting mechanisms. Pre-sintered zirconia has been a focus for some researchers such as Alao and Yin, who published numerous papers on the behaviour of this material under certain conditions. In one such paper (Alao and Yin, 2015) they analysed the elastic and plastic resistance of pre-sintered using nano-indentation. This was done in an attempt to examine the damage induced to the material during the machining process. This work forms an excellent base of knowledge of the elastic and plastic properties of pre-sintered zirconia from which to build on. It does also try to model the cutting mechanism with indentation, but this is a poor representation of what physically occurs during machining due to the time scale and the type of force induced. The evaluation of the elastic and plastic deformation is critical for understanding the cutting mechanism for pre-sintered zirconia and testing could be further expanded to make it closer to machining. Their other works (Alao *et al.*, 2017) have investigated the effects that machining has on the surface of pre-sintered zirconia along with the successive finishing operations such as sand blasting and sintering. This analysis was done using a scanning electron microscope to analyse the surface of the pre-sintered zirconia for phase changes and damage morphology after the operations. It found that sintering induces monoclinic-tetragonal phase and sandblasting led to no detectable phase changes. The study did find that machining created a very rough surface finish scattered with cracks and fractures but that after sintering, the surface roughness is within bacterial retention necessary for dental and surgical purposes. This higher than expected roughness is due to the partial ductile deformation and brittle fracture mechanic that comes from the pre-sintered zirconia physical properties (Kovalchenko, 2013). That study also outlined some problems with the process of milling pre-sintered zirconia discussed the cutting mechanism and gave SEM evidence of the two modes the material is subjected to. However, it did not investigate the extent of the material removal mode and how the mechanism is affected by varying cutting conditions and how that would affect the surface finish.

Few works approach the machining mechanism of pre-sintered zirconia. One such work covered the fracture mechanics of zirconia under laser water jet cutting (LWJ) (Kalyanasundaram, Shrotriya and Molian, 2010). While this is one of the few works that covers how zirconia cracks, it does not use pre-sintered zirconia and LWJ is a different material removal mechanism to milling. However, with the information of partial ductile and brittle fracture material removal modes the literature was broadened to include other materials that share this property and how the material removal mechanism was properly analysed in relation to cutting condition and tooling variation. Some achieved this analysis by treating the material as quasi brittle (Carpinteri, Chiaia and Invernizzi, 2004) and modelling indentation mechanics in FEA. However, that study did not use zirconia and as previously stated, the indentation part of the machining would be very brief. Others have tried to build up models of irregular cutting mechanism; for example, there is a method of finding cutting force independently of the machine parameters (Lee, Cho and Ehmann, 2008) by using tool geometry and chip thickness. This method has shortcomings when it comes to zirconia, as when pre-sintered zirconia is machined there is no conventional chip formation, and the waste material turns into more of a dust when machined.

This non-conventional chip formation causes many problems for the modelling and simulation of machining pre-sintered zirconia, and it also causes a different form of tool wear. As the waste material is formed it is blown around during the machining process, making impact and sliding across the tool surface which causes abrasive wear similar to that which occurs in the machining of carbon fibre (Shen *et al.*, 2015; Gaugel *et al.*, 2016; Muhamad Khairussaleh, Che Haron and A. Ghani, 2016). This tool wear appears as a combination of the rounding of the cutting and rake face wear. This builds up in two stages where the edge rounds off and then the edge deteriorates due to the rake face wear. The same progression of wear has been seen in earlier work with pre-sintered zirconia at the University of the West of England. However, the drilling and milling of carbon fibre causes the face wear in a localised section of the tool causing a crescent shape. This

specific shape of non-uniform wear has not been observed in the machining of pre-sintered zirconia. The crescent shape wear may be directly related to fibre causing the abrasion wear, as the abrasion from machining pre-zirconia comes from the dust-like waste material of zirconia.

## **2.7- Discussion**

This chapter has reviewed the current state of literature in the area of milling pre-sintered zirconia for use in the creation of crowns and other dental restorations, focusing on the areas of the tools that are used and that could be used, the behaviour of zirconia in production and in finished state. It also covered studies that tried to model or simulate the cutting and wear mechanisms from milling materials like pre-sintered zirconia.

Restorative dentistry has existed since the 19<sup>th</sup> century, which has led to the understanding of the framework design, and its impact is very in-depth for many materials used to create copings and crowns. Nevertheless, no effort has been made to adjust the framework for manufacturing. This is due to the bespoke nature of prosthetics having to match as close as possible to the core or tooth. With the adoption of zirconia, the framework was made thinner to take advantage of the increased strength; this allows for less of the tooth being restored to be removed for the fit. The way in which the crown fails is also understood from a fatigue lifetime point of view, but not from a manufacture stance. In many studies, the manufacturing is not reviewed as the work was mainly concerned with the dental application of the crown. This has led to the manufacturing part of the process in essence holding back the development of product. As with better tooling, the induced damage can be reduced leading to stronger parts, which in turn will lead to thinner parts allowing for even less of the tooth to be removed during the restoration.

It has become clear that any of the ball nose end mills used to machine pre-sintered zirconia should be made to resist three-body abrasive wear under dry conditions. Abrasive wear causes many



problems to tool design: firstly, that two stage wear appears more frequently with or without coating, and as the abrasion furthers it will produce multiple wear lands that will converge causing the area to wear at a much higher rate. The majority of tool coatings are not designed to resist abrasion, apart from diamond coating which has excellent abrasive resistance. There are a handful of creative solutions in the form of non-traditional tooling, such as heat pipes, chip breakers or solid lubricant. While these may improve tool life, they need specific testing under machining conditions. The grade of carbide has however been shown to have an impact on the abrasive wear resistance, but which specific grade is still under investigation. Transgranular crack resistance appears to be the critical property when resisting three body abrasion (Antonov *et al.*, 2012), a property that sintered zirconia has itself. However, with the slower nature of the wear presented by the pre-sintered zirconia, transverse rupture toughness may be the more relevant property. Similar abrasive issues have appeared in the machining of other materials such as carbon fibre. In those cases, it occurs as sliding wear which, while missing the impact mechanic of three-body abrasion, is similar and some inspiration could be drawn from the solutions used.

From this literature review, it is apparent that while zirconia is already well understood, the pre-sintered variant is only just being investigated. Its mechanical properties are vastly different from its sintered counterpart, but other properties are very similar. Take for instance hardness: for pre-sintered zirconia it is much lower, but both have very short plastic deformation zones. This split in properties can be attributed to how sintering changes the zirconia, condensing the grain structure down. This process has been previously studied, leading to various methods and pre-treatments to achieve the sintered product in differing time scales with different temperatures, properties and additives. With this background knowledge, it is very clear why zirconia is used for this application. Its wear properties are excellent for both sliding wear and 3-body abrasion. This was attributed to its transgranular crack resistance by Antonov (Antonov *et al.*, 2012), which as the name would suggest is a form of brittle failure. This resistance to crack propagation comes

from the small grain size and hard nature of sintered zirconia. Zirconia's biological behaviour, especially yttria stabilised zirconia, has been covered extensively approaching differing coatings, additives and treatments. For example, hydroxyapatite has outstanding biological compatibility as its structure is very similar to human bone (Yugeswaran *et al.*, 2012) or the plasma treatment of zirconia has shown that it improves the biocompatibility and wettability of zirconia (Zheng *et al.*, 2015).

The creation of pre-sintered zirconia discs for use in the manufacture of dental restoration has been slowly developed to the point where it can create consistent disks of even density and composition. This assists both the machining and sintering of the product as it gives the disk more uniform properties. Where understanding of this material drops off is in the machining mechanics: the maximum shear stress scales with load rate to plateau around 5.5 GPa (Alao and Yin, 2015) but the stress and fracture patterns have not been discussed.

Simulations of zirconia under varying conditions have been conducted, that have given an understanding of the fracture mechanics, but these have not been run for the pre-sintered state of zirconia so is only useful for the finished product post sintering. Some effort has been made to model pre-sintered zirconia indentation mechanics from the various works done by Alao and Yin using conventional calculations. This is a great starting point for modelling the transformations that occur during the machining process. Brittle machining mechanisms have been simulated before, but these use chip formations or assume plastic deformation. Pre-sintered zirconia has a very short plastic deformation zone when subjected to indentation or shear forces, so using plastic deformation to model its cutting mechanics will not give a correct enough representation of the deformation that occurs in material like zirconia. The method of the relevant work (Ma *et al.*, 2017) was also specifically directed at hard materials, of which pre-sintered zirconia is not. Using the chip formation gives inconclusive results, as the chips created from machining pre-sintered

zirconia are dust-like and conventional chip formation relies on plastic transformation. This brittle ductile transition has been studied in the micro milling of glass (Liu *et al.*, 2013); while a different material, the process suffers from some of the same problems such as needing to reduce wear due to the size of tools, but more importantly rapid crack propagation due to a brittle workpiece. That work however has not been applied to pre-sintered zirconia as of yet and in itself only passes comment on the brittle transition without forming any model. However, it does highlight some already suspected machining condition issues such as the spindle speed being too high. Therefore, this modelling method in its current state is insufficiently developed for application to zirconia machining and further work is necessary.

However, what has been well modelled is the fracture mechanics of zirconia. While this was done under different conditions using laser water jet cutting, the propagations prove the similarities between zirconia and other ceramics. The pre-sintered state would however have a much more erratic and rapid fracture propagation. (Liu, Kou and Lindqvist, 2002) modelled the fracture mechanics when cutting rock and rock-like materials; when modelling the fracture pattern it resembles the swarf formation of pre-sintered zirconia. However the model would need to be applied to pre-sintered zirconia to verify its application. Zirconia has also been shown on many occasions to be abrasive by nature but no effort to simulate this abrasion has been made, from a material or tool life standpoint. An effort to develop this tool workpiece interaction into a full model should be made as to increase the understanding of how both the tool and work piece affect each other.

## **2.8- Chapter summary**

In summary, zirconia is abrasive in nature and pre-sintered zirconia shares this nature. Despite this, many tools used in the milling are not designed to resist this. With the addition of the wear becoming three body abrasion, when the waste material becomes abrasive particulates that cannot be controlled by coolant due to the porous nature of pre-sintered zirconia, this abrasion can run rampant across tool faces it would not usually reach. The highly brittle nature and lack of traditional chip formation also makes this material difficult to predict with the current state of supporting literature.

From this review, it has become clear that while zirconia is a well-understood ceramic, machining it in its pre-sintered state is poorly understood, to the point where the cutting condition may not even be optimal! There is also no analysis of the abrasion caused by the pre-sintered zirconia particulate swarf. An effort should be made to research the cutting conditions, tool geometry and tool materials to aid in the machining of accurate restorative parts while maintaining good tool life. The modelling and simulation of materials like pre-sintered zirconia that are highly brittle with non-traditional chip formation should be investigated as to aid further development along with a tool life equation.

### **3- Research Methodology**

This chapter sets out the methods needed to investigate the various aims outlined at the beginning of this thesis, addressing the gaps in the current literature summarised in the earlier chapter. As previously mentioned, the main gaps in the literature that need to be addressed is the understanding of the machining process, therefore the experiments discussed in this chapter were designed with the machining process in mind.

Doing physical experiments in a machining environment allows the research to directly address the gaps however planning out these experiments becomes more difficult.

#### **3.1- Introduction**

With the aims of thesis's work and the literature gaps discovered in mind, this research set out to be more engineering and manufacturing focused. Most medical knowledge was learned through literature and second hand via conversations with other researchers and dental lab technicians to bridge the gap between the engineering approach and patient side practice. Luckily, medical data for the dental restorative sector is extensively researched and documented due to how old restorative dentistry is in comparison to the new usage of pre-sintered zirconia. With the education practice surrounding dentistry being mostly doctoral in nature, this documentation is compiled in medical journals. Whereas with manufacturing being a traditional practice, most of its documentation is entombed in standards, handbooks, and technical memos. This difference in these two fields is what has led to the medical application engineering becoming its own area to bridge these two knowledge bases to bring them closer together.

Keeping the results as actual machining tests helps greatly towards the development of the process of machining of pre-sintered zirconia. This direction was decided as many studies lose their grounding to the original machining process they are trying to aid. Many studies are

modelling things in either over simplified or non-usable manners, through no fault other than trying to simulate a very complex environment. The testing methods being machining based have led to the development of a controllable test that gives as near to the production as can be repeatable, but to keep it relatable to the main machining process. This test was developed at the beginning of this study in co-operation with Prima Dental.

The development of the testing method came from performing two tests alongside each other on two separate machines. The first test, referred to as “the copings test”, involved using a standard desktop router used in the dental industry at the time to machine a series of copings until the marginal fitting edge failed, which is how a dental restoration would fail inspection. The second test, referred to as “the pocketing test” involved machining large pockets from pre-sintered zirconia discs using the same cutting conditions as the dental sector machine, shown in Table 3-1. The smaller tools are for finishing, as many finishing processes use climb milling and much lower feed rates.

*Table 3-1: Machining Conditions of Both Testing Methods*

Tool	Feed rate	Spindle speed	Depth of cut	Step over	Milling strategy
<i>2mm ball nose end mill</i>	1000 mm/min	20,000 RPM	1 mm	0.8 mm	Conventional
<i>1mm ball nose end mill</i>		20,000 RPM	0.5 mm	0.4 mm	Conventional
<i>0.6mm ball nose end mill</i>		20,000 RPM	0.3 mm	0.2 mm	Conventional

This was done to show that the much more controllable, repeatable, and material efficient pocketing testing method would find similar results and to help set an end point. The coping test

found that once the marginal edge failed inspection the tools were worn to around 3.5% of their diameter. The pocketing test removed the same amount of material across a similar cutting time to reach the same wear. This shows that the two methods are alike in nature so either can be used to confirm another hypothesis.

### **3.2- Research Design**

Positivism was the underlying philosophy of this work using quantitative data to objectively confirm or deny the hypothesis of tool wear mechanism.

The research conducted for this study was deductive, confirming and building upon the theory that the wear is third body abrasion and deciding whether other parts of the machining process behave in conjunction with conventional machining or if parts of the process are very different.

The strategy of this work was relied predominately on physical experimentation. This was decided as physical observation as well as data was needed to confirm the mechanism and further investigate the optimal machining conditions of the process. The experiments took the form of tool wear tests based on the ISO 8688 (International Standard Organisation, 1989b), with modifications in the material used as the initial standard used aluminium for standardising the wear mechanism. However, the purpose of the initial phase of testing was to determine the wear mechanism as previous work done at Prima Dental had identified that the wear mechanism was non-conventional.

The experimental strategy was to use the CNC mill to machine simple pocketing programs. This is ideal for high repeatability while allowing for adjustment of the conditions. The milling tool path was programmed inside Feature CAM to generate the machine code (G-code) for the experiments. The resulting G-code was posted to the Denford Micromill, a 3-axis desktop CNC router capable of reaching the high RPM currently used to machine pre-sintered zirconia.

This setup allowed for short run tests to take place in the same environment for instance the subsurface temperature testing. This testing involved thermal couples inserted from beneath the work piece at varying depths to measure how the heat from machining could have affected the material; this test was based upon a previous study (Richardson, Keavey and Dailami, 2006). The aim of this experiment was to show how far the thermal forces travel through the pre-sintered zirconia.

The time setting of these experiments was a mix of longitudinal and cross sectional. The start of the study involved a series of shorter experiments to confirm multiple specifics of the tool workpiece interaction taking place. However the latter half of the work was cross sectional, involving one extensive machining condition test that was used to determine the optimal conditions for surface finish and tool wear.

Much of the data was collected through microscopes, especially for wear propagation. The worn edges of the tools were observed under an optical microscope, from which digital images were captured and measurements taken using a camera and Olympus Stream Start software. This involved aligning the tool at two angles for each tool edge and then again for the tip of the tool to provide images like Figure 3-1.

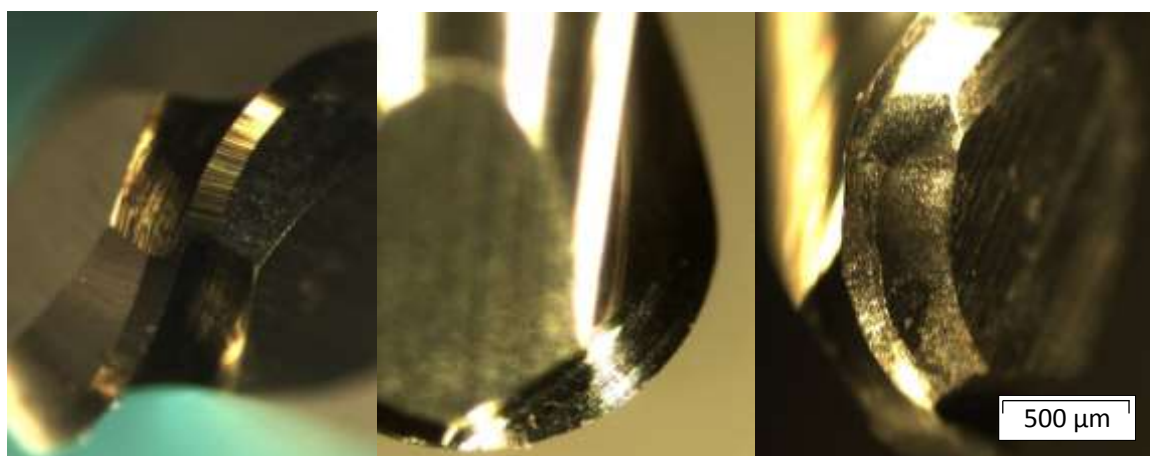


*Figure 3-1: Examples of Images Captured Under Optical Microscope (left to right tip, face, relief)*



Closer observations of the tool material were done using electron microscopes at the Optical Research Centre in Southampton in order to observe the tool's microstructure pre and post tool end life. These observations were taken at the tool edge and at a cross-section at point of highest wear after tool life has been reached. These cross sections were mounted in a polymer mixture and prepped by polishing with a diamond abrasive solution and etched with a one molar hydrofluoric acid solution.

For the larger machining condition test a Taguchi design on a factorial experiment was used to reduce the number of tests runs to an actually achievable amount. The Taguchi method is a statistical method of reducing test runs while still testing each level of each factor against each other factor. The standard experiment design, where one factor is changed each experiment to test each level of each factor against each other, would involve in excess of 600 test runs. With each test taking a day to complete, on minimum, to allow for the ball nose end mill to wear sufficiently, this would result in the full experiment taking well over 2 years, not allowing for machine maintenance or sleep. The design detailed in Table 3-2 is the result of using the Taguchi method to reduce the number of tests runs down to 36.

The method's principle consists in first repeating the first three test runs to confirm accuracy of the results, then changing two factors per run from those first three runs. Each run, the results from these test runs are then fed back into the model to plot the means of means. Minitab was used for this as well as for determining the factors for each test run. Without this method, accurate testing could not have been done on the machining conditions in the time frame of a PhD.

Table 3-2: Taguchi Design of Experiment for Pre-Sintered Zirconia Machining Condition Testing

Run	Tool	Strategy	Feed (MMPT)	Speed (SMM)	a <sub>p</sub> (mm)	a <sub>c</sub> (mm)
1	A	up	0.01250	100.53	0.6	0.6
2	A	up	0.04792	125.66	0.8	0.8
3	A	up	0.08333	150.80	1	1
4	A	up	0.01250	100.53	0.6	0.6
5	A	up	0.04792	125.66	0.8	0.8
6	A	up	0.08333	150.80	1	1
7	A	up	0.01250	100.53	0.8	1
8	A	up	0.04792	125.66	1	0.6
9	A	up	0.08333	150.80	0.6	0.8
10	A	down	0.01250	100.53	1	0.8
11	A	down	0.04792	125.66	0.6	1
12	A	down	0.08333	150.80	0.8	0.6
13	A	down	0.01250	125.66	1	0.6
14	A	down	0.04792	150.80	0.6	0.8
15	A	down	0.08333	100.53	0.8	1
16	A	down	0.01250	125.66	1	0.8
17	A	down	0.04792	150.80	0.6	1
18	A	down	0.08333	100.53	0.8	0.6
19	B	up	0.01250	125.66	0.6	1
20	B	up	0.04792	150.80	0.8	0.6
21	B	up	0.08333	100.53	1	0.8
22	B	up	0.01250	125.66	0.8	1
23	B	up	0.04792	150.80	1	0.6
24	B	up	0.08333	100.53	0.6	0.8
25	B	up	0.01250	150.80	0.8	0.6
26	B	up	0.04792	100.53	1	0.8
27	B	up	0.08333	125.66	0.6	1
28	B	down	0.01250	150.80	0.8	0.8
29	B	down	0.04792	100.53	1	1
30	B	down	0.08333	125.66	0.6	0.6
31	B	down	0.01250	150.80	1	1
32	B	down	0.04792	100.53	0.6	0.6
33	B	down	0.08333	125.66	0.8	0.8
34	B	down	0.01250	150.80	0.6	0.8
35	B	down	0.04792	100.53	0.8	1
36	B	down	0.08333	125.66	1	0.6

### **3.3- Limitations**

This approach was limited by time. Physical tool wear testing (machining a carbide tool till it is worn to its end life while recording the progress of wear at set points) is very time consuming. This was mitigated as much as possible, but each test run still takes a prolonged time, sometimes over a week. The waste material from machining pre-sintered zirconia presents itself as a fine powder, which needs to be safely extracted (while zirconia is medically safe, inhaling large quantities of it can damage the respiratory system in the worst cases). This also caused build-up of the waste material on other parts of the machine, mainly the motor, commutator and axis threads. As the machine used for testing was not designed specifically to machine a material such as this, it resulted in a much more frequent maintenance cycle than would usually be seen while machining. The research being a combination of longitudinal and cross sectional while thorough, is very time consuming and open to scheduling issues. This testing, once started, could not be redirected a great deal. So once committed to the direction, if any unseen circumstances were to have occurred or a discovery was made the test could not be adjusted to react. While a deductive basis of these experiments did allow for a building upon pre-existing theories confirming or denying hypothesis, it does not however lend itself toward open discovery.

### **3.4- Conclusion**

The core of the machining tests performed in this work were based upon the ISO end mill wear test standard (International Standard Organisation, 1989b). However the material is changed out for pre-sintered zirconia as the wear mechanism is different. While this test standard is designed for measuring tool life it can be easily expanded for analysing the wear mechanism and work piece surface typography. A Taguchi design was used for establishing the impact that each factor had on the tool wear and surface integrity. Observations were taken during and after the experiments to support data findings. Post-machining analysis was done using Excel and Minitab, and both optical and SEM microscopes were used depending on requirements.

## **4- Tool Wear Testing**

This chapter introduces the experimental work conducted, investigating the interactions between the carbide cutting tool and the pre-sintered zirconia work piece and focusing on how the tool was worn and what can be done to reduce this wear.

### **4.1- Introduction**

Tool wear is a natural side effect of machining, no matter how robust the material being used is. This wear, while unavoidable, can be reduced and investigations into this wear allow for the identifying of these preventative measures. This analysis starts with the wear pattern. Understanding the wear pattern allows for identification of the primary source of the wear so the tool material can be designed to resist it. If the wear was caused by abrasion, then the wear pattern will present in specific ways. If the wear is plastic deformation of the cutting edge, where the wear comes backward as the edge falls away, the wear rate slows in a predictable manner. With abrasive wear, the location can start away from the edge and causes an increase in the wear rate as the surface area increases, increasing the contact area to worn away.

After machining, the part is sintered by placing it in an oven and heating for upwards of 5 hours; however, if the heat is localised it can cause partial sintering which would lead to large, hardened pieces of zirconia present in the machining environment. To understand the heat present in the work piece during machining, a series of tests were performed to see how the heat moves through the material and whether some form of coolant could be necessary. As the work piece is formed of cold, isostatically pressed powder, it returns to its powdered state when machined. The individual particulate of the powder is what makes up the swarf of machining pre-sintered zirconia. Like in conventional machining, uncontrolled swarf leads to high wear rates. The final part of this chapter discusses machining condition manipulation.

A series of tools were subject to 2-point loading in order to demonstrate the sudden breakage that happens. This test involved clamping the tools as if they are being held in a collet in a universal testing machine and loaded at the cutting depth until breakage occurs. The breakage is measured as force drops off, as shown in Figure 4-1. This shows the general maximum cutting force of these tools when the tool is “fresh” and unworn. This limits the overall cutting depth and materials it could machine. These forces should not be reached while machining zirconia, unless trying to rapid machine sintered zirconia.

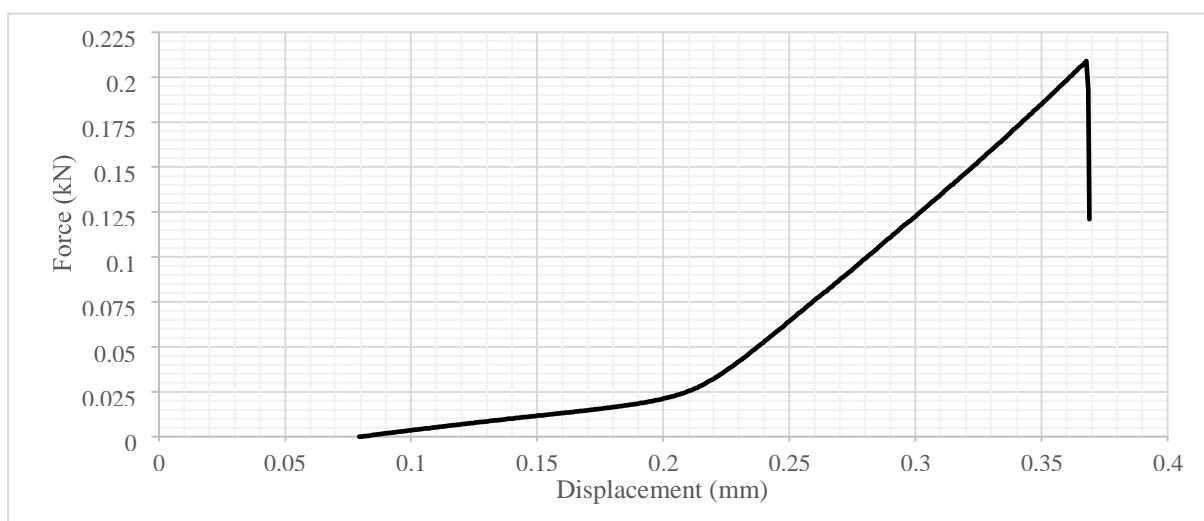


*Figure 4-1: Results for 2 Point Bending Test of 2mm Ball Nose End Mills*

The ball nose end mills used started as conventional 2mm 2 flute ball nose cutters. These cutters are small, so like much micro tooling they tend to have zero rake angle to resist plastic deformation. This design is carried across to these tools even in the current iterations of the tools. Through various tests prior this doctoral study, high relief was found to be necessary to allow for space between tool and work piece for the swarf to move as, it is the swarf that caused the tools to fail. The flutes do not remove all the waste material and much of the swarf tries to pass around the tool due to its fine, dust-like nature. This goes for the flutes as well: reducing the flute count increases the clearance between cutting faces for the swarf to be moved away from the cutting area with more ease.

## 4.2- Tool Wear Pattern

The tool wear pattern is how the tool tends to wear and eventually fail. This testing was aimed at expanding on the abrasive wear reports of previous testing and finding the locations and magnitudes of wear propagation so that the tool can be better designed to resist it. This testing was also used to define and prove testing methods for future testing.

### 4.2.1- Method

This testing involved a previously used method where 98mm in diameter by 20mm deep pre-sintered sintered zirconia discs were machined in regular patterns under constant conditions. These conditions are listed in Table 4-1.

Table 4-1: Machining Conditions for Wear Pattern Testing

Process	X,Y Feed (mm/min)	Z Feed (mm/min)	Spindle speed (rpm)	Step over (mm)	Depth of Cut (mm)
Rough	2000	1000	20,000	0.8	1

The tool pathing for this testing was laid out so that it mimicked the milling of the dental prosthesis. This was done by setting up a pocketing feature that is 96 mm across. This pocketing was used instead of machining individual dental restorations as it is more repeatable and uses fewer discs per test, as more material is removed per disc.

### 4.2.2- Observations and Results

From the machining of the pre-sintered zirconia, it is obvious from the get-go that the nature of the waste material is very different from the classic chip-like waste material created during the machining of metals. The waste material generated during the machining of pre-sintered zirconia is dust-like in form and is propelled outwards by the forces and air currents created by the tool spinning and the work interface. This dust is harder to control than conventional chip-style waste material due to its size and weight. This erratic movement of the waste material

caused some wear to occur on surfaces that usually would not be worn, such as the secondary relief as shown by the silver area in the blue circle in Figure 4-2. Unusually high wear on the cutting face of the tool in the form of stair wear also occurred; however this is far steadier than the flank wear which tails off and then peaks again, becoming the main source of tool failure.



*Figure 4-2: Example of Wear Occurring on Secondary Relief of Tool After Machining Pre-Sintered Zirconia*

After machining was completed, samples of the tooling and waste material were taken to the optical research centre in Southampton for SEM analysis, in order to verify the occurrence of abrasive wear and how the material could cause such wear to occur. This analysis showed concentrated areas of wear on many of the tools in similarly found regions, as shown in Figure 4-3. The topography of this concentrated wear gives way to high volumes of the abrasive material passing through this section of tool.

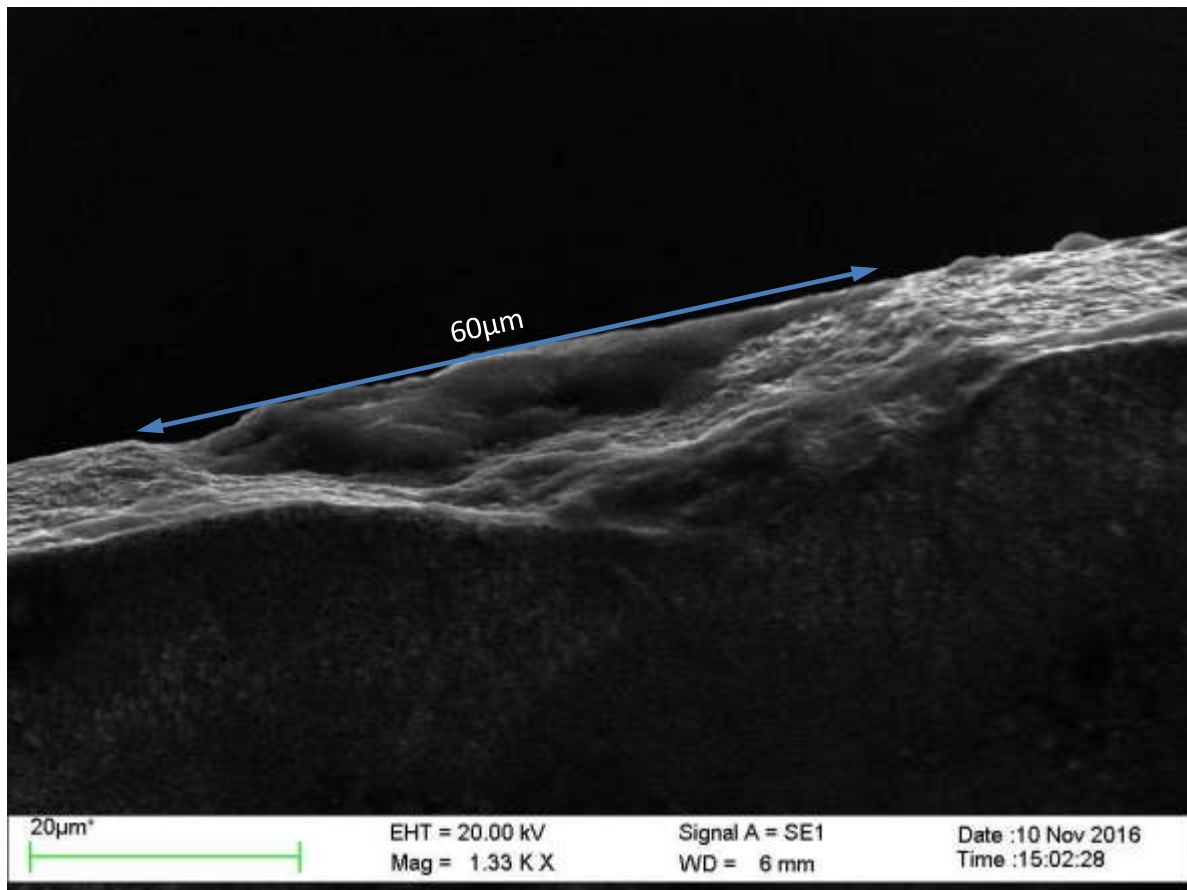


Figure 4-3: SEM Image of the concentrated wear that occurred from machining pre-sintered zirconia

Some surface welding of the pre-sintered zirconia on the tool surface was also present, as shown in Figure 4-4. This would have been caused by constant high forces pressing the zirconia against the tool at the tool work interface, combined with the heat generated during machining. This caused the zirconia to partially sinter to the worn away, rough surfaces on the relief. This changes the shape of tool, reducing its effectiveness. There is also the danger of the build-up breaking away and taking some of the tool material with it, weakening the tool's structure.



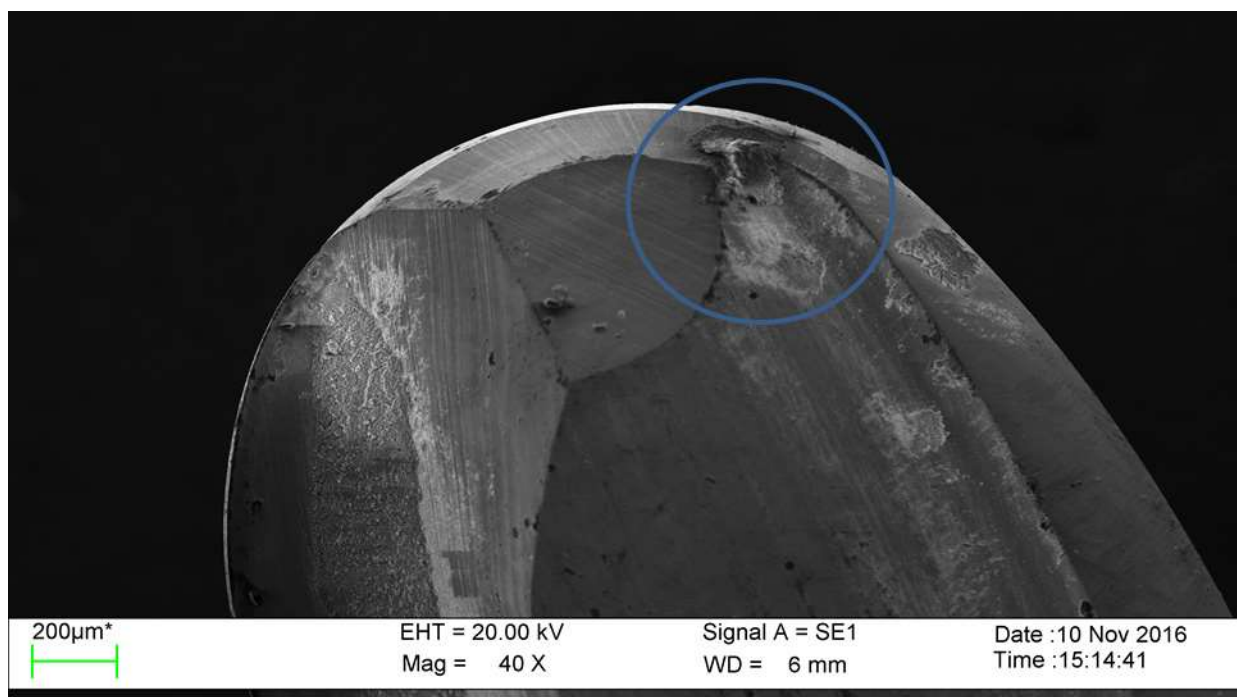


Figure 4-4: Example of Surface Welding on Relief Surface of Tool Highlighted in the Circle

#### 4.2.3- Discussion

The wear rate curve and formation of wear does point towards abrasive wear. If the tool wear involved more plastic deformation, then uniform flank wear would be more prevalent with an increase towards the outer cutting edge. The chipping and cratering are highly affected by the particles: as a chip starts to form, the increased surface area allows for an increased abrasive wear. This is what causes the increasing wear rate toward the end of a tool's life, as the fractures turn to craters and rapidly expand. In many cases of tool wear testing seen in this research, it was this rapid tool edge degradation that led to tool failure. The surface welding on the rear faces may have also been happening on the tool edge but breaking away, causing further degradation. Further investigation is needed into what happens to the core material to give an indication of which of these effects was taking place and what can best be done to resist the cause of wear. This study found the wear pattern of machining pre-sintered zirconia to be predominantly abrasive, in particularly third body abrasive wear and not typical plastic deformation. This is shown from the non-uniform nature of the wear.

### **4.3- Tool Material Changes**

The core material of the ball nose end mills is cemented tungsten carbide. This section covers the testing and analysis that were conducted to determine how the core material was changed by the abrasive wear mechanism of machining pre-sintered zirconia.

#### **4.3.1- Introduction**

For decades, dental prosthesis has been a common method of restoration, but like many other medical sectors the method, material and technology used to create these restorations has evolved throughout the application of these procedures. The most recent of these evolutions is the shift in material to using zirconia for structural parts of these restorations, such as crowns and copings, due to its high strength, excellent wear properties and biocompatibility. To create these the generally implemented method is Computer Numerically Controlled (CNC) milling of zirconia in a pre-sintered state, as it allows for access to this material and others along with the repeatable accuracy precision and high-quality control (Buhner Samra *et al.*, 2016). This happens in the dental laboratories or in milling centres and has become known as dental CAD-CAM. Pre-sintered zirconia is machined instead of its sintered counterpart as the latter is high in hardness and poor in thermal conductivity, giving it low machinability. Presintered zirconia has a hardness around 66 Vickers hardness. Once the same block is fully sintered, the hardness value increases to be above 1600 Vickers hardness. This increased hardness comes from the consolidation of grains. The pre-sintered zirconia can also sustain greater amounts of mechanical damage and absorb more energy (A. R. Alao and Yin, 2014). This allows it to resist cracking induced damage during machining.

Dental restorations, such as copings and crowns, have the main purpose of repairing damaged teeth to a state where they can again be used for mastication. The ability for restorations to resist wear and impact comes from the material. The need for an aesthetic matching of the

surrounding teeth is another factor in material choice. The dental material should be able to blend in with the natural colour of teeth or be semi-translucent. This has caused the shift to zirconia with the development of yttria-stabilized zirconia. The speed of generating restorations as well as the accuracy needed on final restorations has led to the shift away from the classic hand tooling towards CAD and CAM in dentistry. The machining process in dental labs typically uses a small desktop 5-axis CNC machines. These machines are usually set up for machining discs of pre-sintered zirconia, as in Figure 4-5. Geometry and dimensions of the restoration are taken directly from the patient's mouth using impression moulding or laser scanning. This gives a highly accurate model to work with that the CAM package can build straight from.

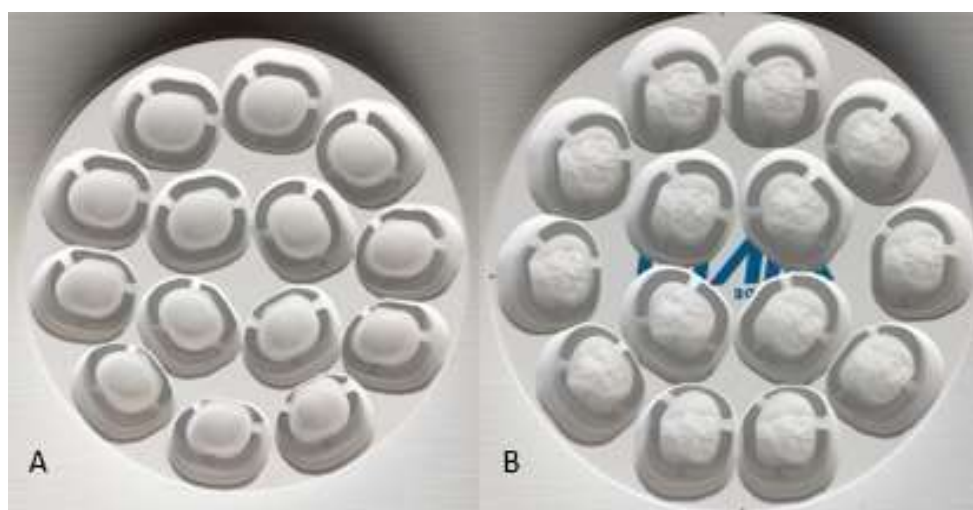


*Figure 4-5: Machined Zirconia Dental Crowns from a 100mm Disc A) Under/Fitting Side B) Top/Visible surface*

The process also uses extraction and air blasts to control the waste material for dry milling and coolant or water for wet milling. The pre-sintered zirconia discs that are used in the manufacture of restorations are formed by cold isostatically pressing powdered, or what is referred to as green state zirconia. From the dentist's perspective, the actual process of machining is not a main priority in their working function, beyond the points that the process must be simple to operate and accurate in the final output. Issues such as tools wearing, changing the surface geometry of the crowns, or even damaging the material are certainly unwanted and would be

undesired effects for both the dentist and the tooling manufacturer. To build an understanding of the tool wear that occurs during the prosthesis production, the remainder of the chapter presents a modified ISO 8688:1989 test method for investigating tool wear in machining pre-sintered zirconia using carbide tools.

#### **4.3.2- Tool life**

Tool life is the measure of how long a tool can be used until it can no longer achieve its specified purpose. Much work has shown the direct effect that tool wear has on the surface finish of the machined surface and the stresses induced during the machining process (Diniz and Filho, 1999; Tamizharasan, Selvaraj and Noorul Haq, 2006). Both affect the product of dental restorations especially at the high tolerance areas such as the marginal fitting edge, which is where failures occur the most (Nasrin *et al.*, 2016). It is therefore important to understand the propagation of wear and the effect it has on both the tool and work surface. Tool wear classifications that have been set in stone by ISO8688:1989 (International Standard Organisation, 1989a) are: flank wear, face wear, chipping, cracking, and catastrophic failure. Flank wear is the gradual loss of tool material from the tool's flank or edge during cutting which leads to the progressive development of flank wear land. This flank wear land is a newly formed surface created from the worn away edge. Face wear is a gradual loss of material from the cutting tool's leading face, or rake face, during cutting. This can result in one of two differing forms known as crater wear and stair formed wear, which form craters or a sloping land, respectively, on the face. Wear occurs due to friction and heat generated during cutting and of course the properties of material being machined. Zirconia, which is to be studied in this chapter, is abrasive in nature (Suh, Chae and Kim, 2008).

#### **4.3.3- Test Method**

To analyse wear, three carbide grades with different properties as summarised in Table 4-2 were used to make tools. The aim was to identify which carbide grades wears out the least when

machining pre-sintered zirconia and what was the wear mechanism. Tests were conducted on a 3-axis router. The cutting conditions used are summarised in Table 4-3. These conditions were adapted from those used in desktop milling machines in dental labs. Ø2mm ball nose end mills made from three different carbide grades were tested. These tools were uncoated. Each tool milled a circular pocket until it wore out. The stopping criterion used was when the flank wear of a tool reached 3.5% of the tool diameter. For a Ø2mm tool, this was 70 microns. Flank wear on the tool was checked at 15 minute intervals until the stopping criterion was reached. However, when tools broke halfway through the test or it caused a margin of the milled pocket to crack, the tool would be considered as worn and no measurement would be taken on this tool for comparison purposes. Figure 4-6 shows pre-sintered zirconia discs in the CNC router that had a bed large enough to accommodate multiple discs at once. Vacuum extraction and air blasts were to control dusts that were formed from machining.

*Table 4-2: The Material Properties of Carbide Grades*

<b>Carbide grade</b>	<b>CARBIDE A</b>	<b>CARBIDE B</b>	<b>CARBIDE C</b>
<b>Transverse rupture toughness (MPa)</b>	3700	4000	4200
<b>Fracture toughness (MPa)</b>	10	10.4	9
<b>General grain size (µm)</b>	0.8	0.5-0.8	0.5
<b>Hardness (Hv 30)</b>	1590	1600	1920

*Table 4-3: Cutting Conditions*

<b>Process</b>	<b>X,Y Feed (mm/min)</b>	<b>Z Feed (mm/min)</b>	<b>Spindle Speed (rpm)</b>	<b>Step over (mm)</b>
Roughing	2100	1200	25,000	0.8

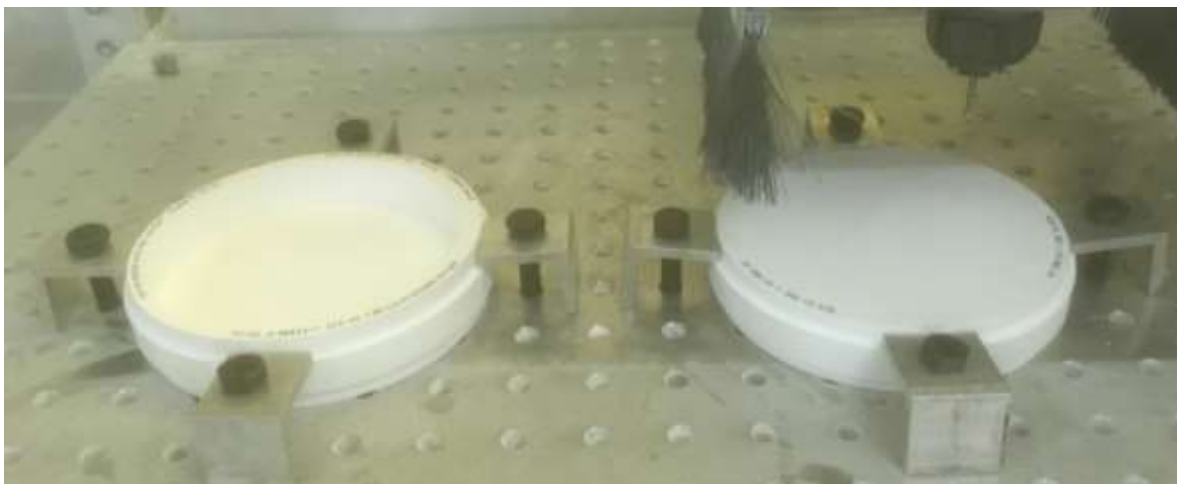


*Figure 4-6: Pre-Sintered Zirconia 100mm Disc Inside the CNC Router*

Figure 4-7 shows the flank wear of tools, with the left image showing flank wear after 15 minutes and the right showing flank wear after 310 minutes. The width of wear was measured using an Optical Microscope coupled with Stream, a measurement software from Olympus.

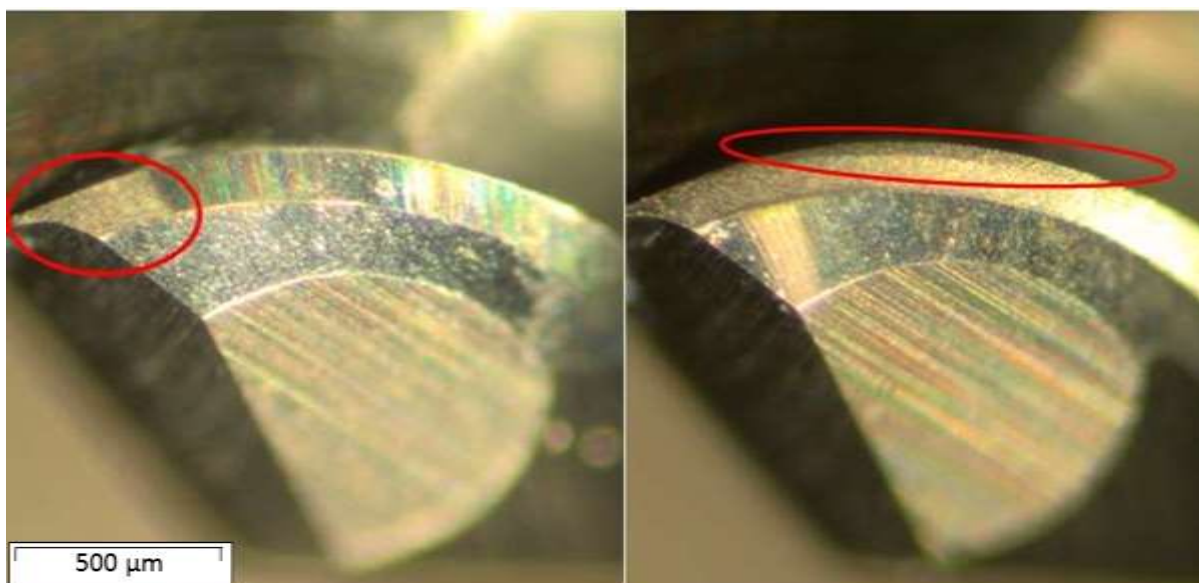


*Figure 4-7: Tool Wear Progression on a Ball Nose End Mill After 15 Minute (left) and 310 Minutes (right) at X8 Magnification*

#### **4.3.4- Results and Analysis**

The flank wear measured at the 15 minute interval was plotted as shown in Figure 4-8, with the horizontal line representing the tool end life criteria, which was the stopping criterion of 70 microns used in the test. The final tool life in minutes is summarised in Table 4-4.

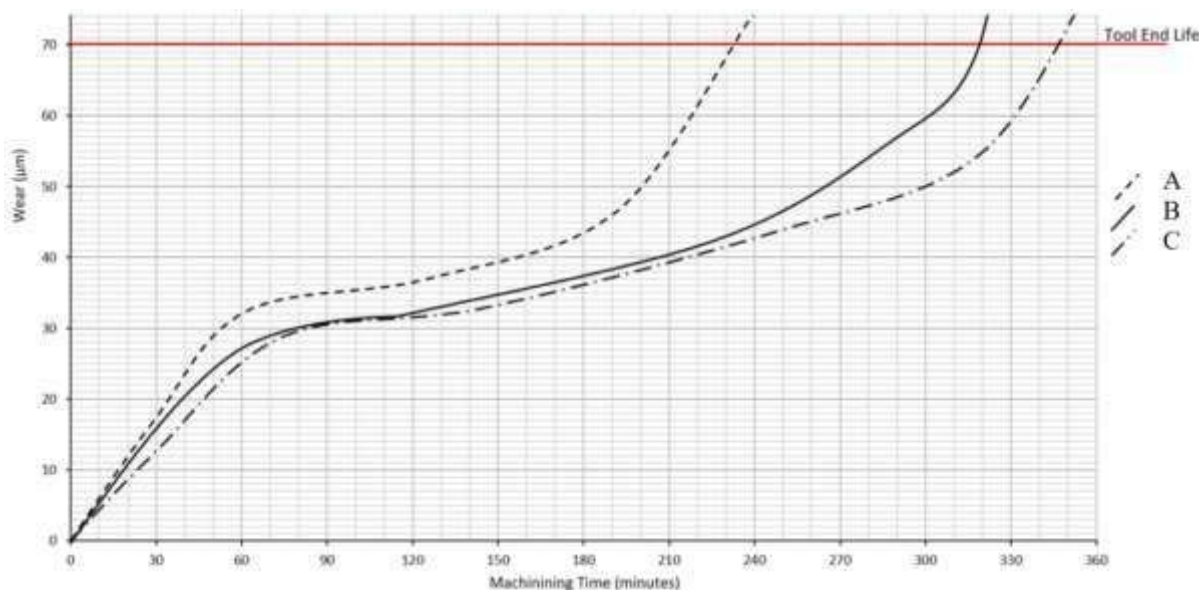


Figure 4-8: Tool Wear Curves

Table 4-4: Average Tool Life for Carbide Grades and Material Properties of Carbide Grades

Carbide grade	CARBIDE A	CARBIDE B	CARBIDE C
Average tool life (minutes)	240	315	350

After testing was completed, the tools were prepped for observation under SEM. This was to observe the effect that three-body abrasive wear has on the microstructure of the cemented carbide and to determine which properties might be causing the failure of the tool. This was done by mounting the tested tools in resin, and polishing and etching the worn area so that a decent image can be taken of the grain structure around the worn faces and tool tips. These samples were then observed under the SEM in the clean rooms at the Optical Research Centre (ORC) in Southampton. From these images, observations can be made of how the grain has deformed after the tool life has been reached. Figure 4-9 shows the images taken of the three carbide grades when unworn by the machining process. These images were used as a reference point to make a series of initial observations, such as the grain density and grain size. As can be seen in Figure 4-9C, carbide C has a very fine grain structure that is tightly packed, while the other two are medium and mixed grain carbide for A and B respectively.

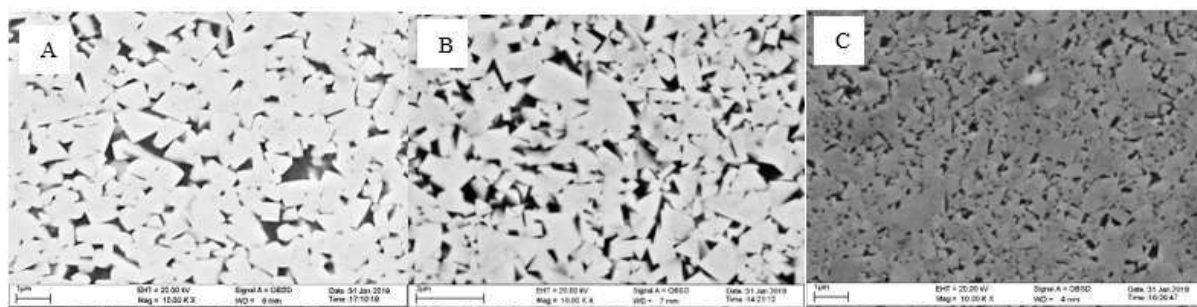


Figure 4-9: Unworn Carbide Grades Left to Right A, B & C

This disparity in grain size is very common for cemented carbide due to the sintering forming process which allows for it to be such a tailorable tool material. The crystal structure is what leads to poor grain tessellation especially at larger grain sizes, which in turn causes the brittle nature of the material. Figure 6-6 shows how the first grade of carbide resisted the tool wear. This tool shows the most transgranular fracturing, having entire rows of crystals sheared in a straight line ignoring the grain boundaries. This can be seen especially well in Figure 4-10B toward the top of the image.

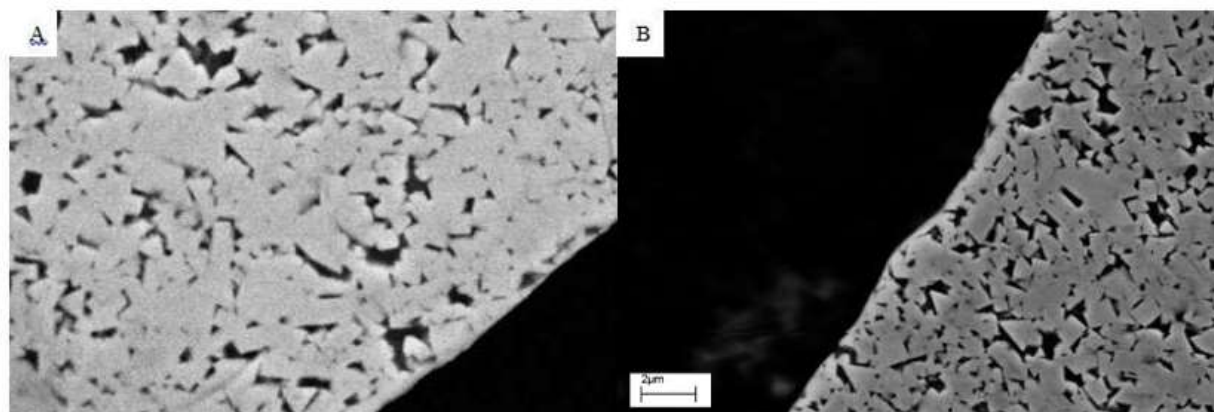
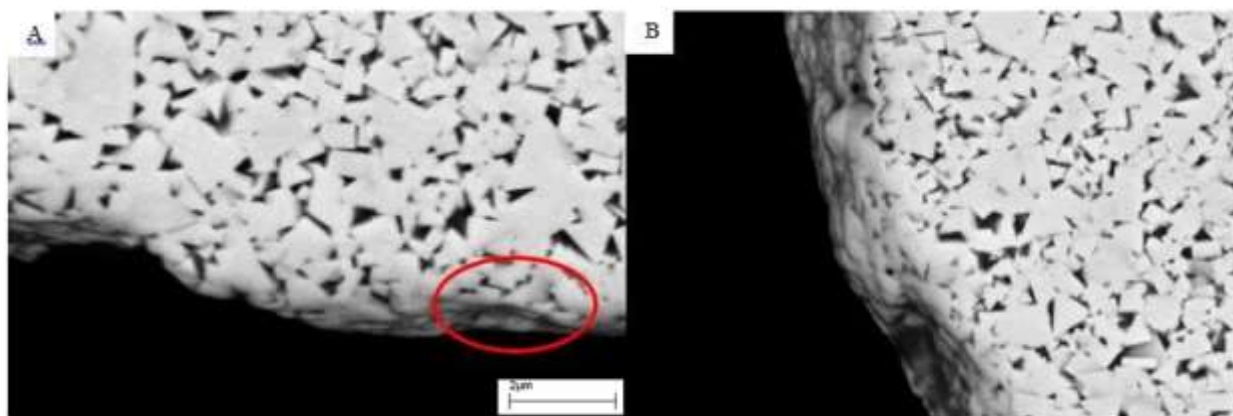


Figure 4-10: QBSD Images of Carbide a Worn Edges at 10 kX Magnification

This grade of carbide also had the shortest tool life by more than an hour. This form of fracturing happens in place of intergranular fracturing where the fracture follows roughly the grain boundaries of each crystal. This can be seen to be happening in some cases in both Figure 4-10 and Figure 4-11. This tends to happen more in materials where the grains align or the intergranular interactions are much weaker than the grains themselves, or when the material



removal mechanism provokes a reaction such as hard particle abrasion. The images of the tool edges reveal how the edge deteriorates and resists the forces of the machining process such as in carbide B, shown in Figure 4-11. This deformation is typical of abrasive wear causing the grain to round in some places. It also causes grains to break away, but where the grain breaks some of the grains break through their own boundaries. This again is transgranular fracturing and can be seen in the highlighted in Figure 4-11A.



*Figure 4-11: QBSD Images of Carbide B Worn Tool Edges at 10 kX Magnification*

This is a product of poor transgranular fracture toughness. However, most of the fracturing happens around some of the grains unlike the wear that occurs in carbide C. As can be seen in Figure 4-12B, the grains are compressed at the tool edge increasing the crystal density drastically. This is part of the forming process of the tool to harden the tool. This tool also had the longest tool life and highest transgranular fracture toughness. This is more than likely due to the hardened surface grain. In the area where the tool wear is more concentrated, the edge looks like Figure 4-12. This show much more intergranular fracturing along the edge than previously observed. The tools made from this grade of carbide failed due to localised chipping quite rapidly toward the end of its tool life whereas the other tools gradually developed a flank land slowly.

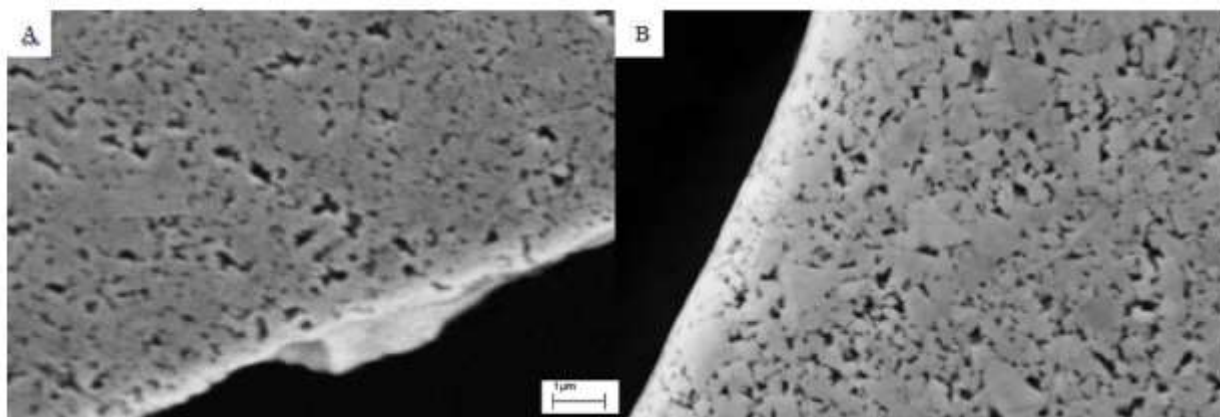


Figure 4-12: QBSD Images of Carbide C Worn Edges 10 kX Magnification

This shows that transgranular fracture toughness key to resisting the three-body abrasion that occurs during the machining of pre-sintered zirconia. This is more than likely due to the fact that individual crystals of zirconia can still be hard, especially in comparison to the hardness of a whole disc of pre-sintered zirconia.

#### 4.3.5- Discussion

The three carbide grades show fewer and fewer signs of transgranular fracturing from carbide A to carbide B to carbide C (left to right of Table 4-2). This points toward transgranular fracturing being the leading cause of tool failure. This further highlight that when machining pre-sintered zirconia, three body abrasion is the primary wear mechanism as these go hand in hand. Oddly enough, zirconia has a very high transgranular fracture toughness allowing it to resist three body abrasion itself (Antonov *et al.*, 2012). This resistance comes from the fine grain size of the C grade carbide. As carbide is a brittle failure material with a consistent grain structure, it minimalizes the amount of material that is removed with each removal of the tool edge. Carbide C grade tools failed in a slightly different way to the other tools. Most of the tools had a progressive increase in flank wear land growth to point of failure, as shown in Figure 6-3. Carbide C tools did this but much slower, then a small chip formed that rapidly propagated to point of failure as shown in Figure 4-13. This rapid propagation pointed towards this occurring due to the upper surface of this grade of carbide being harder, therefore once a

chink had been made in this layer the abrasion had two things going for it: the increased surface area and the softer material.

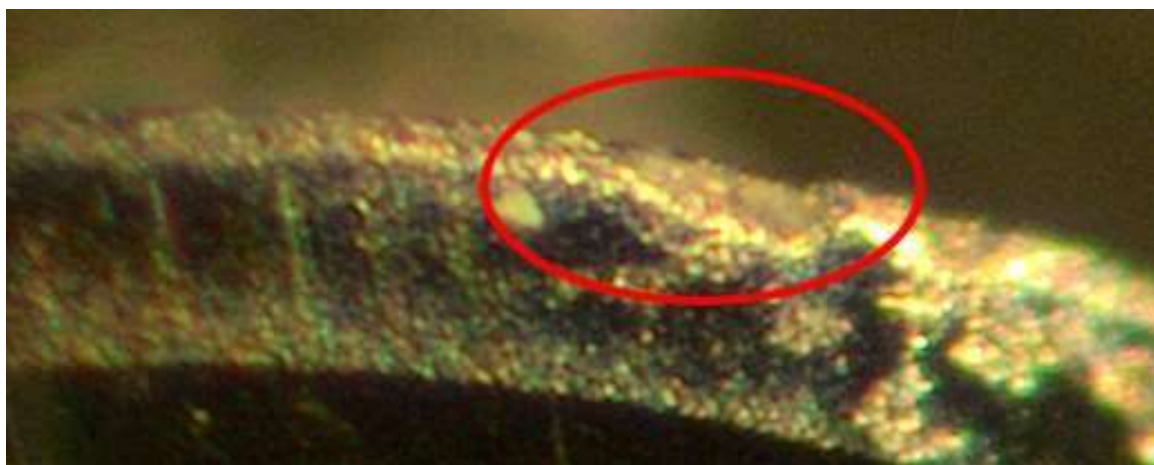


*Figure 4-13: Chipping on Tool Edge of Carbide C*

This information will be especially useful to tool manufacturers when selecting carbide for creating tools to machine pre-sintered zirconia and materials that cause the same wear mechanism. In addition, in many dental labs technicians are typically not from an engineering background and tool wear is not something greatly understood in the sector. This has led to many parts failing inspection as the worn tool fails to create an accurate fitting edge.

During machining, zirconia dusts could get entrapped between the tool and the zirconia surface to create a three-body abrasion effect. Such effect has caused two types of material fracture on carbide, namely transgranular and intergranular fractures. Carbide A and B with submicron grain exhibited higher transgranular fracture as compared to the ultrafine grain, Carbide C. While Carbide C exhibited lower transgranular fracture, it also experienced intergranular fracture. Carbide C, which had finer grains, had a higher hardness value. Hence, it was able to withstand abrasion caused by machining longer than any other carbide grades.

With the increased application of zirconia in digital dentistry, there is a need to have an in-depth understanding of the mechanisms of wear that are likely to happen as crowns and other restorations are manufactured. This is important from two perspectives: the manufacturer of

the cutting tools needs to provide a product that does not fail in operation, and the dentist needs to have confidence that the tools will remain intact and that the final crown meets the geometry they expect. Through SEM analysis and pattern of tool wear it was observed that the wear is third body abrasion, as theorised by other works. This is potentially problematic as only tooling with diamond coatings is likely to have the abrasive properties to withstand hard particle three body abrasion. However, further analysis of the fracture, including mean free path between grains, needs to be conducted to complete the analysis.

## **4.4- Machining Condition Manipulation**

This testing was done to analyse the effect that the various conditions have on the tool wear rate. The recorded data enabled additional analyses once the machining was concluded. This analysis, combined with observations taken during machining, allowed for a more in-depth investigation of the effect that the machining conditions have on the tool wear rate and other factors after the machining was concluded. This section outlines the method of testing for the various testing parameters conditions such as spindle speed, feed rate and cutter depth.

### **4.4.1- Method**

The process of this testing involves machining pre-set volumes of pre-sintered zirconia discs. This volume is pre-set instead of machining until the tool's end of life, to allow for more expeditious testing and a more controlled end point. This volume of pre-sintered zirconia was set to just over 0.4 m<sup>3</sup> which is equivalent to 4-disc 98x20 mm discs of pre-sintered zirconia. This volume was decided as it is similar to the amount of material needed to wear most tools past their end life in testing completed prior to this. The tools used are simple ball nose end mills to the specification shown in Figure 4-14. Both tools use the same geometry but have slightly different core materials that are of varying transgranular rupture toughness for tools A and B respectively. These materials were chosen for their differences in trans-granular rupture toughness to confirm if a reduction in force would reduce the dependency on the transgranular rupture toughness.

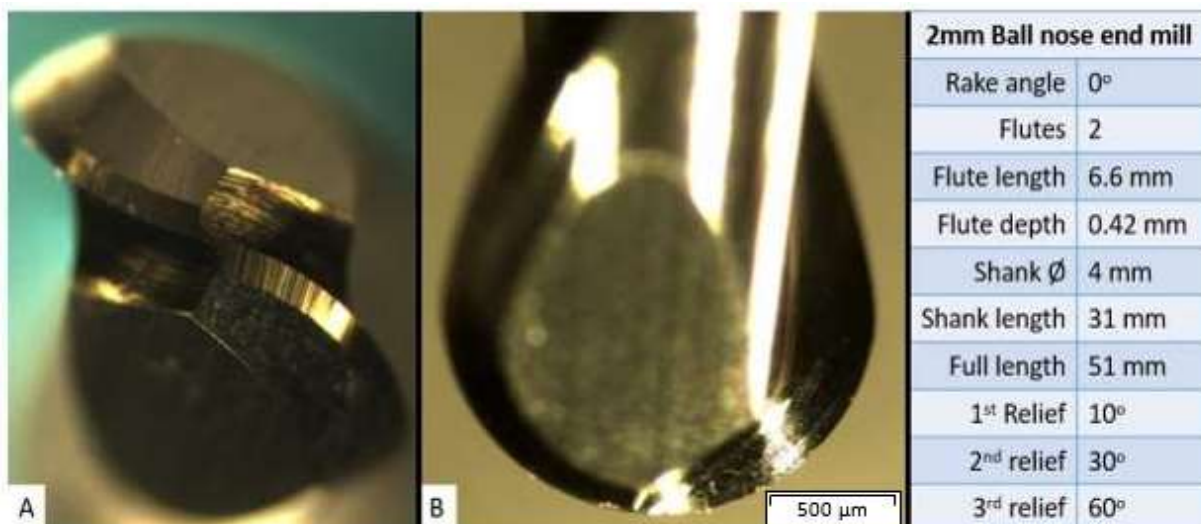


Figure 4-14: Ball Nose Tool Geometry for Tip (A) and Face (B) Along with Data

The machine conditions were divided into levels as shown in Table 4-5.

Table 4-5: Machining Condition Test Levels

Level	Strategy	Feed (MMPT)	Spindle (RPM)	$a_e$ (mm)	$a_p$ (mm)
1	Conventional	0.01667	16,000	0.6	0.6
2	Climb mill	0.05	20,000	0.8	0.8
3		0.08333	24,000	1	1

These conditions were selected for various reasons. While down milling has been shown to give better surface finish and up milling better tool life, this is still a useful condition to test against others. The depth of cut and step over were divided into 0.6, 0.8 and 1mm. As 1mm is the max work of the tool in both  $a_e$  and  $a_p$  for a ball nose end mill of this radius, 0.8 is the recommended working depth for general materials and 0.6 would be what is referred to as safe working depth used for harder materials than pre-sintered zirconia. Using the same values for both depth and width gave an easy insight by looking at the ratios between these two conditions. The two main conditions are spindle speed and feed rate. These two are little more complicated as many speeds and feeds are quoted for use in dental CAD-CAM. The upper-level spindle speed is set as the machine maximum at 24,000 RPM so no machining can be done above that speed. It is also stated in previous studies (Liu *et al.*, 2013) that higher spindle speeds on brittle

materials deteriorate the surface quality. The other spindle speeds were decided by reviewing previous testing done both here at the University of the West of England and by other research bodies. The machining conditions as laid out by Roland DWX-50 dental CAD-CAM instructional manuals have the RPM set to 24,000 for both 2mm and 1mm diameter tools. The lower level was extrapolated from this using like materials as some works found that lower surface speed assists in machining such materials, but with tools this size the RPM cannot be too low otherwise there is not enough force at the cutting edge to effectively shear the pre-sintered zirconia. The feed rate is manipulated in many works, however with pre-sintered being relatively new this is not overly extensive. A testing approach (Demarbaix *et al.*, 2018) uses feeds in the range of 0.006 – 0.09 millimetres per tooth (MMPT), which is one of the largest ranges used in the testing of machining pre-sintered zirconia. This is also one of the only works that is concerned with standard machining conditions in pre-sintered. This range was reduced substantially, mainly at the low end, as 0.006 MMPT equates to 192 mm/min at 16000 rpm which is too slow to be considered as production times would be very long; therefore, the low end is increased. This has led to a more production sensible 0.0125 MMPT. This is still slow but on the low end of what is acceptable for lead times in production. The high end is set at just below the 0.09 MMPT as the machine max was 4,000 mm/min and at 24,000 rpm that makes the feed 0.08333 MMPT, which was decided to be close enough to tested values at the high end. The middle level is simply taken midway between these two.

With these levels in mind, the experimental design was created to facilitate the testing of the machining conditions. If one condition was changed at a time it would involve more than 600 tests with each test run taking over a day each, which at minimum would have taken 2 years. So, a Taguchi style of design of experiment was implemented. This entails changing select factors in each test run so that each factor is tested against every other factor, so that the impact of each factor can be measured against the others. This experimental design was set out as

shown in Table 4-6. This layout of 36 test runs ensures that there are confirmative repeats of each condition, and each variable gets tested against each other variable. As each of these runs machines four discs of pre-sintered zirconia, some of these test runs took upwards of 14 hours so careful planning of these tests was needed which took more than 400 hours. As can be seen in Table 4-6, the first three test runs were repeated to confirm the stability of results at each level. From there onwards, certain values are changed to ensure that each variable's impact on the other variables is tested.

These test runs were done by mounting five discs of pre-sintered zirconia that are 98mm diameter and 20mm thick in the CNC router so that an 8mm pocket can be machined out off one side of each of these discs. The discs are then flipped and additional observations on the tool taken. The discs are flipped for two reasons: this allows for more samples when looking into the surface typography, and the ball nose end mills used have a flute length of 8mm and only a max cutting depth of 12mm. This leaves 4mm thickness between the two sides for rigidity to retain the integrity during further observations.

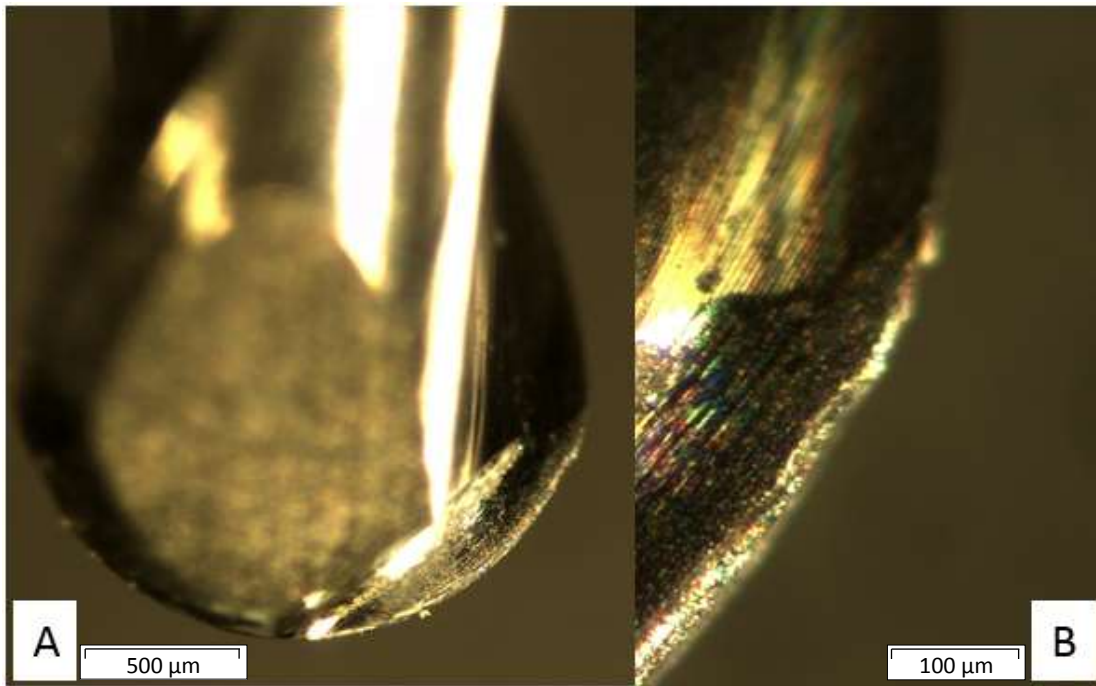


Table 4-6: Taguchi Design of Experiment for Condition Manipulation Testing

Run	Tool	Strategy	Feed (MMPT)	Speed (SMM)	$a_p$ (mm)	$a_e$ (mm)
1	A	up	0.01250	100.53	0.6	0.6
2	A	up	0.04792	125.66	0.8	0.8
3	A	up	0.08333	150.80	1	1
4	A	up	0.01250	100.53	0.6	0.6
5	A	up	0.04792	125.66	0.8	0.8
6	A	up	0.08333	150.80	1	1
7	A	up	0.01250	100.53	0.8	1
8	A	up	0.04792	125.66	1	0.6
9	A	up	0.08333	150.80	0.6	0.8
10	A	down	0.01250	100.53	1	0.8
11	A	down	0.04792	125.66	0.6	1
12	A	down	0.08333	150.80	0.8	0.6
13	A	down	0.01250	125.66	1	0.6
14	A	down	0.04792	150.80	0.6	0.8
15	A	down	0.08333	100.53	0.8	1
16	A	down	0.01250	125.66	1	0.8
17	A	down	0.04792	150.80	0.6	1
18	A	down	0.08333	100.53	0.8	0.6
19	B	up	0.01250	125.66	0.6	1
20	B	up	0.04792	150.80	0.8	0.6
21	B	up	0.08333	100.53	1	0.8
22	B	up	0.01250	125.66	0.8	1
23	B	up	0.04792	150.80	1	0.6
24	B	up	0.08333	100.53	0.6	0.8
25	B	up	0.01250	150.80	0.8	0.6
26	B	up	0.04792	100.53	1	0.8
27	B	up	0.08333	125.66	0.6	1
28	B	down	0.01250	150.80	0.8	0.8
29	B	down	0.04792	100.53	1	1
30	B	down	0.08333	125.66	0.6	0.6
31	B	down	0.01250	150.80	1	1
32	B	down	0.04792	100.53	0.6	0.6
33	B	down	0.08333	125.66	0.8	0.8
34	B	down	0.01250	150.80	0.6	0.8
35	B	down	0.04792	100.53	0.8	1
36	B	down	0.08333	125.66	1	0.6

#### **4.4.2- Results and Analysis**

After the testing was completed, all tool wear was measured under a microscope across three surfaces: rake face, flank, and nose. Several images were taken for each test run using different magnifications, focal lengths, exposures, and shadowing. Only a few selected examples are shown in this chapter.



*Figure 4-15: Examples of Rake Face Microscope Image Capture A-4x Full Edge, B-11x Focus Wear*

These images were used to identify areas of high wear. In the case depicted in Figure 4–15, there is heavy wear toward the outer section of the edge along with abrasion across the rake face. This heavy wear is focused on under higher magnification, as shown in Figure 4-15B in order to identify the form of the wear. In this case it is uniform flank wear then a wide chip out of the edge. This is consistent with the tool life testing. Chip wear can be seen in Figure 4-16B which demonstrates an example of the relief faces post testing using the test run.

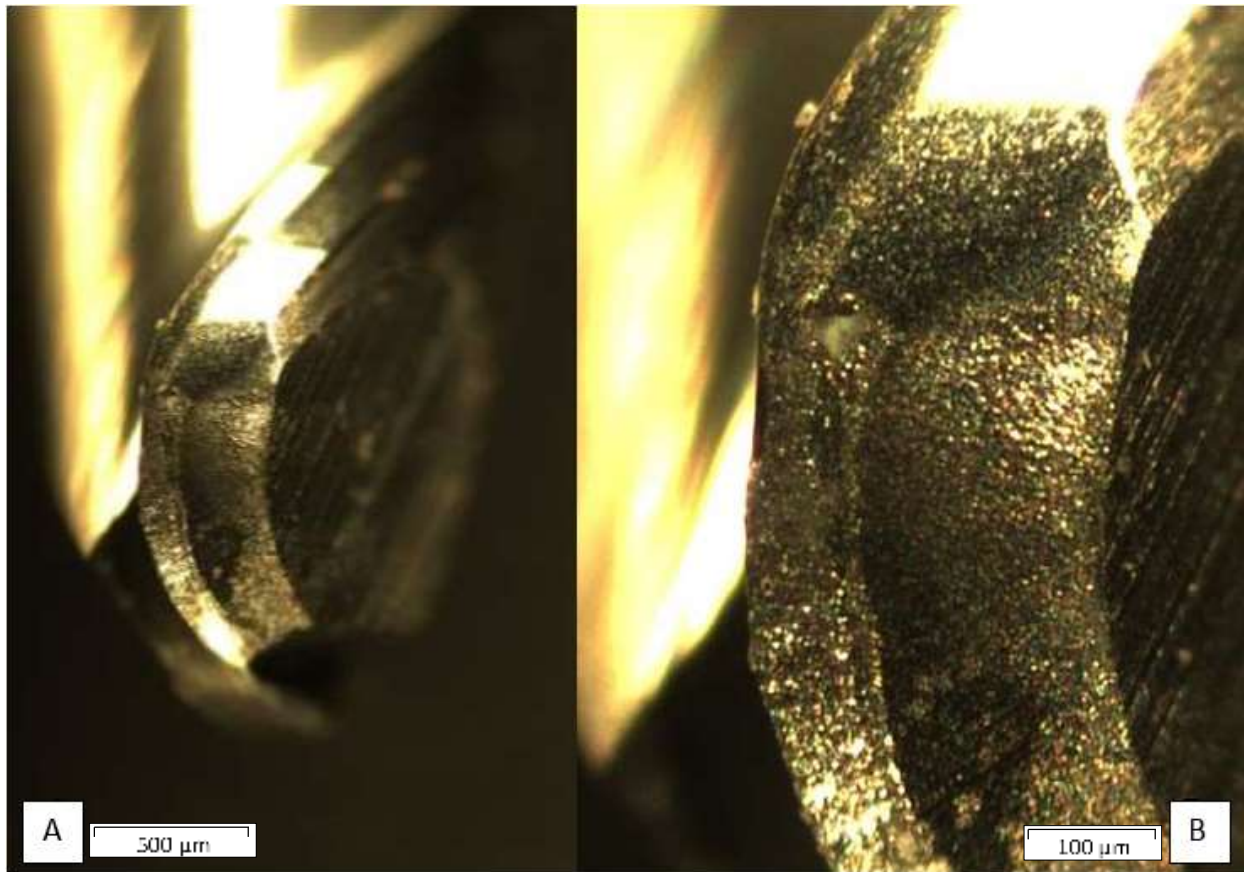


*Figure 4-16: Examples of Relief Face Microscope Image Capture A-4x Full Edge, B-11x Focus Wear*

These were used to check the relief faces for any additional wear forms or failure modes. They are also used to support observations and measurements of the flank wear from the images of the rake face. As relief faces receive an abnormally high amount of wear during the machining of pre-sintered zirconia, these images help to track how well the machining conditions control the removal of swarf from the cutting area. The images of the tip allow for measure of flattening of the nose which would be drastic for geometric accuracy. Images of this effect are shown in Figure 4-17.

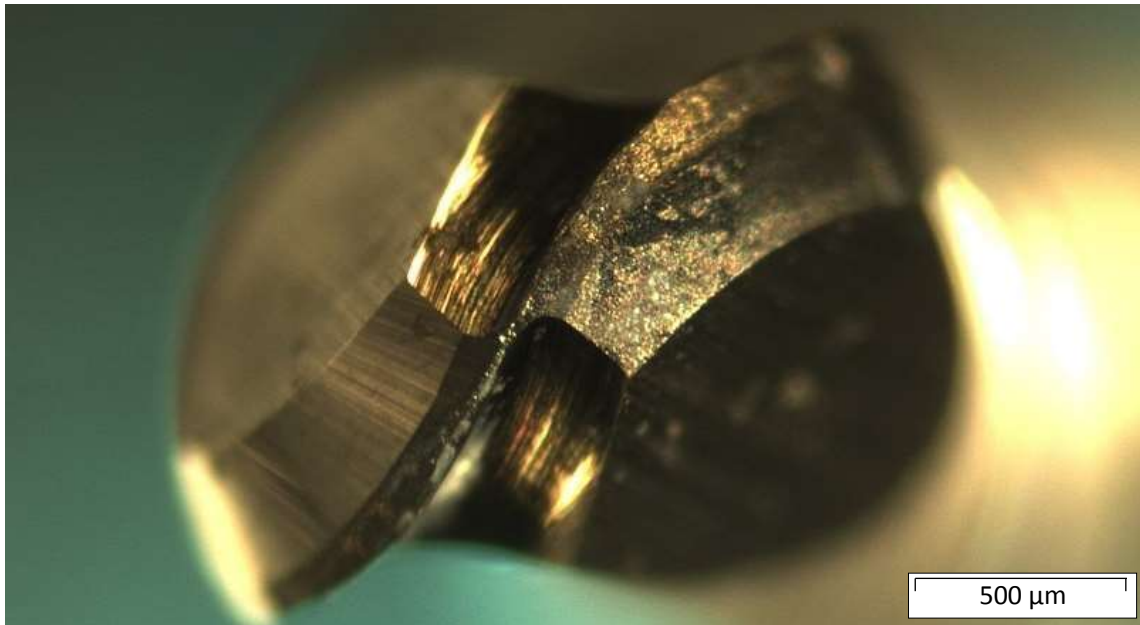


*Figure 4-17: Examples of Tool tip Microscope Image Capture at 4x*

Detailed in the rest of this section are the measurements and observations of the tool wear.

Table 4-7: Measure of Flank Wear for All 36 Test Runs

Run	Edge 1 ( $\mu\text{m}$ )	Edge 2 ( $\mu\text{m}$ )	Total wear ( $\mu\text{m}$ )	Average wear ( $\mu\text{m}$ )
1	72.67	30.02	102.69	51.345
2	81.59	21.95	103.54	51.77
3	75.6	26.38	101.98	50.99
4	79.07	11.05	90.12	45.06
5	38.39	24.45	62.84	31.42
6	72.14	48.66	120.8	60.4
7	58.1	24.45	82.55	41.275
8	78.35	7.94	86.29	43.145
9	62.85	13.01	75.86	37.93
10	55.3	35.71	91.01	45.505
11	28.08	20.03	48.11	24.055
12	50.05	38.79	88.84	44.42
13	51.31	41.27	92.58	46.29
14	66.96	58.92	125.88	62.94
15	136.17	27.36	163.53	81.765
16	45.18	42.06	87.24	43.62
17	66.51	23.01	89.52	44.76
18	88.1	6.2	94.3	47.15
19	47.19	23.59	70.78	35.39
20	55.72	12.92	68.64	34.32
21	38.16	166.3	204.46	102.23
22	52.63	15.41	68.04	34.02
23	66.91	58.92	125.83	62.915
24	50.19	36.82	87.01	43.505
25	51.52	21.37	72.89	36.445
26	70.37	1.12	71.49	35.745
27	75.4	12.61	88.01	44.005
28	53.66	12.92	66.58	33.29
29	62.84	27.03	89.87	44.935
30	53.26	18.1	71.36	35.68
31	65.4	15.75	81.15	40.575
32	69.88	24.69	94.57	47.285
33	72.95	31.6	104.55	52.275
34	74.83	5.08	79.91	39.955
35	84.13	3.97	88.1	44.05
36	69.04	43.82	112.86	56.43

Table 4–17 details the various measures of wear taken from the images. This data was put back into Minitab for statistical analysis and generated this means of means, shown in Figure 4-18.

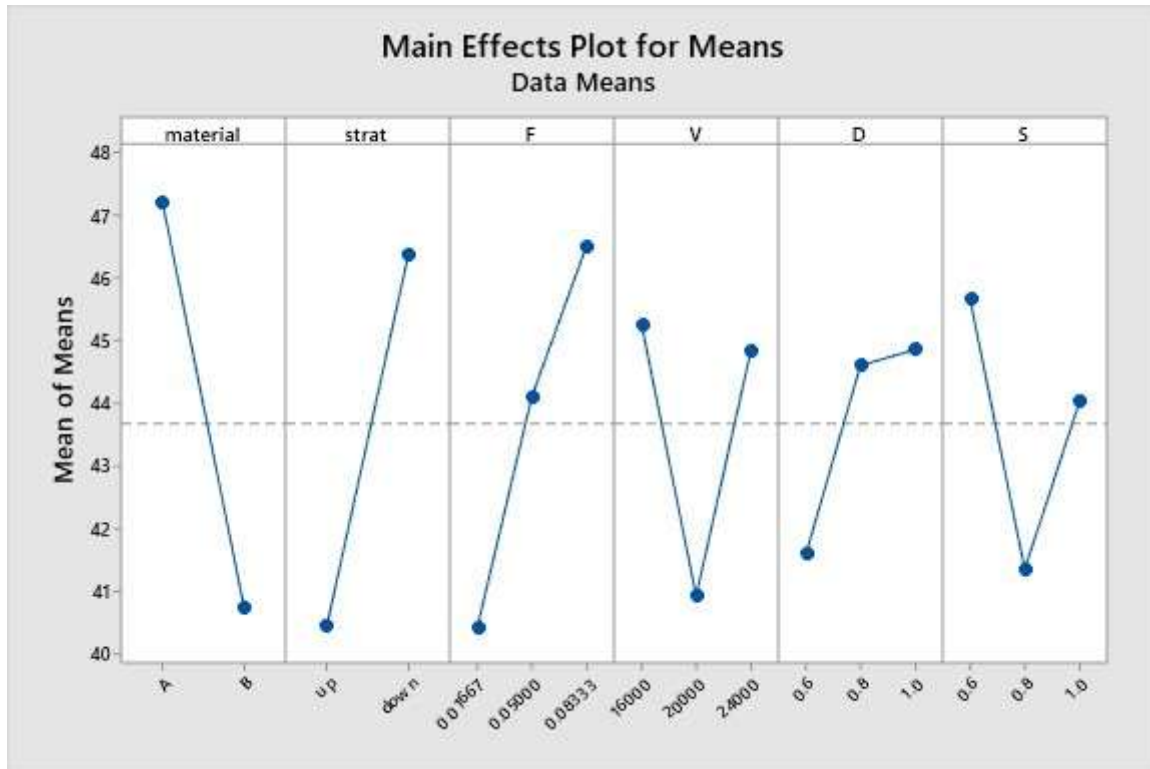


Figure 4-18: Mean of the means of tool wear for each machining condition

From this analysis we can reach the following conclusions.

1. For the tool material, (A or B) in all cases the lower the trans-granular rupture toughness, the lower the tool wear. This supports the previous experiment on tool material properties.
2. Up milling was indeed better for tool wear and there is a large difference between the two strategies, which is in line with metal machining.
3. Lower feed rate means lower wear rate. This however heavily affects the lead time of the part being machined.

4. Spindle speed has an optimal of 20,000 RPM or 125.66 SMM. This indicates that the optimal cutting force is within this range. A few brief test runs were done either side of 20,000 RPM at 21,000 and 19,000, and the difference in tool wear rate between these was the same in magnitude and direction. This points toward 125.66 SMM being the optimal speed.
5. Depth of cut is more complicated as the lower the depth the better, but the relationship is inversely exponentially related, with the start of the plateau just between 0.8 and 1 mm.
6. The step over is another condition that has an optimal of around 0.8 mm which makes sense as less step over does not reduce force but rather increases contact time, leading to more abrasion. However, when the step over goes past the 0.8 it starts to become over worked and swarf cannot leave the area properly.

The detailed analysis of the surface wear obtained from these experiments is described in Chapter 5.

#### **4.4.3- Discussion**

The use of the Taguchi method was necessary for the design of the experiment to keep the testing within a reasonable time frame, while still allowing for a comprehensive comparison between each variable. It also highlights the major contributing factors towards wear rate. From the analysis, the ideal operating conditions for the router while machining pre-sintered to attain minimal wear are displayed in Table 4-8.

*Table 4-8: Machining Conditions for Minimal Tool Wear*

<b>Tool material</b>	<b>Strategy</b>	<b>Feed (MMPT)</b>	<b>Spindle (RPM)</b>	<b>a<sub>e</sub> (mm)</b>	<b>a<sub>p</sub> (mm)</b>
B	Conventional	0.01667	20,000	0.6	0.8

This was interesting as many dental labs use 24,000 rpm as the standard spindle speed, due to recommendations from machine manufacturers. As spindle speed does not affect cycle time, changing this would be highly recommended. The rest of the results were standard for machining abrasive materials. The depth ( $a_e$ ) being lower would heavily affect the cycle time by reducing the affective cutting area. The affective step over ( $a_p$ ) of 0.8 mm is in line with general tool recommendations of 80% of the tool radius. While the lower the feed rate the lower the wear is true, and appears to have no lower limit, feed rate has the highest impact on cycle time.

#### **4.5- Chapter Summary**

The experimental method established in earlier work was adapted for specific investigation. The testing of the wear pattern backs up the hypothesis from earlier work that the wear is combined abrasion and third body abrasion. This comes from the waste material being very different to conventional waste material observed during the machining of more traditional materials such as plastics and metals. This makes the swarf harder to control, especially without the use of coolant to flush it away from the work area. Much of the wear is located on the relief faces, the tool tip and in craters along the edges.

The thermal forces during machining were found to not move away from the point of contact due to the low thermal conduction of pre-sintered zirconia. The temperatures just below the tool's point of contact were not high enough nor lingered long enough to enact changes in the material towards sintering. However, it should be noted that when higher temperatures are reached inside the machine, then the material build up rate is higher which can lead to faster tool failure.

Testing the machining conditions was a very lengthy experiment involving months of long hours that pushed the router used for testing to its limits involving much more maintenance



cycles than initially expected. The amount of data from this run of tests was very large and worth the time investment even with the extra time from unexpected delays. The aim of the analysis in this chapter was to discern the effect that differing machining conditions have on the tool wear rate and final tool life when machining pre-sintered zirconia.

The optimal spindle speed being around 20,000 RPM for the 2mm ball nose end mills instead of the 24,000 RPM used in some dental labs is something that was highlighted as a key finding, as it has little impact on the cycle time and a large impact on the wear rate.

This section was very intensive in both lab time and resources, however the data and observations from it allowed for the filling of key gaps in the knowledge base and reinforcing findings from previous studies.

## **5- Pre-Sintered Zirconia Work Piece Testing**

This chapter covers all the testing concerned with what happened to the pre-sintered zirconia when it was machined in the process of making dental restorations. It contains the analyses of the surface integrity and the thermal forces introduced into the work piece during machining.

### **5.1- Introduction**

After the tool testing, additional investigation could be done using the tools and test blanks from the various machining tests. These analyses consisted of changes in the workpiece during machining and changes in the surface of machined pre-sintered zirconia. The first analysis of the workpiece was how temperature permeates thorough the material during the machining process. If high heat was to reside within the stock for too long, then the pre-sintered material could begin to sinter. The machined surface analysis was done to investigate any difference between the optimal conditions for tool wear and optimal conditions for surface integrity. Poor surface integrity is what causes the machined parts in dental prosthesis to fail inspection, so a bad condition selection would cause the tool wear to be meaningless. This analysis was done through the tool's life as well to show the change in machined surface integrity as the tool wears.

Yttria stabilized zirconia (YTZP) data on these properties is presented in Table 5-1. This data is from the manufacturer's specifications and in-house testing where applicable. Pre-sintered data is usually not supplied by manufacturers as it is not in its end state, so some additional testing was necessary.

Table 5-1: Physical Properties of YTZP

Property	Units	Sintered YTZP	Pre-sintered YTZP
Density	kg/m <sup>3</sup>	6000	550
Hardness	HV	1600-1800	60-80
Fracture toughness	MPa m <sup>1/2</sup>	10	0.7
Flexural strength	MPa	1165.5	100
Tensile strength	MPa	620	N/a
Compressive strength	MPa	3985	N/a
Young's modulus	GPa	210	32
Poisson's ratio		0.3	0.3
Thermal conductivity	W/m K	2.1	1.2

The difference in these materials is not just apparent in these figures but also from just handling the material: pre-sintered zirconia is very smooth and holds a below-room ambient temperature, making it cool to the touch. The process of sintering pre-sintered zirconia involves heating the material at 1100 °C for 8 hrs or at 1500 °C for 6 hours, with a gentle increase in temperature at the start of the process and decrease at the end of the process. This stops the cermet from breaking due to thermal shock and can be done by simply leaving the work piece in the oven as it heats up and cools. The heating times change depending on work piece manufacture specification. This is due to what the makeup of pre-sintered zirconia is and what sintering agent is used.

## **5.2- Thermal Effects**

This testing was concerned with the temperature increase, due to heat transfer between the tool and work piece, which occurs in all cutting operations. This had to be tested because like with many other physical properties of pre-sintered zirconia, thermal properties are much more inconsistent than metals.

With this testing certain key parts of the process that were addressed:

- How much heat is transferred from the contact area away from the tool?
- How much of an effect do the machining conditions have on the temperature change?
- How fast does the work cool and how much heat is retained after?
- Does the extraction and air blast assist the cooling process?
- How much heat is taken away with the swarf?

The effects that machining conditions and the extraction have on the temperature, the cooling rate after the machining process and how much heat is retained, and how much the heat transfers from the tool contact area away from the tool (i.e., how far the thermal forces will penetrate the work piece) were all important factors to be considered. The testing was therefore designed chiefly with these factors on mind.

### **5.2.1- Methods**

During some machining testing, temperature readings were conducted both at surface levels and inside the workpiece. This was done in two separate ways, both detailed in the following section. The need for separate methods is that due to the poor conductivity of zirconia, the impact of heat deeper into the workpiece needed to be investigated.

The measure of the subsurface temperature was done using thermal couples inserted up through the workpiece at set levels to read the temperature difference at these distance from the surface.

As shown in the Figure 5-1, an additional thermal couple was set inside the CNC router to measure the air temperature.

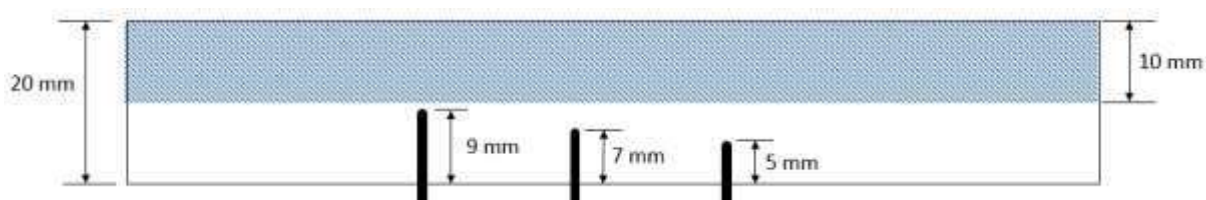


Figure 5-1: Thermal Couple Set up for Subsurface Thermal Testing

A series of cuts were then made to derive different information. The first of these was to face the pre-sintered zirconia workpiece down by 10mm to 1mm above the highest thermal couple, as shown in Figure 5-1. This was to measure how temperature would build in the material through the machining process and how far thermal forces would penetrate through the zirconia.

The second series of tool paths was to machine 2mm wide slots in a block of pre-sintered zirconia, as shown in Figure 5-2. Each of these slots would be machined at different feed rates and spindle speeds. The thermal couple probes were inserted to be 2mm below the finish depth and for each slot probes were put in the channels next to the slot to record the temperature spread in the horizontal direction as well.

Table 5-2: Speeds and Feeds for Slot Milling of Temperature Tests

Slot	Spindle speed (rpm)	Feed Rate (mm/min)
1	20000	1000
2	17000	1000
3	22000	1000
4	20000	600
5	20000	1400
6	24000	2000

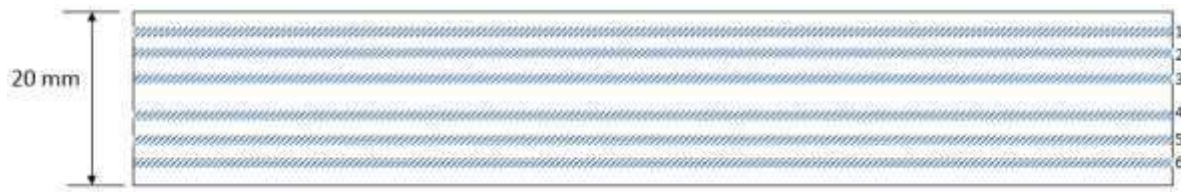


Figure 5-2: Set up of Slots for Condition and Thermal Forces Testing

The surface temperature was observed via infrared camera during a machining operation run at the same conditions as the subsurface testing. Following a test memo from Prima Dental, the heat radiated in a comet like fashion with temperatures of 473 K.

### 5.2.2- Results and Discussion

The temperature was recorded in real time in a Pico log, and is shown in Figure 5-3

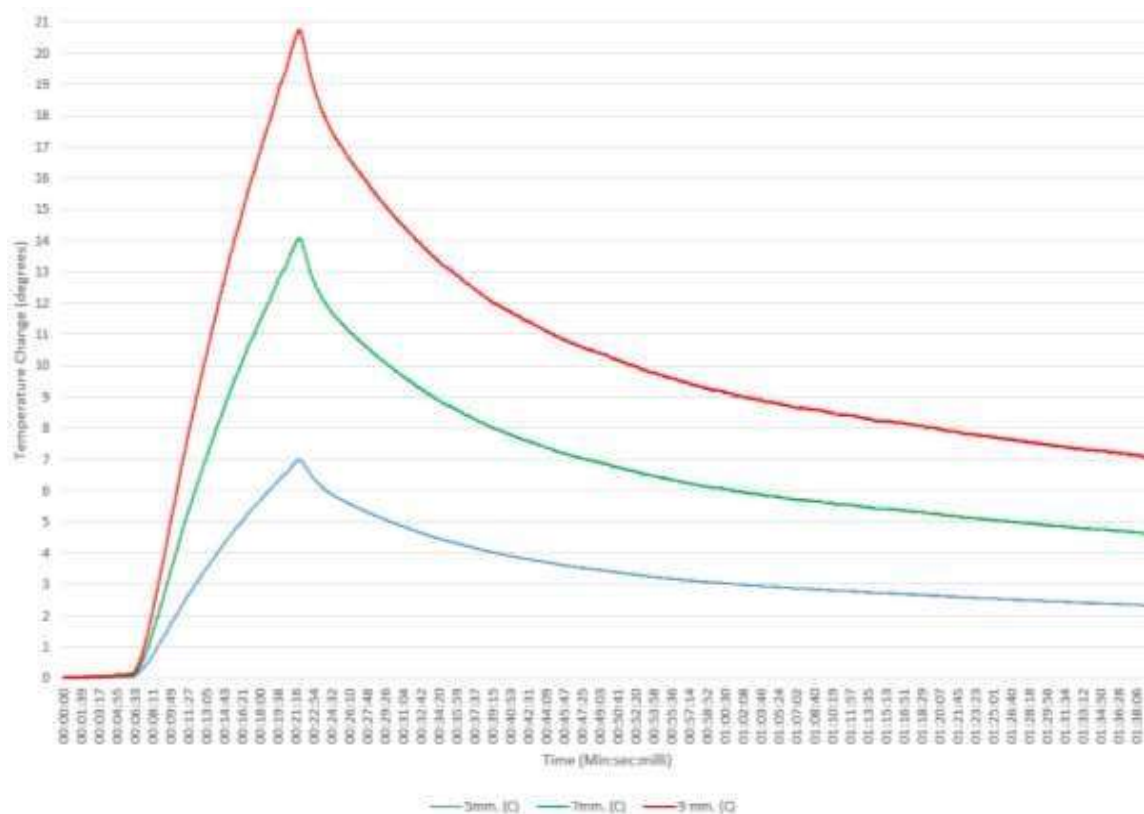


Figure 5-3: Sub-surface temperature readings across time

As shown in Figure 5-3, the thermal forces do not penetrate through the work piece in any great degree, as the work piece tends to only heat up with the air temperature. This was due to the low thermal conductivity of pre-sintered zirconia.

However, the heat at the point of contact it is quite high and directly under the tool. So, for heat penetration peak temperatures were recorded in Table 5-3. This shows the sub surface temperature does not penetrate very deep; even at its highest, it is 15 degrees lower than just under the surface.

*Table 5-3: Peak Temperatures for Probe Height*

	Probe height			
	9 mm	7 mm	5 mm	air
Peak temperature (K)	324.6	319.3	309.7	308.8

Each of the test runs were very quick, but during preliminary testing one longer machining operation was conducted to observe the temperature increase over longer time. This showed that in general, the workpiece temperature would increase at the same rate as the air temperature inside the machine until the tool passed over the thermal couple. At this point, the heat would increase moderately then decrease slowly as the tool moved away. It should also be noted that while extraction doesn't reduce the temperature at point of contact, it does reduce overall ambient temperature slightly while also removing the waste material. This is the key component to improving the machining process, as while the temperature is not high enough to begin the sintering process, it is enough to cause surface welding in small amounts. This phenomenon can be very problematic for many reasons: it changes the geometry of the tool and can lead to sudden edge failure from build-up edge (BUE) wear.

There is also the chance of the small particles "re-joining" the machined surface; however, on inspection, this seems to either be non-existent or unnoticeable. Forcing the waste material away from the cutting area will reduce build up on the tool, however during preliminary testing extraction had little effect on tool wear. Taking the Prima Dental tests into account, the

temperature difference between the point of contact and 1 mm beneath the point the contact was 148.4 degrees, which is a large difference for such a small distance. The tool does not dwell during machining though, so with a material that has as low a thermal conductivity as zirconia does, the tool would have to dwell to transfer its contact heat through the workpiece. For this reason, and for the sake of the tool as carbide does not like to dwell while the spindle is on, dwelling would not be advised.

### **5.2.3- Discussion**

The temperature appears to not penetrate the material at all, however there is still high heat at the surface where the material is removed and in the air around the workpiece. This will firstly increase the work for electrical parts such as the spindle motor. It also affects the material that has been cut away; it was noted that during long operations when the temperature inside the machine gets high, the swarf binds to surfaces in higher frequency and volumes. So prolonged machining will have an adverse effect on tool wear and the condition of the router unless proper cooling and shielding are implemented. Shielding is achieved thoroughly in most dental routers. Cooling, however, is a more difficult problem as due to the permeability of pre-sintered zirconia, any liquid coolant will be absorbed into the work piece. This permeability is why coolant is not used for swarf control during the machining process. Air blasts and extraction help somewhat, but they mainly help to disperse the heat rather than lessen it. To cool the work environment inside the router, a heat pump combined with the air blasts could work but further investigation would be needed. However, the temperatures recorded inside the machine and at the tool workpiece contact point are not enough to enact permanent change in the material towards sintering, but could explain the surface welding of the waste material on to the tool that occurs during long machine processes.



### **5.3- Pre-sintered Zirconia Surface Analysis**

This section is a compilation of the surface analysis of pre-sintered zirconia after the machining process.

#### **5.3.1- Introduction**

Surface integrity is linked to tool wear, thus tracking it is very important if the finished part is to maintain a uniform marginal fitting edge. Surface integrity however is related to many surface imperfections on a macro level, such as: surface roughness, cracking, discoloration, and introduction of foreign material. Many micro level integrity defects such as phase change, porosity, recrystallizing layer can also be present. As a consequence, these surface imperfections could lead to failure modes such as fracturing, chipping or fit interference.

Surface integrity can be thought of as a classification of one of the conditions of a material after being manufactured in some form such as: grinding, forging, forming, or cutting (Davim, 2010). Understanding how materials respond to the applied manufacturing process has aided manufacturing in producing parts with high tolerances. Ensuring that high surface integrity is maintained has become essential in today's products, especially wear resistant ones or products where the interface between two surfaces is critical. The study of surface sciences originates in the 19<sup>th</sup> century so is well understood and standardised.

Zirconia, being a ceramic, has a fragile relationship with surface integrity. The material is capable of a very smooth surface topography, but it can fall part with the slightest fracture, such is the brittle nature of ceramics. In most cases, zirconia manufactured for medical and dental purposes is machined then sintered. If the surface integrity of the pre-sintered zirconia workpiece is too damaged by the machining process, the thermal stress of sintering will cause heavy fracturing. A few heat treatments methods can reduce this damage (Kurtulmus-Yilmaz and Aktore, 2018), but the best solution is to not cause it in the first place. In most cases, the

loss of surface integrity first presents as surface roughness. Even this form of integrity loss can cause problems in the field of prostheses, as the accuracy of the marginal fitting edge is crucial to the finished product.

Any loss of surface integrity can lead to fracturing of the part during finishing or use. This can be seen in many forms of machining from conventionally milled aluminium to electrical discharged cemented carbide (Llanes *et al.*, 2004). Llanes et al and similar studies come to the same conclusions regarding how these surface imperfections cause micro-fracturing that registers as roughness in most cases. However, the severity of the of the integrity loss changes depending on material and conditions. A study was thus initiated to discover the effect that machining pre-sintered zirconia has on its surface. The aim was to determine how best to reduce any machining induced surface imperfections, so that the standards of the part created and of the manufacturing increase.

### **5.3.2- Method of Analysis**

For this analysis, a series of blanks were chosen at random from other experiments before they were machined in order to establish a base line for the surface topography. The topography was measured using a R<sub>Z0</sub> stylus. This uses a touch probe to drag across a surface over a specified distance, and the probe reads any change in height over this distance. If suitable recorders are used, the change in height is averaged over a set distance; this distance can be adjusted to meet circumstances and detect specific flaws (Esmaeilzare, Rahimi and Rezaei, 2014).

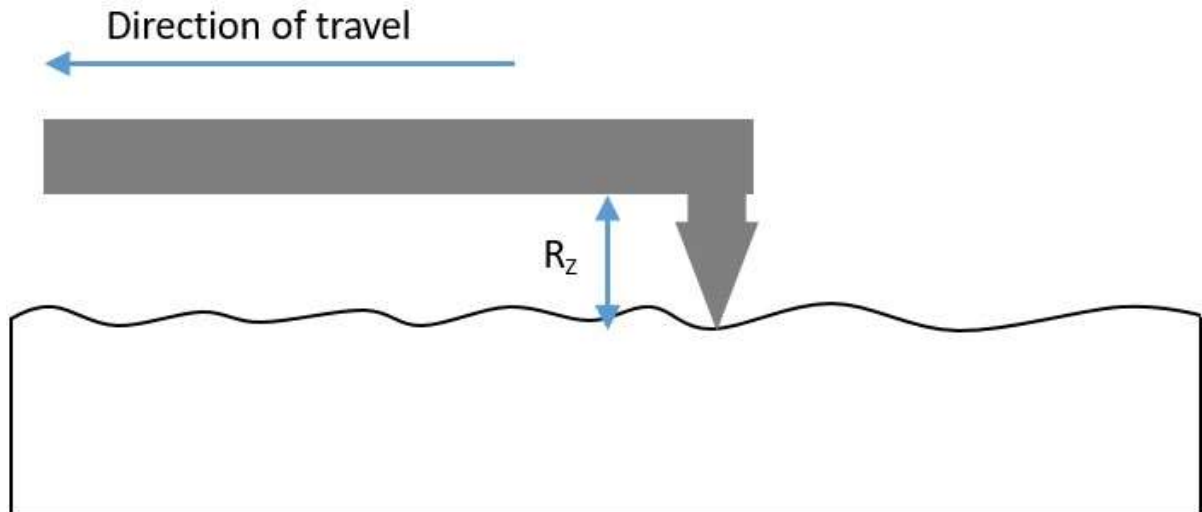


*Figure 5-4: Demonstrating Rz0 Stylus Set Up*

For this set of testing, a series of passes were done at the longest distance both in-line and with the cutter feed direction and across-the-cutter feed direction. In-line readings show how the surface integrity was affected at the bottom of the cut by the cutting edges closest to the tip, while across-the-cut shows the edge of the cut by the outer edges. The peaks of these edges should be consistent and solid if the integrity is high. When the integrity fails, the edges of the cut will be non-uniform where the micro fractures lead to cracking, much like with the failure of the marginal fitting edge when machining dental crown.

For the measuring of the surface roughness after the zirconia has been cut, the two main questions were: does the surface degrade as the tool does, and how does machining condition selection affect the surface roughness.

For the first question, a series of pre-sintered zirconia disks from previous tool wear testing were taken and selected sections measured for their surface roughness. The measurements and observations were taken between tool passes and programmed cuts and plotted on a graph. For the machining conditions analysis, this also used pre-sintered zirconia blanks previously machined in a tool wear testing the conditions as described in Table 4-6. For the measurements of this part, the test blanks were machined in such a way that readings could be taken of certain

parts of the run after the fact. Then a notch was taken out the side with a grinding wheel to allow the probe access to the machined face, as shown in Figure 5-1.

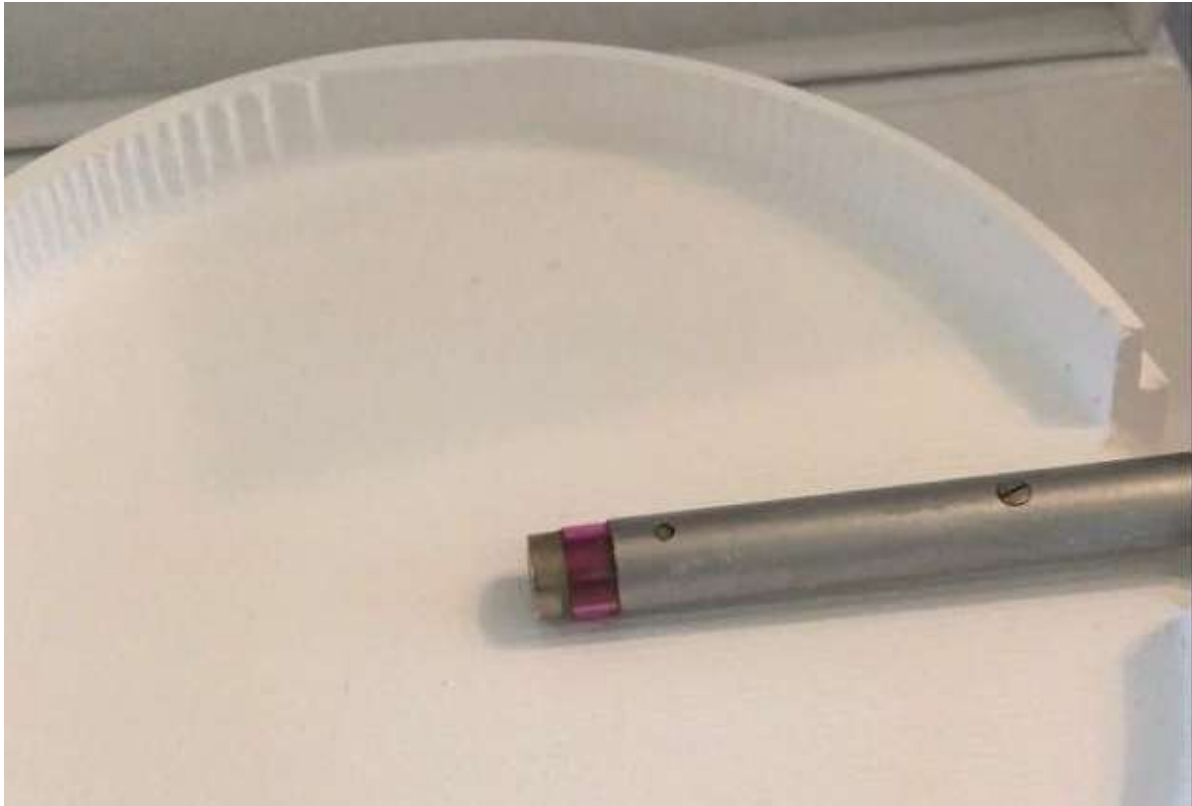


*Figure 5-5: The RZo Stylus on Machined Zirconia Surface*

Each test blank was specifically machined to allow for two surface readings per disc and eight readings per test run, with each reading interval at a volume difference of  $57,900 \text{ mm}^3$ . Measurements were then taken in-line with the cut direction and varying points across the direction of the cut. This decision was made so that in-line readings gave a measure of the surface roughness in the cut of each pass. The across-the-cut measures the peaks that occur from rough cutting with a ball nose end mill if the RZO was much lower than expected, while the surface roughness is higher in-line, it points toward the degradation of structural integrity at the wall as it has crumbled away. Any test run that had this result was flagged for further observations.

### 5.3.3- Results

Using the benchmark test runs from the design of experiment (runs 1-6), we can plot the tool wear against the surface integrity. For this surface roughness through the tool's life, it was averaged between identical material removal stamps and plotted in Figure 5–6.

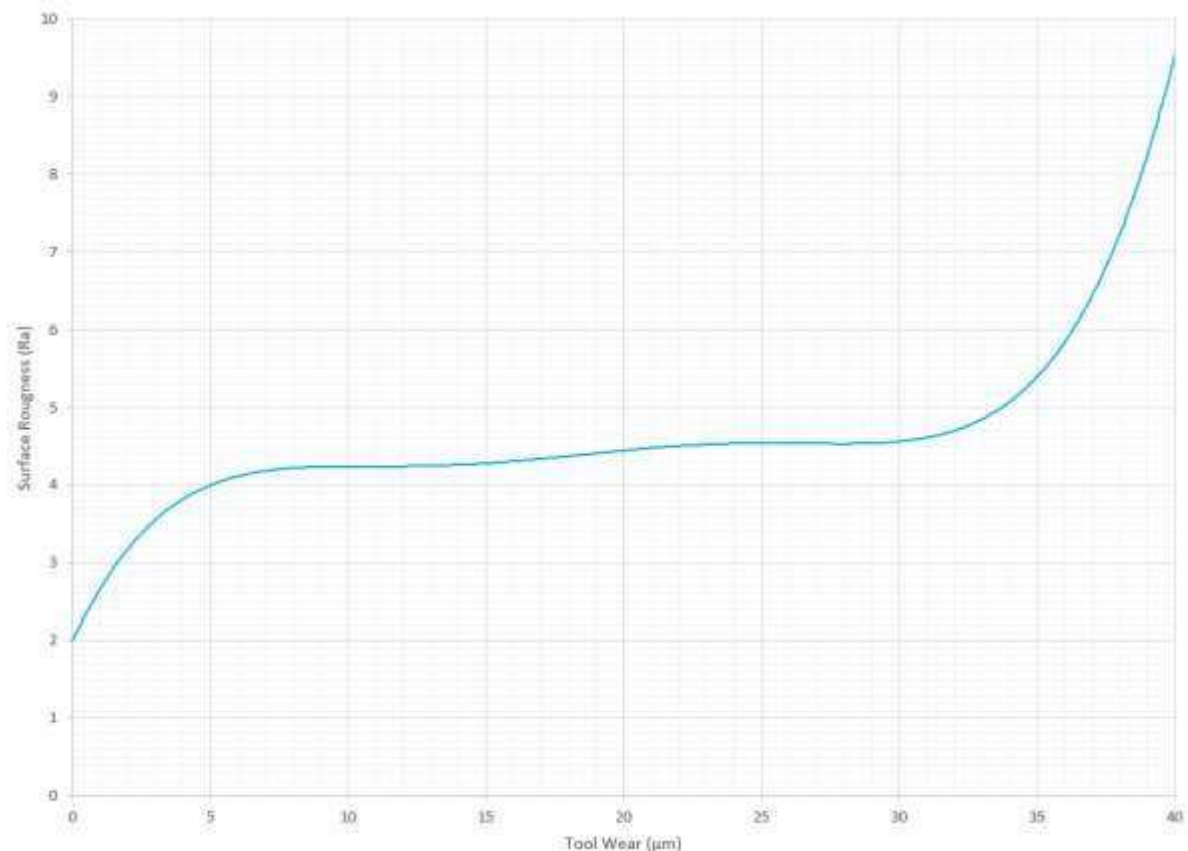


Figure 5-6: Surface Roughness Against Tool Wear

The initial rapid increase in roughness is the result of stock material being much smoother than any machined zirconia surface. The graph also shows that, as predicted, the surface integrity reduces as the tool wear increases. However, the integrity rapidly degraded until it reaches its failure point. This curve is very similar to the tool wear rate curve discussed in Section 4.2. This supports the assumption that tool wear and surface integrity are correlated.

To determine the effect that machining conditions have on the machined surface, the surface readings were fed back into the design of the experiment. The analysis generated the following

two graphs: one for in line with the cut direction (Figure 5-7), and one for across the direction of the cut (Figure 5-8).

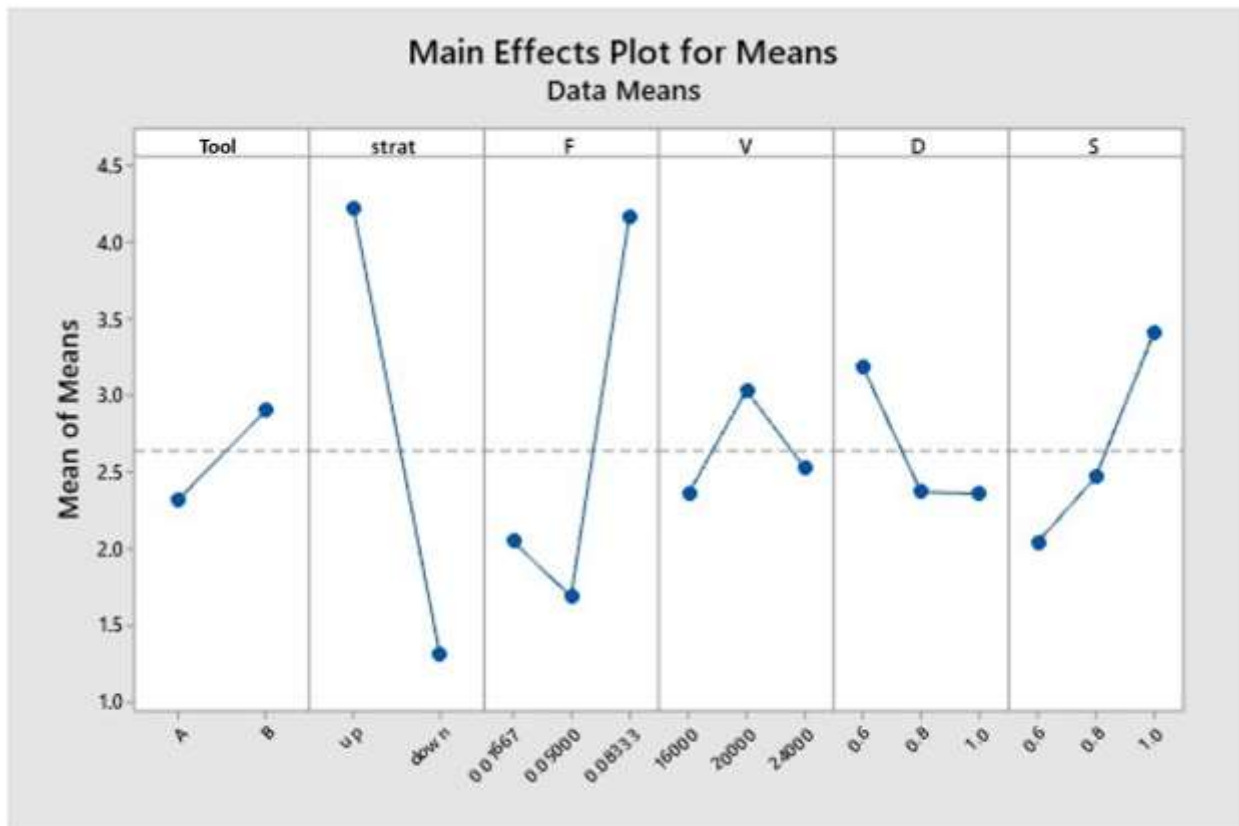


Figure 5-7: Mean of Means for Machining Conditions Against Surface Roughness in Line with the Direction of Cut

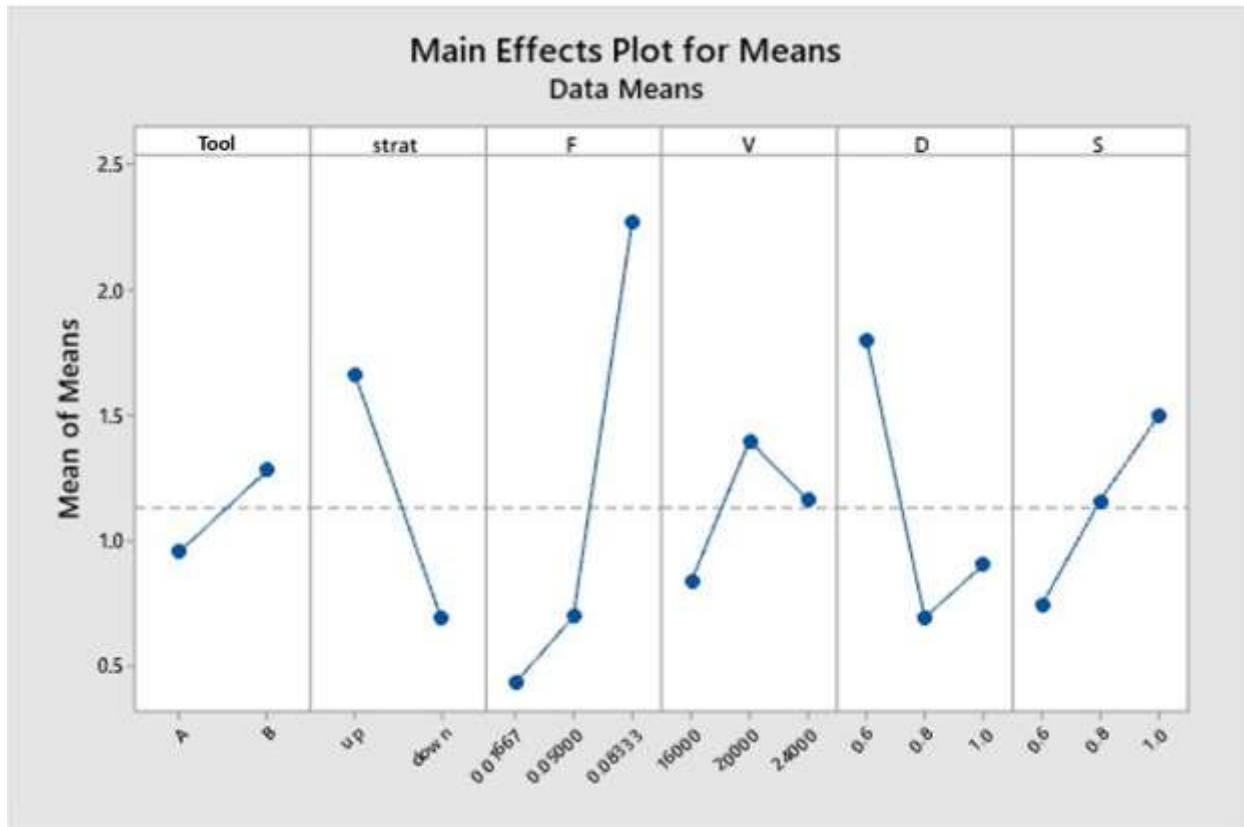


Figure 5-8: Mean of Means for Machining Conditions Against Surface Roughness Across the Direction of Cut

The tool material has minimal effect on the surface roughness; however material B does wear faster which led to rougher machined surfaces over time. The cutting direction, on the other hand, had a large impact on the roughness as down milling delivered a much better finish. The feed rate and spindle speed are optimal at 0.5 mm per tooth and 20,000 RPM respectively. For step over, the smaller the better in a linear trend. The depth of cut created a bit of an oddity: the effect it has on roughness in the cut direction gets better the higher the cut, plateauing around 0.8 mm. However, across the direction it has an optimal value around the 0.8 mm mark. The curve for the spindle speed also inverses for measurements across the cut direction.

This flipping in roughness in variation to these conditions was perplexing. Some explanations to this could be a weakening in the ridge of the cut causing breakage at these ridges, changing the average reading for the RZ<sub>0</sub>. These results should be discounted until further investigation can be done into the cause. However, if measurements across the cut should be used then a

typographical map should be created for an in-depth analysis; sadly, this could not be completed due to travel restrictions during the COVID-19 pandemic.

### 5.3.4- Discussion

*Table 5-4: Machining Conditions for Ideal Surface Finish*

<b>Strategy</b>	<b>Feed (MMPT)</b>	<b>Spindle (RPM)</b>	<b>a<sub>e</sub> (mm)</b>	<b>a<sub>p</sub> (mm)</b>
Climb Mill	0.02	16,000	0.8	0.6

As the results show, surface roughness increases with tool wear which was to be expected as with any machining process. However, for a material such as pre-sintered zirconia, when surface imperfections are introduced, they could quickly lead to failure at key areas of the produced part. In dental restorations, these would be the chips and cracks at the marginal fitting edge. This is how most parts that fail inspection present themselves.

The top three key contributing machining conditions have towards surface finish are the feed, cutting direction and step over. This shows that force could be the contributing factor toward surface roughness. This is consistent with the method with which material is removed, as if it is being smashed apart on very small scale. Another contributing factor is the size of the cut. If, with each rotation, the tool is cutting away a larger area, then more abrasive material is generated faster that in turn leads to more abrasion taking place. So, with more abrasion happening at each given moment it is more likely that some will happen on the workpiece.



## **5.4- Chapter Summary**

The first part of this chapter outlines the difference between sintered and pre-sintered zirconia along with some important information for any further work with this material. The work within this chapter discovered that the thermal forces from machining have little to no effect on the pre-sintered zirconia workpiece. This confirms that coolant is not needed outside of air cooling for the sake of the electrical components in the router motor and actuation. It should be noted that prolonged machining operations in excess of 30 minutes without tool rest do lead to high surface welding occurring on flute and relief surfaces, like that seen in Figure 4-4 (page 52).

On the other hand, the mechanical impact that machining has is significant. The surface integrity degrades as tools reach their end life, and certain machining conditions have higher impacts than others – mainly feed rate – which should be kept as low as possible. The tool material only has an effect as tool B wears quicker than tool A.

Therefore, conditions should be adjusted during finishing operations and tools should be changed before their end life is reached. This is especially true around marginal fitting edges and other areas of high tolerance, as poor surface integrity will lead to parts failing inspection, especially once subjected to sintering.

## **6- Tool Life and Optimisation**

This chapter covers the two major outputs of this research: the tool life equation and the optimisation assist. The tool life equation is used for determining the maximum recommended tool life based on the machining conditions. The optimisation tool is used to determine a set of conditions for machining pre-sintered zirconia with respect to wear, time, and surface finish.

### **6.1- Introduction**

Tool life and tool optimisation are two intertwined outputs of this work. Tool life equations are what allow for the estimation of tool life depending on certain factors for which Taylor's tool life is the basis. Optimisation is the balance between throughput and surface integrity and can take many forms, from an equation to tool assist. Both sections use data collected from all the testing through this doctoral work and some extra experimentation performed within the overall work, as well as some limited additional tests to validate these predictive measures. The first section concerns the tool life equation; its creation and related issues. The issues with the tool life equation derive mainly from the shift in material removal mechanism being different to conventional machining. Instead of the material being cut away in chips, it is more akin to being smashed away from the workpiece. The second section is concerned with the optimisation of the machining process to ensure the parts are made expediently without sacrificing the tool or the surface finish. It covers this process and supplies the data necessary to carry out optimisation and display how adjusting the machining conditions changes variables of time, wear, and surface finish. This process is a bit niche in application but is the starting point to transferring it to a digital format to allow for easy digesting by dental lab technicians.

### **6.2- Tool Life Equation**

The Taylor's tool life equation has been adapted many times to suit different circumstances. For this model, a modified version of the Taylor's tool life equation was used. This section

details how the constants of this equation are found and why this equation was used in place of others.

*Equation 6-1: Taylor's Tool Life Equation*

$$VT^n = C$$

Where V is cutting speed in metres per minute, T is tool life in minutes, and n is the tool material index. C is a constant, representing the cutting speed that would result in a tool life of one minute ( $C = V \times 1^n$ ). This constant is also sometimes referred to as CT or tool life constant.

### **6.2.1- Introduction**

Taylor's tool life is an excellent base from which to start the construction of a tool life equation as it is generally used for predicting tool life when deciding cutting speed. The main things that needed adjusting when concerning the tool life of machining pre-sintered zirconia are the tool life constant (CT) and an allowance for the third body abrasion mechanic of the wear. Both can be added into the existing calculation with little disturbance. The machining constant is derived empirically from data recorded from the various machining experiments detailed throughout this thesis. The wear mechanism was much more of an issue, as many tool wear equations are not designed for edge build-up or rely on chip thickness for the bulk of the equations, such as the Colding model. These types of models do not account for the material removal mechanism, and so the subsequent wear pattern falls outside the general purpose of these models.

The Colding equation is more accurate for general machining of conventional materials (Johansson *et al.*, 2017), but relies on chip thickness for generating constants. For this reason, the equation has not seen use outside of conventional materials that produce a consistent chip thickness. If used to predict the tool wear of machining pre-sintered zirconia, it will start to deviate from the actual tool wear rapidly. The Colding equation is too specific in its form of prediction and is not excellent at predicting anything that is slightly off model. Using base

Taylor's tool life is not advised as it is based on spindle speed having proportional relation to tool wear. Whereas with the machining of pre-sintered zirconia, the optimal spindle speed is very apparent, as the tool wear increases massively when the spindle speed moves away from optimum. Feed rate and depth of cut have a similar impact on wear rate.

However, Taylor's modified tool life equation is expanded to include more machining conditions:

*Equation 6-2: Modified Taylor's Tool Life*

$$VT^n f^a d^b = C$$

Sometimes written as:

$$T = \frac{C^{1/n}}{V^{1/n} f^{a/n} d^{b/n}}$$

where V is spindle speed in m/min, T is tool life in minutes, f is feed rate in mm/rev and d is depth of cut in mm. n, a and b are machining exponents that depend on condition and tool material that follow the general rule

$$\frac{1}{n} > \frac{1}{n_1} > \frac{1}{n_2}$$

This means that cutting speed has a greater effect, followed by feed, followed by depth of cut.

Determining these constants involves determining the relationship between these variables and the tool wear.

Determining the machining exponents involves plotting the log of tool life against the log of the variable for each exponent. The gradient of the line plotted is then used to find the machining exponents, as shown in Figure 6-1.

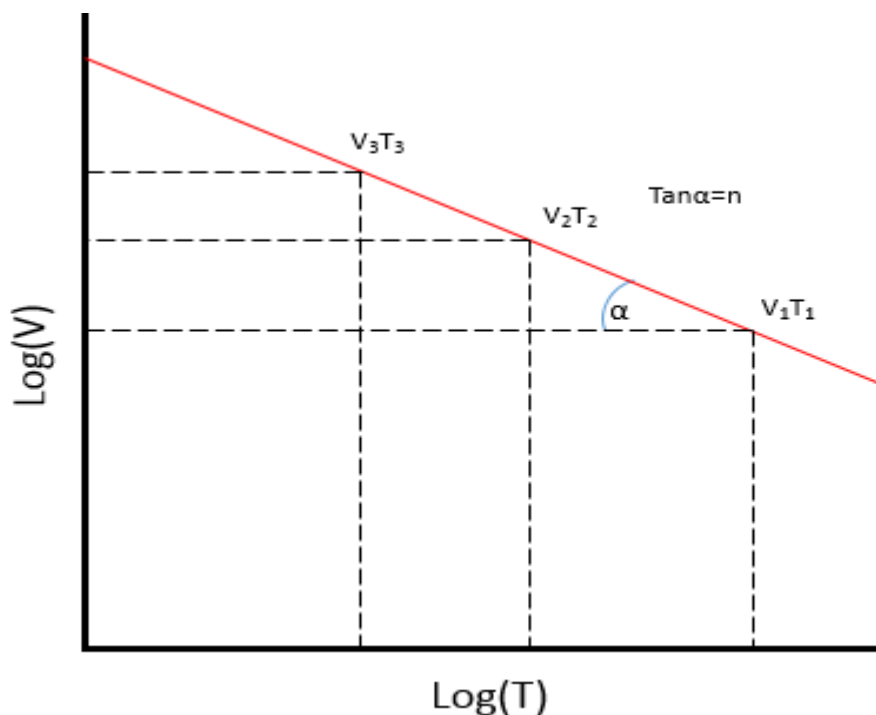


Figure 6-1: Demonstration of Determining  $n$  for Taylor's Tool Life Formula

These exponents were then used to determine the tool life constant ( $C$ ), by back substitution into the modified tool life with machining conditions and a known tool life from experimentation.

### 6.2.2- Adaption and Machining Constant

The machining constant is a material property that illustrates a material's ability to wear a tool as it is being machined. But firstly, the exponents for each machining condition must be found which is done by determining the gradient of the log plots for each variable. The log plots for the machining variables for feed rate and depth of cut are as follows.

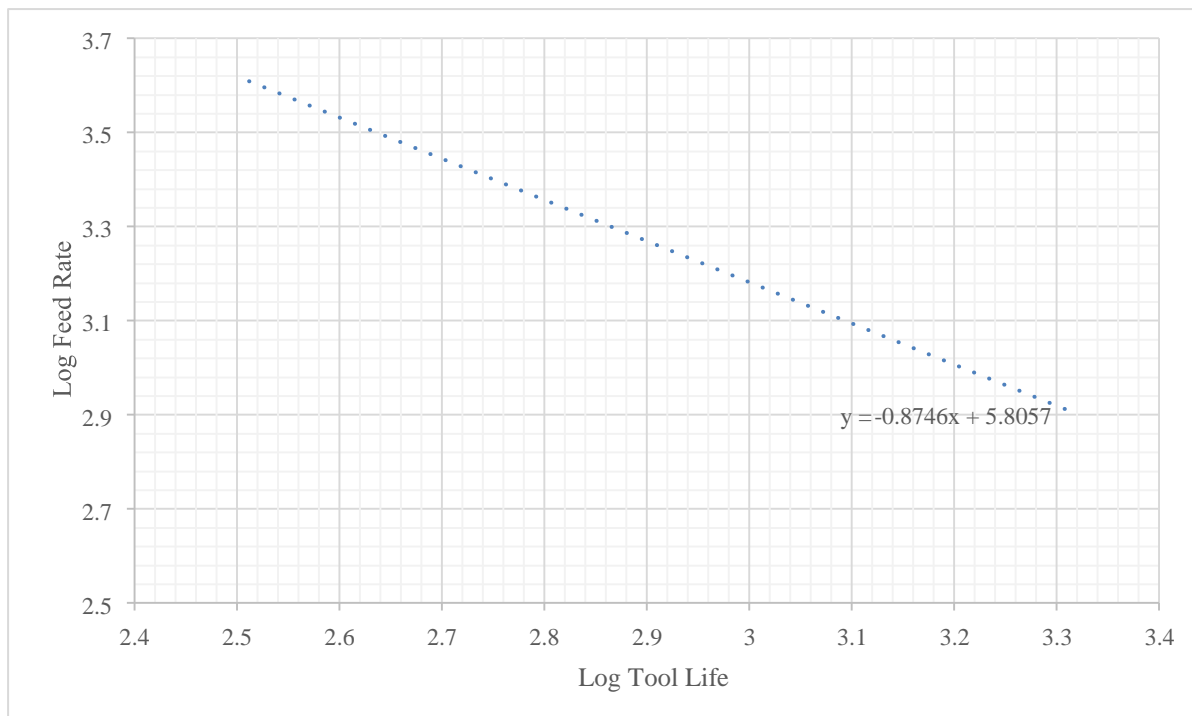


Figure 6-2: Log Plot of Tool Life Against Feed Rate

The machining exponents (n) being equal to the modulus of the gradient of the line. The feed rate being simple and linear in its log plot so the n value can be taken from the gradient of the line, and  $n_1$  is 0.8746. This is the same for depth and  $n_2$  is 0.7601.

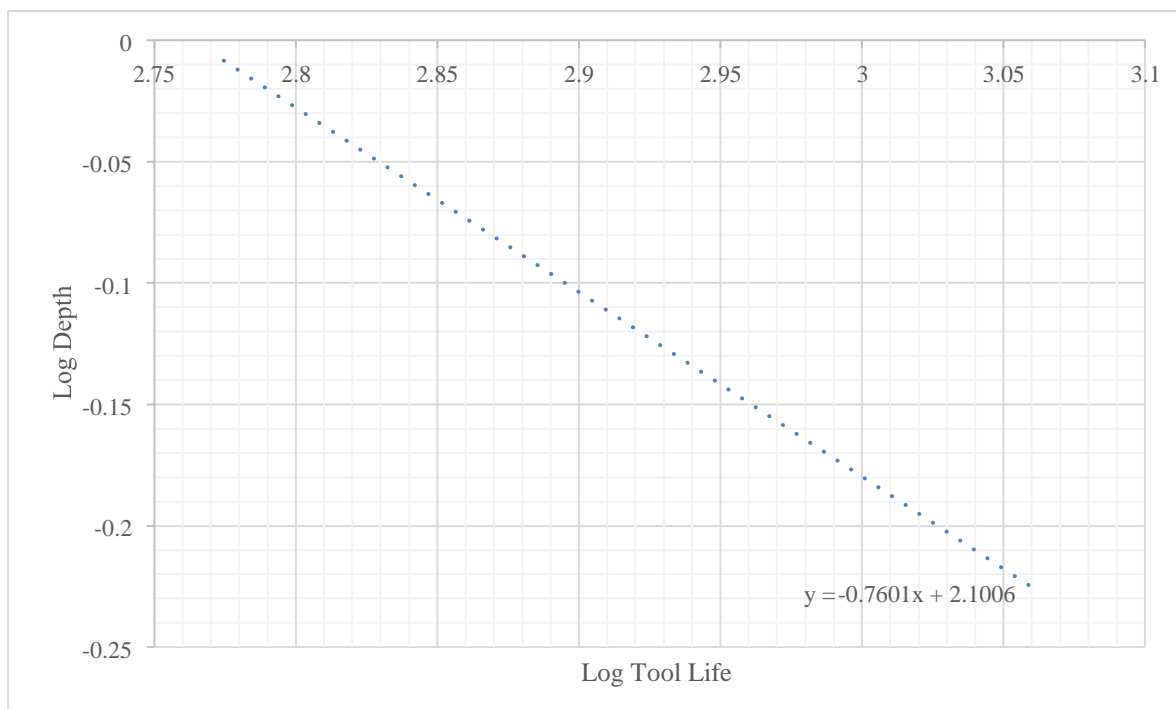


Figure 6-3: Log Plot tool Life Against Cutting Depth

There is an issue with determining the exponent for the speed variable. This variable has an optimum for tool wear while having minimal effect on time. This makes the line of graph different to the other variables.

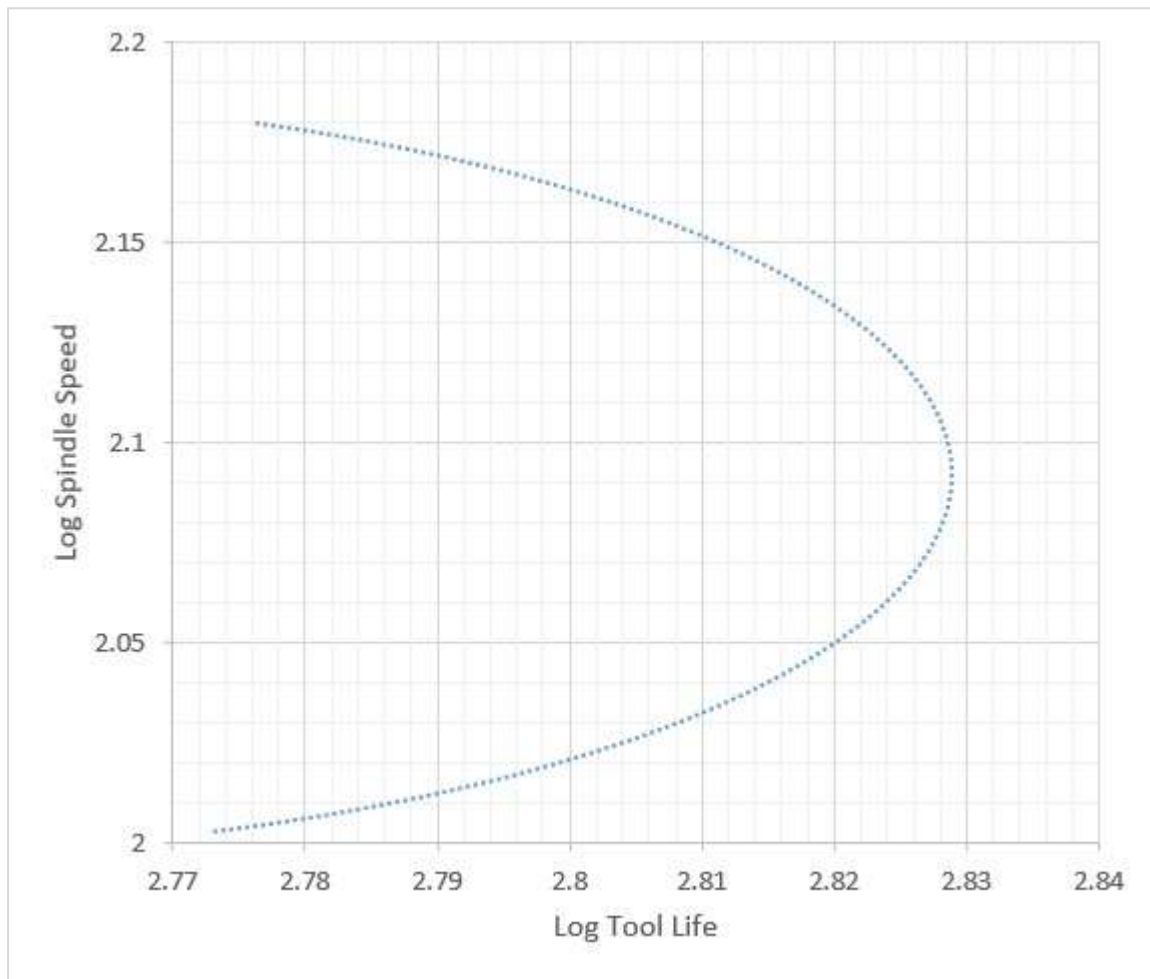


Figure 6-4: Log Plot Tool Life Against Spindle Speed

While this plot does not give an exponent like it normally should the tangent of the angle gives the gradient of the line so n can be expressed as a differential of the trend line for the log plots.

The equation for the log plot of the spindle speed is as follows:

Equation 6-3: Equation Log Tool Life, Log Spindle Speed Curve

$$x = -7.0638y^2 + 29.548y - 28.071$$

The differential of this equation is:

Equation 6-4: Differential of Equation 6-3

$$\frac{d}{dx} = \frac{1}{29.548 - 14.1276y}$$

Using this derivation as the exponent where y is the logarithm of the cutting speed V leads to:

Equation 6-5: Machining Exponent n

$$n = \frac{1}{|29.548 - 14.1276 \log V|}$$

Having this equation also allowed for determining of the optimum by solving the denominator for zero. The final modified Taylor's tool life equation would look like:

Equation 6-6: Modified Taylors Tool Life with Exponents

$$VT^{\frac{1}{|29.548-14.1276\log V|}}d^{0.7601}f^{0.8746} = C$$

Replacing with experimental values to determine C gives the following:

Equation 6-7: Determining Tool Life Constant

$$100.53 \times T^{\frac{1}{|29.548-14.1276\log 125.66|}} \times 0.8^{0.7601} \times 0.09584^{0.8746} \approx 2071.11$$

This equation does not consider the step over of the tool path, however step over has an optimum that is dependent on the design of the tool but would almost always be around three-quarters the tool diameter.

Table 6-1: Three Sets of Conditions and Their Corresponding Theoretical Tool Life

Feed	Spindle speed	Depth	Rake wear	Tool life (mins)
0.0125	100.53	0.6	51.345	406710815.6
0.04792	125.66	0.8	51.77	2.64994E+56
0.08333	150.8	1	50.99	49727.92605

These three sets of results show the huge variance in tool life prediction where the tool wear was fairly uniform. The second run especially was much too high.



This equation quickly fails validation. The reason for this is the non-linear relationship of spindle speed to tool life. Taylor's tool life was originally created with linear tool life relations in mind.

However, if the spindle speed is assumed to not change from its optimum then the tool life equation can be re-written to adjust for feed rate and depth and cut still. This adjustment follows the same structure of Taylor's tool life but with a different constant (C).

*Equation 6-8: Corrected Comparative Tool Life Equation*

$$Td^{0.7601}f^{0.8746} = C$$

Where T is tool life in minutes, f is feed rate in mm/rev and d is depth of cut in mm. It should also be noted that it only estimates the tool life, and this estimation gets very loose towards the extremes of machining limits, so should only be used for comparative analysis between two possible conditions. This equation however has inaccuracies and is very simplified. Further test data and possibly targeting experimentation would be needed. The equation created in this section can be used for quick comparisons instead of determining operating life.

## **6.3- Optimisation Assist**

Optimising the machining of a part becomes more of a rule of thumb in actual practice. This section lays out how adjusting the conditions affects not just the tool wear but the finish and time.

### **6.3.1- Introduction**

As with any production, there is always a balance of time, cost, and accuracy. With the machining of zirconia dental prostheses, the time to the patient and the delivery of an accurate part are both very important. The accuracy of these parts comes from the machining condition and the condition of the tool, so a balance must be found between leaving enough time to produce a decent part while not overworking the tool and delivering it quickly enough. A tool had to be developed so that the balance can be found to tailor to the needs of the dental lab.

### **6.3.2- General theory**

Balancing these factors for some machining conditions was easy, for example 20,000 rpm for a 2mm ball nose end mill (SMM of 125.66) gave the best surface tool life but the worst surface finish; balancing these machining variables for the desired outcome is the purpose of this tool. To achieve this, a series of steps are followed. The first step consists in determining which factors need to be balanced. In the case of machining the key factors are time, finish, and tool wear. The next step, as with any model building, is to simplify the problem by eliminating factors that have no or minimal effect on multiple factors. Another simplification is to find variables that have the same or similar effects in all factors and create a general rule for those variables. When comparing factors that counteract each other, we can consider the example of feed rate. For surface finish, a low feed rate is good, but a low feed rate is bad for time. This is the balancing act that optimisation tools allow for, giving an operator the ability to see what effect machining a part at higher speeds would have.

The data for this optimisation was collected from varying tests performed in chapters 4.4 (page 64) and 5.3 (page 84) for tool wear and surface finish respectively. The machining time was found by running each of the levels through a virtual CAM environment and noting the times which are then recorded on the graph (Figure 6-5). The tool path for this was similar to that used in wear testing, but the 8mm deep pocket was done in spiral pockets instead of zigzags to more accurately represent tooling paths used rather than for controlled testing procedures.

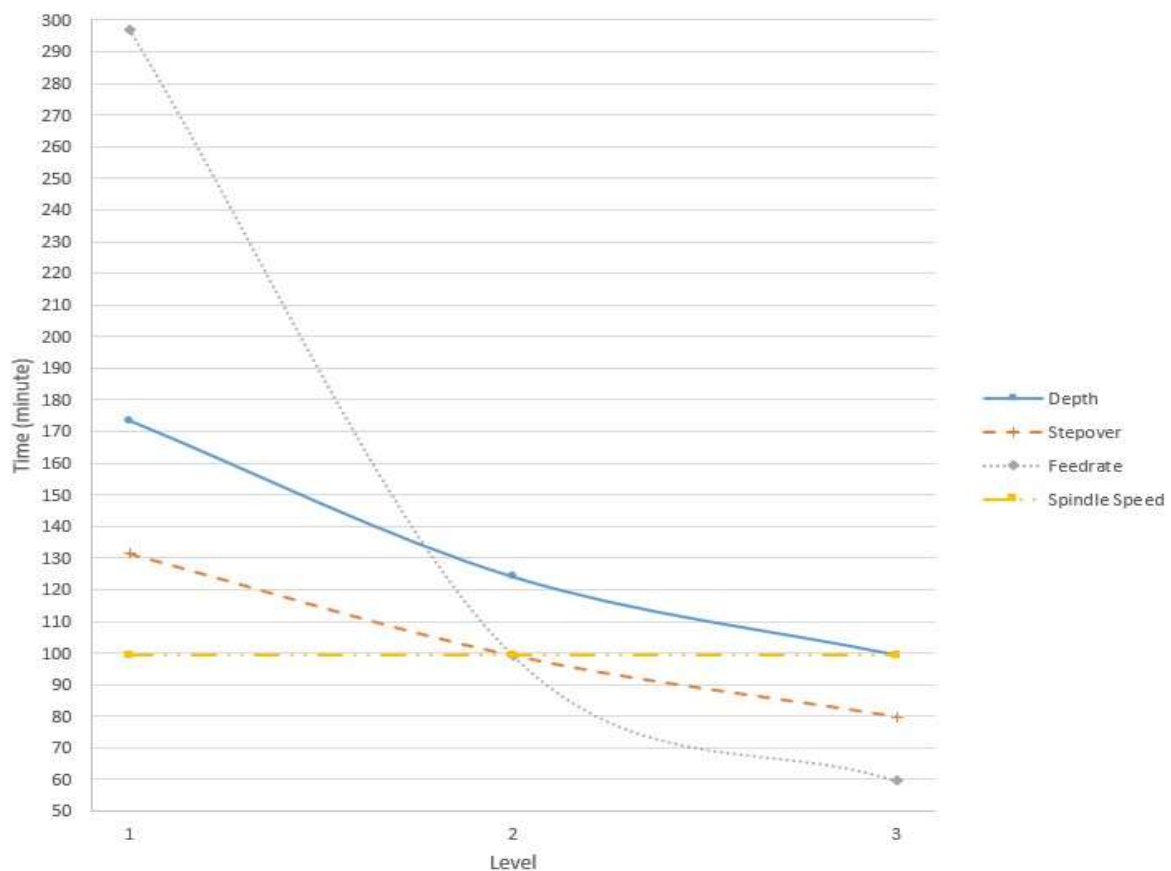


Figure 6-5: Machining Conditions Against Time

To keep consistency, the levels for this graph are the same as those used for the wear and surface wear tests and detailed in Table 4-5 (page 65), allowing for direct comparison. Tool material and cutting direction had no effect on machining time so were omitted from the graph. Spindle speeds appear to have had no effect on time but could have a very small effect as feed rate levels were input in mm per revolution, so there is a very small decrease in time with an

increase in spindle speed. Feed rate has the biggest effect on time and has a more exponential like relationship. While step over and depth have similar relationships, depth has a slightly greater effect than step over.

The following figures show how roughness and wear are affected by the levels, mainly the magnitude and direction of these relationships.

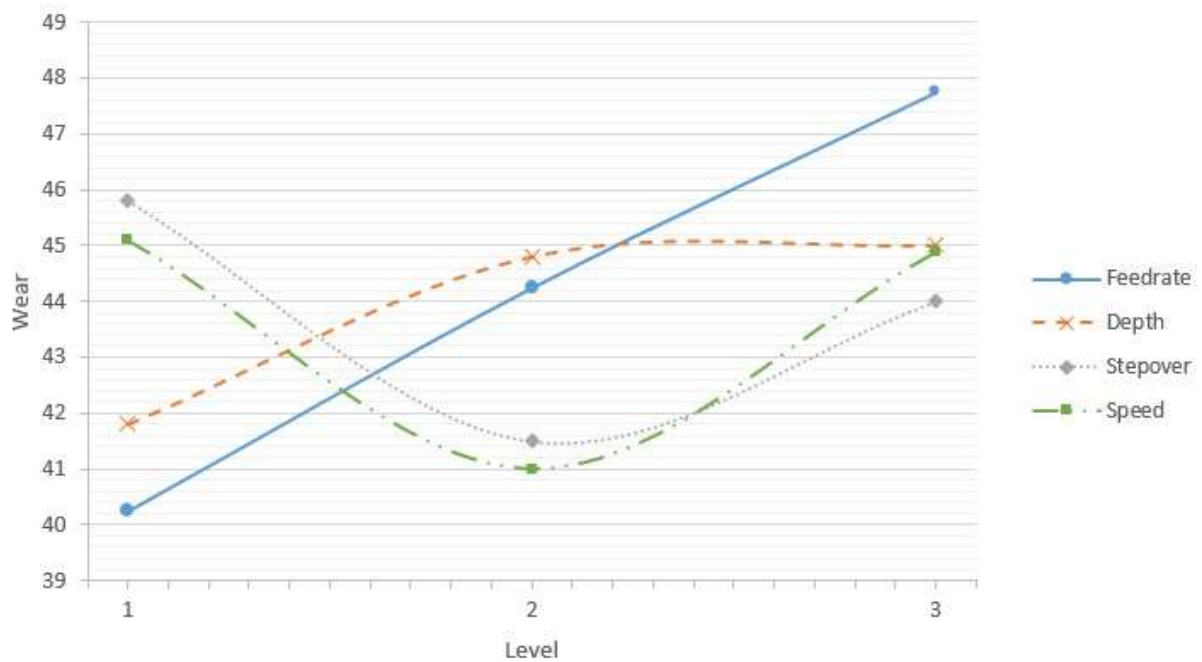


Figure 6-6: Machining Conditions Against Tool Wear

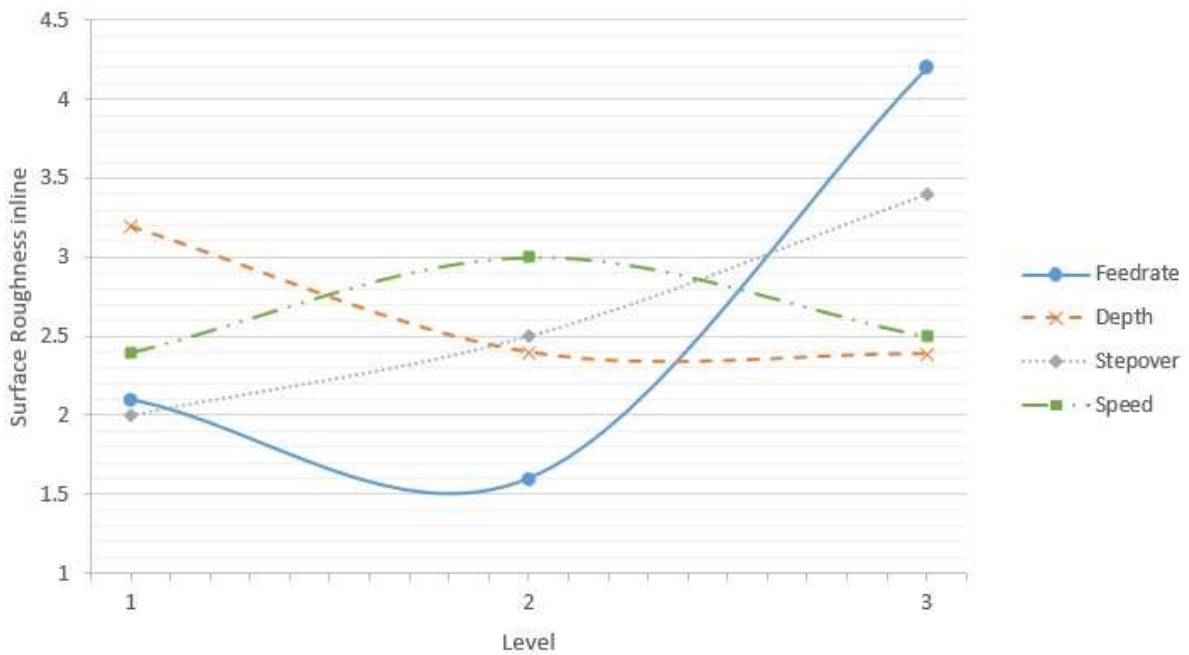


Figure 6-7: Machining Conditions Against Surface Roughness in Line with the Cut Direction

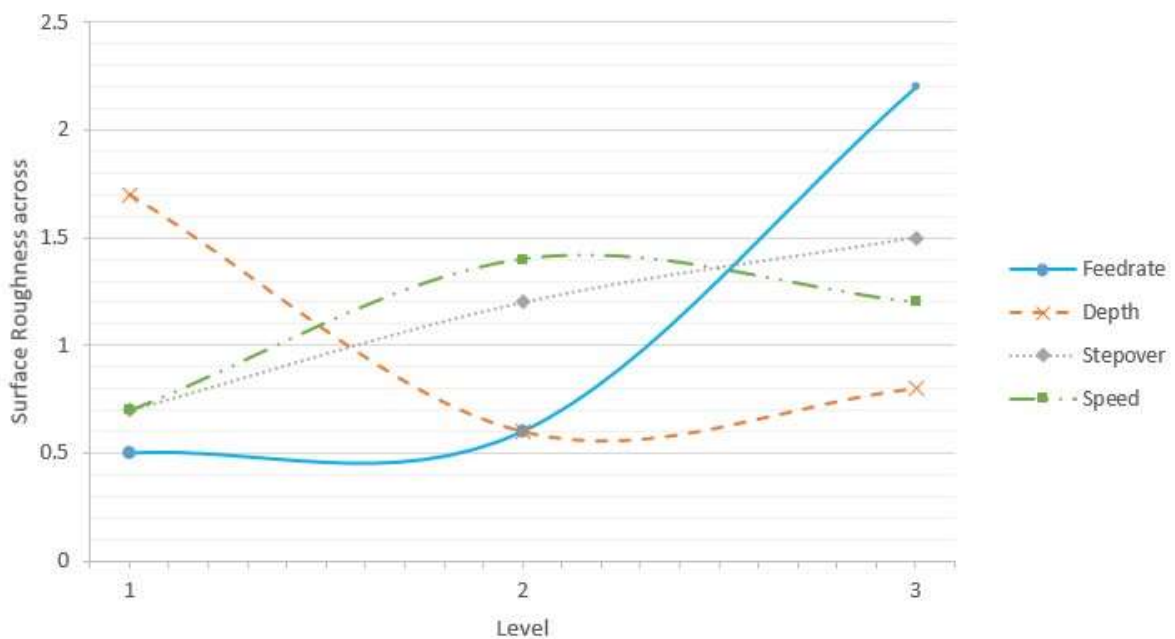


Figure 6-8: Machining Conditions Against Surface Roughness Across the Direction of the Cut

These are key to understanding the relationships and visualising how changing one condition affects the other factors. Some operators can use this information to make decisions on production operations. The purpose of an optimisation tool is to streamline this information into a more manageable bundle so that it can be used by operators with less experience.

### **6.3.3- Tool creation**

To simplify the optimisation tool, the tool material can be eliminated as it only has a minor effect on tool wear. So, a tool with high transgranular rupture toughness should always be selected. The second simplification is the cut direction, as this variable is categorical and has no effect on time. If reducing tool wear is the aim, such as in rough cutting, then conventional (up) milling should be used. If surface finish is the concern, as in finish cutting, then climb (down) milling should be used instead.

The next step concerns factors that share linear variables. From looking at Figure 6-7 and Figure 6-8, the step over's relation to surface roughness is near linear and not very high. The same goes for machining time, but the line is inverted. The only nonlinear factor is for tool wear, where step over is optimal at around 0.8 mm. Because of this, most cutting operations should not exceed 0.8mm or 40% of the tool's diameter step over; this should give the fastest time without sacrificing the performance of the tool. However, for finishing operations, this should be shifted to 30% of the tool's diameter.

While for tool wear, there is a very definite optimum for spindle speed; it is the opposite for surface finish, where 20,000 rpm is among the worst spindle speeds for finish. The effect on machine time is negligible. The effect on surface roughness is a lot lower than on tool wear so, for a large portion of operations, the spindle speed should be 20,000 rpm. Tool wear has a much greater impact on surface roughness than spindle speed does. However, for crucial areas such as finishing, the marginal fitting edge spindle speed should be reduced.

The last three variables have more optimums and curved relationships than the others. Feed rate, step over and depth all have the biggest impacts on machining time out of all the machining conditions. Feed rate has the highest impact. As found in Chapter 5, the lower the feed rate the lower the tool wear; this relation is nearly linear and has a very high impact on tool wear.

However, it also has the highest impact on machining time. The relationship between feed rate and machining time is the lower the feed rates the longer the time, with the ratio rapidly increasing as it reaches 0.06 MMPT. As can be seen in Figure 6-5, the curve flattens out past this point. This means that past 0.06 MMPT tool wear will keep increasing, however the machining time will not decrease a great deal. With just these two factors in mind, the feed rate should not be increased above 0.06 MMPT. When the feed rate was reduced to 0.01667 MMPT the machining time more than tripled, which would mean that a single coping that would usually take around 7-9 minutes to machine would take 23-30 minutes, and during tool life testing this resulted in weeklong test runs. Having routers run for long times is not only not cost effective, but can lead to more frequent maintenance. For this reason, when aiming to keep the machining time under 20 minutes, it is advised to keep the feed rate above 0.034 MMPT. Where surface roughness is concerned, feed rate gets more complicated. Surface roughness, both in line and across the cut direction, have an optimal point around 0.04 MMPT. However, across-the-cut direction the optimum is where the curve plateaus, whereas the in line curve returns upwards around this point. This means that in finishing operation, the feed rate should be close to this optimum, especially at key areas such as the marginal fitting edge. For roughing operations it can be higher, although from 0.05 MMPT to 0.06MMPT the machining times does not decrease drastically so if not machining many pieces, then leave the feed rate below 0.05MMPT.

With depth, the machining time increases as depth decrease. Across the maximum range of cutter depth, the time barely doubles. With the other factors however, depth was not so straight forward; tool wear increases as depth increases until 0.8 where it plateaus, but before this plateau it increases at much the same rate as feed rate. Surface roughness, both in-line and across-the-cut, share a similar but slightly different curve with both having an optimum around 0.85mm. This leaves no perfect selection for rough cutting when it comes to depth. For

finishing however, 0.85mm cutting depth should be used. With roughing, the understanding of reducing cutter depth below 0.8mm will protect the tool, although if a part must be rushed then using 1mm is the same as 0.8mm for all intent and purpose.

Step over shares the same relationship as spindle speed, where there is an optimum for tool wear just past 0.8mm. As step over increases, machining time decreases in a near linear manner. However, this has a lot less of an impact than cutter depth, as the time does not even double across the range of the step over. When it comes to surface roughness, it increases with step over both in line and across the cut. This means that for this variable, it would be advised to perform finishing operations at as low a step over as possible. For rough cutting, the optimal tool wear should be used: 0.8mm or 40% of the tool diameter.

#### **6.3.4- Implementation**

The collection of data and comparison of how the machining conditions affect the time, tool wear and surface finish machining conditions are presented here. This is broken into what operation is being done, as a finishing is primarily concerned with surface finish and tool wear is a secondary concern; the conditions are laid out in Table 6-2.

*Table 6-2: Advised Machining Conditions for Finishing Operations*

<b>Feed rate</b>	<b>Spindle speed</b>	<b>Depth of cut</b>	<b>Step over</b>	<b>Strategy</b>
0.015-0.04 MMPT	16,000 RPM	40-45% of ball Ø	≤30% of tool Ø	Climb mill

These conditions are optimised purely for surface finish, apart from feed rate as below 0.02MMPT is far too slow to produce a part in any reasonable amount of time. For non-



finishing operations however, there is more balance to be found as it comes down to the target tolerances and time frame. However there is an advisable range that each variable should operate within, as shown in Table 6-3.

*Table 6-3: Range of Advisable Machining Conditions for Machining Pre-Sintered Zirconia*

<b>Feed rate</b>	<b>Spindle speed</b>	<b>Depth of cut</b>	<b>Step over</b>	<b>Strategy</b>
0.02-0.05 MMPT	20,000 RPM	30-37% of ball $\emptyset$	40-42% of tool $\emptyset$	Conventional

These ranges are suggested for keeping the tool wear rate low enough to remove at least 0.4 m<sup>3</sup> of pre-sintered zirconia before tool life is reached. Conventional milling (or upward milling) is used for this precise reason, as climb milling causes a lot of tool wear. Spindle speed range covers the optimal for tool wear and does not affect the machine time greatly. If the spindle speed does have to be reduced, then it should not be reduced past 17,000 RPM; this spindle speed will also give a decent finish.

A feed rate of 0.05 MMPT is on the cusp of being too high when it comes to wear rate. Reducing the feed rate below this value, however, causes the machining time to increase very rapidly. Each reduction of 0.02 MMPT nearly doubles the machining time. A sensible feed rate would be 0.04-0.045 MMPT for roughing operations.

The depth has a short range for 2mm tools at 0.6-0.74mm. Going above 0.75mm is where the tool life is too short; depth has a much lesser effect on machining time than feed does, but a similar effect on wear. A depth of 0.6mm can be used with a feed rate 0.05MMPT to offset the increased tool wear while reducing machining time.

The Following flow Chart is a rough guide through this decision making process and how best to handle deciding machining conditions when programming an operation. Of course there are numerous other concerns and inputs: type of operation, grade of tool, size of operation, length of cutting time etc.

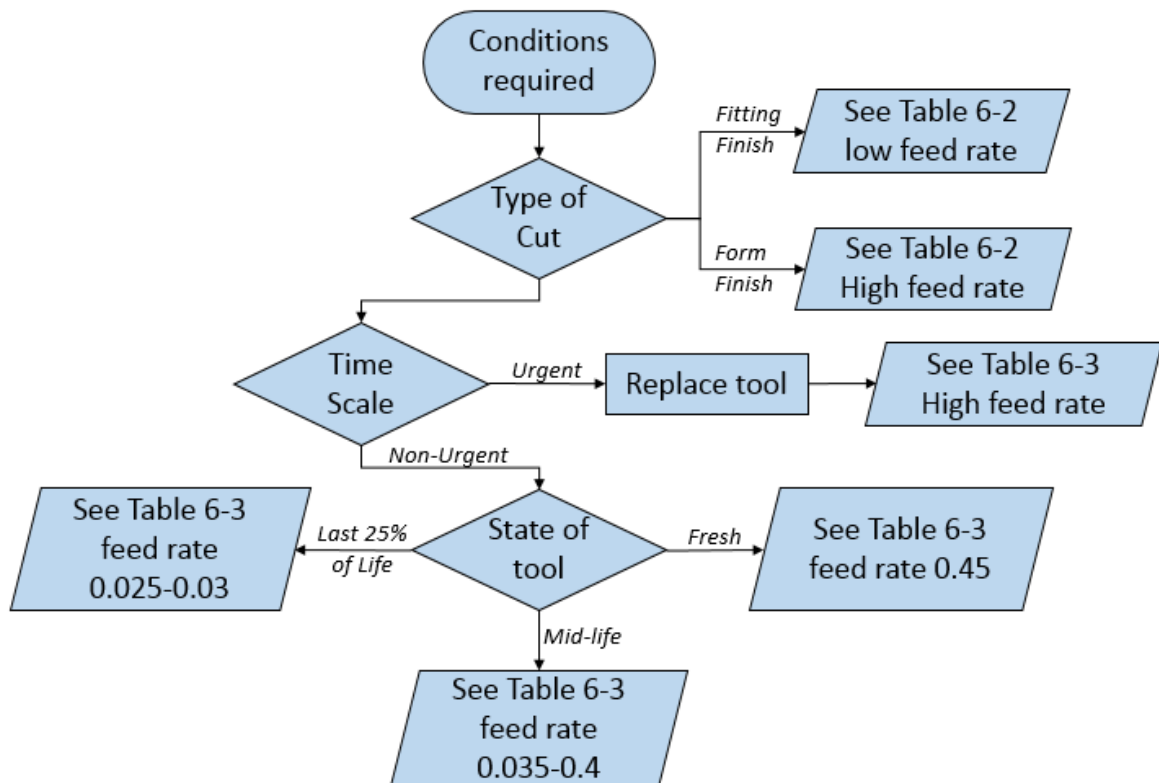


Figure 6-9: Decision Flow Chart for Optimisation Assist

## 6.4- Chapter Summary

This chapter gives a pair of tools for machining pre-sintered zirconia with cemented carbide ball nose end mills. The modified tool life equation was found to be as below:

$$Td^{0.7601}f^{0.8746} = C$$

This equation was selected due the classic Taylor's tool life equation relying on a linear relationship between spindle speed and tool wear. The Colding equation is based on a phenomenon that does not occur in the machining of pre-sintered zirconia. However, further validation was not possible due to the COVID-19 lockdown restricting access to repeat testing. It should also be noted that it is still not precise in its prediction, so tools should be changed before the predicted tool life estimated by this equation.

The optimal running conditions were found by capping the limits of each variable, then comparing them across each factor. This found the following rough guides for general machining.

Table 6-4: Machining Conditions for Differing Operations

<i>Operation</i>	<b>Feedrate MMPT</b>	<b>Speed RPM</b>	<b>Depth % of ball Ø</b>	<b>Step over % of tool Ø</b>	<b>Strategy</b>
<i>Finish</i>	0.04	16,000	40	30 or lower	Climb
<i>Rough</i>	0.045	20,000	35	40	Conventional
<i>Rapid</i>	0.05	20,000	40	42	Conventional

These are conditions that achieve the aims for their respective operations. More detailed ranges are outlined in the chapter, but these are good bases to work with. Roughing does keep the tool wear rate low enough to manufacture plenty of parts. Rushing pushes the tool past this, just

enough, while trying to keep the tool wear rate low enough to not aggressively wear the tool. This could be used for one off rush jobs or prototype runs.

## **7- Conclusion**

This chapter summarises the thesis, outlining the contributions and suggesting future research possibilities. The aim of this research was to analyse the carbide tool wear that occurs in machining pre-sintered zirconia.

*Objective 1: To analyse how the cemented carbide tool is affected by the machining of pre-sintered zirconia.*

During the machining of pre-sintered zirconia, the tool undergoes third body abrasion from the particulate style waste material sliding and impacting across the tool surfaces, which in turn changes the nature of the tool wear; this was shown in Chapter 4 during the investigations into tool wear. This chapter also investigated how the wear occurs on a microscopic level. It was found that the abrasive wear causes transgranular rupture in the carbide ball nose end mills.

*Objective 2: To understand the tool wear pattern and propagation along with the mechanism of this wear, and how these are affected by mechanical, chemical, and thermal properties of the workpiece and the tool and process.*

The tool wear propagation was also detailed in Chapter 4. This wear propagation occurs in two stages, starting normally along the tool edge. Once the initial sharpness of the tool is worn away, a chip forms towards the top of the cutting edge on the flank. This creates more surface area to be subjected to abrasive wear, accelerating the wear rate. The acceleration continues until the tool fails. The wear also happens away from the main cutting edges, noticeably along the relief faces.

*Objective 3: To understand the effect the material removal process has on the workpiece mechanically, topographically, and thermodynamically and how these factors influence further machining and final products.*

Understanding how the workpiece was affected by machining is mostly covered in Chapter 5. The surface roughness of the machined surface degraded with the tool wear, much like any other machining process. With pre-sintered zirconia, the effect that tool wear has on the topography is more exaggerated, when the tool reaches its end life as shown in Figure 5-6 (page 88). The thermal forces introduced to the workpiece are low at any meaningful distance from the tool. The mechanics of the material removal were not detailed in this chapter; this was observed to be less of a cut caused by shear forces and more similar to smashing the material apart.

*Objective 4: To develop the basis of a tool life equation for the machining of pre-sintered zirconia and other materials that share the same waste material properties.*

The tool life equation was covered in Chapter 6, however due to the non-conventional wear and material removal mechanism, standard tool life models such as Taylor's or Colding's cannot work. Because the relationships are assumed to be linear in these models, instead of being non-linear: such as tool life and spindle speed or chip thickness per revolution. To fully develop this tool life equation more time would be required, possibly building a fresh model.

*Objective 5: Creation of a tool to assist the operators and manufactures in optimising the machining efficiency, by increasing tool life and decreasing damaging to the workpiece to supply consistent dental restoration.*

The machining conditions were tested throughout the work for how they affect tool wear and surface finish. This data was all brought together in Chapter 6 to determine an optimal method of machining. These conditions allow for excellent tool life while not sacrificing production lead times or surface integrity, as fully maximising tool life would lead to mediocre finish and machining times being significantly longer than their current average of 7 to 10 minutes per a part.

## **7.1- Impact**

Through this work, many facets of machining pre-sintered zirconia were investigated. Focus has been given to the tool workpiece interaction and how understanding this assists the dental prosthesis sector, from operators to tool manufacturers.

- **Understanding of tool wear and creating tool wear curves.** Investigating and detailing the how the tool wears during the machining of pre-sintered zirconia and how this wear happens on microstructure level. Defining a material that resists abrasion and transgranular rupture to be most favourable.
- **Defining optimal running conditions and developing the tools to do so.** Optimising the machining conditions involved collecting a vast data set of the range of machining conditions and comparing these to varying desirable factors such as time, wear and surface finish. This data is available in graphical format to assist in the selection of differing machining conditions for this material.
- **Proof of how the material is affected by the machining process.** It was theorised that the pre-sintered workpiece was only significantly mechanically affected by the machining. The lack of thermal forces penetrating the below the immediate surface of the work piece show this.

## **7.2- Limitations and Future Work**

This section details how the work was limited and future work that could be done to overcome this following this thesis.

- Further investigation in tool life equation

While Chapter 6 outlined a comparative tool life equation, further investigation and testing would be needed to fully define a model for predicting the tool life. This would involve more machining of pre-sintered zirconia for additional data and more vigorous validation.

- End product testing

Due to the interruption of the COVID-19 pandemic, some final testing was cancelled such as the final product testing which involved sintering machined blocks to validate the failure point of the tool. This study would involve a large amount of time with ovens capable of heating and cooling consistently over the periods needed to sinter the samples.

- End mill design

While tool geometry was not within the scope of the research, the current tools are not the most optimal. While improvements have been made to the original adaption of metal cutting tools, further exploration should be done towards improving them such as higher reliefs or removal of flutes.

- Virtual milling model

With the development of virtual engineering, a virtual milling model for assisting dental lab technicians would be very useful in machining parts, as they can simulate and visualise the process before committing to production with what is an expensive material. This interface could also be adapted to show remaining tool life, predicted surface finishes and adjust for shrinkage to allow for a better fitting part.



## 8- Bibliography

‘Porcelain Margins’ (no date), p. 23320.

Abdulmajeed, A. A. *et al.* (2017) ‘Fracture of layered zirconia restorations at 5 years: A dental laboratory survey’, *The Journal of Prosthetic Dentistry*, 118(3), pp. 353–356. doi: 10.1016/j.prosdent.2016.11.009.

Abduo, J., Lyons, K. and Swain, M. (2010) ‘Fit of zirconia fixed partial denture: A systematic review’, *Journal of Oral Rehabilitation*, 37(11), pp. 866–876. doi: 10.1111/j.1365-2842.2010.02113.x.

Agapiou, J. and Stephenson, D. (2016) ‘9-Tool Wear and Tool Life’, in *Metal Cutting Theory and Practice*. 3rd edn. Taylor & Francis Group, pp. 529–573.

Agapiou, J. and Stephenson, D. (2016) ‘6-Mechanics of Cutting’, in *Metal Cutting Theory and Practice*. 3rd edn. Taylor & Francis Group, pp. 393–447.

Agapiou, J. and Stephenson, D. (2016) ‘4-Cutting Tools’, in *Metal Cutting Theory and Practice*. 3rd edn. Taylor & Francis Group, pp. 159–280.

Ahearne, E. and Baron, S. (2017) ‘Fundamental mechanisms in orthogonal cutting of medical grade cobalt chromium alloy (ASTM F75)’, *CIRP Journal of Manufacturing Science and Technology*. CIRP, 19, pp. 1–6. doi: 10.1016/j.cirpj.2017.02.001.

Alao, A.-R. and Yin, L. (2014) ‘Prediction of the resistance to machining-induced cracking in zirconia by nanoindentation’, in *Recent Advances in Structural Integrity Analysis - Proceedings of the International Congress (APCF/SIF-2014)*. Elsevier, pp. 580–584. doi: 10.1533/9780081002254.580.

Alao, A. R. and Yin, L. (2014) ‘Nano-scale mechanical properties and behavior of pre-sintered zirconia’, *Journal of the Mechanical Behavior of Biomedical Materials*. Elsevier, 36, pp. 21–31. doi: 10.1016/j.jmbbm.2014.03.019.

Alao, A. R. and Yin, L. (2016) ‘Assessment of Elasticity, Plasticity and Resistance to Machining-induced Damage of Porous Pre-sintered Zirconia Using Nanoindentation Techniques’, *Journal of Materials Science and Technology*. Elsevier Ltd, 32(5), pp. 402–410. doi: 10.1016/j.jmst.2016.02.009.

Alao, A.-R. *et al.* (2017) ‘Surface quality of yttria-stabilized tetragonal zirconia polycrystal in CAD/CAM milling, sintering, polishing and sandblasting processes’, *Journal of the Mechanical Behavior of Biomedical Materials*. Elsevier, 65, pp. 102–116. doi: 10.1016/j.jmbbm.2016.08.021.

Alao, A.-R. and Yin, L. (2015) ‘Nanoindentation characterization of the elasticity, plasticity and machinability of zirconia’, *Materials Science and Engineering: A*. Elsevier, 628, pp. 181–187. doi: 10.1016/j.msea.2015.01.051.

Almas, K. (2018) *Glossary of dental implantology*. Hoboken: Wiley-Blackwell.Amat,

N. F. *et al.* (2019) ‘Effect of sintering temperature on the aging resistance and mechanical properties of monolithic zirconia’, *Journal of Materials Research and Technology*. Brazilian Metallurgical, Materials and Mining Association, 8(1), pp. 1092–1101. doi: 10.1016/j.jmrt.2018.07.017.

Anand, P. S. P., Arunachalam, N. and Vijayaraghavan, L. (2018) ‘Study on grinding of pre-sintered zirconia using diamond wheel’, *Materials and Manufacturing Processes*. Taylor & Francis, 33(6), pp. 634–643. doi: 10.1080/10426914.2017.1364761.

Anderson, D., Warkentin, A. and Bauer, R. (2008) ‘Experimental validation of numerical thermal models for dry grinding’, *Journal of Materials Processing Technology*, 204(1–3), pp. 269–278. doi: 10.1016/j.jmatprotec.2007.11.080.

- Antonov, M. *et al.* (2012) 'Effect of temperature and load on three-body abrasion of cermets and steel', *Tribology International*, 46(1), pp. 261–268. doi: 10.1016/j.triboint.2011.06.029.
- ASM Handbook Committee (1997) 'Materials Selection and Design', in *ASM International: Materials Park, OH*, p. 2005. doi: 10.1007/978-981-4560-38-2.
- Astakhov, V. P. and Davim, J. P. (no date) 'Tools ( Geometry and Material ) and Tool Wear'.
- Basílio, M. de A. *et al.* (2016) 'Failure modes of Y-TZP abutments with external hex implant-abutment connection determined by fractographic analysis', *Journal of the Mechanical Behavior of Biomedical Materials*, 60, pp. 187–194. doi: 10.1016/j.jmbbm.2015.12.042.
- Belli, R. *et al.* (2017) 'Chairside CAD/CAM materials. Part 1: Measurement of elastic constants and microstructural characterization', *Dental Materials*. Elsevier Inc., 33(1), pp. 84–98. doi: 10.1016/j.dental.2016.10.009.
- Bhuiyan, M. S. H. and Choudhury, I. A. (2015) 'Investigation of Tool Wear and Surface Finish by Analyzing Vibration Signals in Turning Assab-705 Steel', *Machining Science and Technology*, 19(2), pp. 236–261. doi: 10.1080/10910344.2015.1018531.
- Boitelle, P. *et al.* (2018) 'Evaluation of the marginal fit of CAD-CAM zirconia copings: Comparison of 2D and 3D measurement methods', *Journal of Prosthetic Dentistry*. Mosby Inc., 119(1), pp. 75–81. doi: 10.1016/j.prosdent.2017.01.026.
- Boitelle, P. *et al.* (2018) 'Evaluation of the marginal fit of CAD-CAM zirconia copings : Comparison of 2D and 3D measurement methods', *The Journal of Prosthetic Dentistry*. Editorial Council for the Journal of Prosthetic Dentistry, 119(1), pp. 75–81. doi: 10.1016/j.prosdent.2017.01.026.
- Bona, A., Pecho, O. and Alessandretti, R. (2015) 'Zirconia as a Dental Biomaterial', *Materials*, 8(8), pp. 4978–4991. doi: 10.3390/ma8084978.
- Bouzakis, K.-D. *et al.* (2004) 'The effect of coating thickness, mechanical strength and hardness properties on the milling performance of PVD coated cemented carbides inserts', *Surface and Coatings Technology*, 177–178, pp. 657–664. doi: 10.1016/j.surfcoat.2003.08.003.
- British Standard Institution (2001) 'BS EN 725-12:2001 Advanced technical ceramics — Methods of test for ceramic powders — Part 12: Chemical analysis of zirconia', *London: BSI*. London.
- Buhrer Samra, A. P. *et al.* (2016) 'CAD/CAM in dentistry – a critical review', *Revista Odonto Ciência*, 31(3), p. 140. doi: 10.15448/1980-6523.2016.3.21002.
- Camposilvan, E. *et al.* (2015) 'Enhanced reliability of yttria-stabilized zirconia for dental applications', *Acta Biomaterialia*. Acta Materialia Inc., 17, pp. 36–46. doi: 10.1016/j.actbio.2015.01.023.
- Carpinteri, A., Chiaia, B. and Invernizzi, S. (2004) 'Numerical analysis of indentation fracture in quasi-brittle materials', *Engineering Fracture Mechanics*, 71(4–6), pp. 567–577. doi: 10.1016/S0013-7944(03)00037-7.
- Cassie, A. B. D. and Baxter, S. (1971) 'Front matter', *Transactions of the Faraday Society*, 67(2), p. P001. doi: 10.1039/tf97167fp001.
- Chavali, R., Nejat, A. H. and Lawson, N. C. (2017) 'Machinability of CAD-CAM materials', *Journal of Prosthetic Dentistry*. Editorial Council for the Journal of Prosthetic Dentistry, 118(2), pp. 194–199. doi: 10.1016/j.prosdent.2016.09.022.
- Che, D. *et al.* (2014) 'Machining of Carbon Fiber Reinforced Plastics/Polymers: A Literature Review', *Journal of Manufacturing Science and Engineering*, 136(3), p. 034001. doi: 10.1115/1.4026526.

- Chen, W. (2000) 'Cutting forces and surface finish when machining medium hardness steel using CBN tools', *International Journal of Machine Tools and Manufacture*, 40(3), pp. 455–466. doi: 10.1016/S0890-6955(99)00011-5.
- Chew, W. J. K. *et al.* (2014) 'Sintering properties of zirconia-based ceramic composite', *Materials Research Innovations*, 18(sup6), pp. S6-105-S6-108. doi: 10.1179/1432891714Z.000000000939.
- Damyantov, N. D. *et al.* (2010) 'Dental Laboratory Production of Prosthetic Restorations in a Population in Sofia, Bulgaria: A Descriptive Study', *International Journal of Dentistry*, 2010, pp. 1–6. doi: 10.1155/2010/286192.
- Davim, J. P. (2010) *Surface integrity in machining*, *Surface Integrity in Machining*. doi: 10.1007/978-1-84882-874-2.
- Dds, D. J. F. (2010) 'The CEREC system', *The Journal of the American Dental Association*. American Dental Association, 141(September 1985), pp. 3S-4S. doi: 10.14219/jada.archive.2010.0354.
- Dearnley, P. A. and Trent, E. M. (1982) 'Wear mechanisms of coated carbide tools', *Metals Technology*, 9(1), pp. 60–75. doi: 10.1179/030716982803285909.
- Demarbaix, A. *et al.* (2018) 'Behaviour of pre-sintered Y-TZP during machining operations: Determination of recommended cutting parameters', *Journal of Manufacturing Processes*, 32, pp. 85–92. doi: 10.1016/j.jmapro.2018.01.020.
- Denkena, B. *et al.* (2017) 'Impact of Hard Machining on Zirconia Based Ceramics for Dental Applications', *Procedia CIRP*. The Author(s), 65, pp. 248–252. doi: 10.1016/j.procir.2017.04.055.
- Denry, I. and Kelly, J. R. (2008) 'State of the art of zirconia for dental applications', *Dental Materials*, 24(3), pp. 299–307. doi: 10.1016/j.dental.2007.05.007.
- Diniz, A. E. and Filho, J. C. (1999) 'Influence of the relative positions of tool and workpiece on tool life, tool wear and surface finish in the face milling process', *Wear*, 232(1), pp. 67–75. doi: 10.1016/S0043-1648(99)00159-3.
- Dolinšek, S. and Kopač, J. (2006) 'Mechanism and types of tool wear ; particularities in advanced cutting materials', *Journal of Achievements in Materials*, 19(1), pp. 11–18. doi: <http://www.doaj.org/doaj?func=openurl&genre=article&issn=17348412&date=2006&volume=19&issue=1&spage=11>.
- Donaldson, T. K. *et al.* (2013) 'Risk of Impingement and Third-body Abrasion With 28-mm Metal-on-metal Bearings', *Clinical Orthopaedics and Related Research*®, 472(2), pp. 497–508. doi: 10.1007/s11999-013-3399-3.
- Esmailzare, A., Rahimi, A. and Rezaei, S. M. (2014) 'Investigation of subsurface damages and surface roughness in grinding process of Zerodur ® glass-ceramic', *Applied Surface Science*. Elsevier B.V., 313, pp. 67–75. doi: 10.1016/j.apsusc.2014.05.137.
- Fallqvist, M., Olsson, M. and Ruppi, S. (2007) 'Abrasive wear of multilayer  $\kappa$ -Al<sub>2</sub>O<sub>3</sub>-Ti(C,N) CVD coatings on cemented carbide', *Wear*, 263(1–6), pp. 74–80. doi: 10.1016/j.wear.2007.01.113.
- Fang, Z. Z. *et al.* (2009) 'Synthesis, sintering, and mechanical properties of nanocrystalline cemented tungsten carbide - A review', *International Journal of Refractory Metals and Hard Materials*, 27(2), pp. 288–299. doi: 10.1016/j.ijrmhm.2008.07.011.
- Fernandes, C. M. and Senos, A. M. R. (2011) 'Cemented carbide phase diagrams: A review', *International Journal of Refractory Metals and Hard Materials*. Elsevier Ltd, 29(4), pp. 405–418. doi: 10.1016/j.ijrmhm.2011.02.004.

Fiset, M. *et al.* (1998) 'Three-body impact-abrasion laboratory testing for grinding ball materials', *Wear*, 217(2), pp. 271–275. doi: 10.1016/S0043-1648(98)00154-9.

Flavio Augusto de Moraes Palma, Izabela Lima Gois, Carol Ellen Silva Tavares, Luiza Gabriella Vale Teixeira, Tamires Mirely Reis Silva, L. M. (2021) 'Indication and Use of Zirconia Crowns on Decidual Teeth', *International Journal of Dental Research and Reviews*, p. 48. doi: 10.28933/ijdr-2021-06-2805.

Fu, Q. (2019) 'Bioactive Glass Scaffolds for Bone Tissue Engineering', in *Biomedical, Therapeutic and Clinical Applications of Bioactive Glasses*. Elsevier, pp. 417–442. doi: 10.1016/B978-0-08-102196-5.00015-X.

Gale, W. F. (2003) *Smithells metals reference book*. 8th edn. Oxford: Butterworth-Heinemann. Available at: <https://www.vlebooks.com/Product/Index/32921?page=0>.

Gaspar, M. and Weichert, F. (2013) 'Integrated construction and simulation of tool paths for milling dental crowns and bridges', *CAD Computer Aided Design*, 45(10), pp. 1170–1181. doi: 10.1016/j.cad.2013.04.007.

Gaugel, S. *et al.* (2016) 'A comparative study on tool wear and laminate damage in drilling of carbon-fiber reinforced polymers (CFRP)', *Composite Structures*. Elsevier Ltd, 155, pp. 173–183. doi: 10.1016/j.compstruct.2016.08.004.

Ghani, J. A., Choudhury, I. A. and Masjuki, H. H. (2004) 'Wear mechanism of TiN coated carbide and uncoated cermets tools at high cutting speed applications', *Journal of Materials Processing Technology*, 153–154(1–3), pp. 1067–1073. doi: 10.1016/j.jmatprotec.2004.04.352.

Groesser, J. *et al.* (2014) 'Retention forces of 14-unit zirconia telescopic prostheses with six double crowns made from zirconia—an in vitro study', *Clinical Oral Investigations*, 18(4), pp. 1173–1179. doi: 10.1007/s00784-013-1093-1.

Grzesik, W. (2017) 'Advanced Machining Processes', in *Advanced Machining Processes of Metallic Materials*. 2nd edn. Cambridge USA: Elsevier, pp. 285–397. doi: 10.1016/B978-0-444-63711-6.00015-6.

Guilemany, J. M. *et al.* (2001) 'Role of three-body abrasion wear in the sliding wear behaviour of WC–Co coatings obtained by thermal spraying', *Surface and Coatings Technology*, 140(2), pp. 141–146. doi: 10.1016/S0257-8972(01)01033-7.

Hafli, L. (2009) 'Automation is not just about robots Manufacturing, Computer Aided', *American Machinist*, 153(1), pp. 30–32. Available at: <https://web-b-ebsohost-com.ezproxy.uwe.ac.uk/ehost/pdfviewer/pdfviewer?vid=1&sid=8333d863-3f06-4fb1-90d2-997ac3b484a0%40sessionmgr101>.

Hedenqvist, P., Olsson, M. and Söderberg, S. (1989) 'Influence of Tin Coating on Wear of High Speed Steel Tools as Studied by New Laboratory Wear Test', *Surface Engineering*, 5(2), pp. 141–150. doi: 10.1179/sur.1989.5.2.141.

Higgins, R. A. (1993) *Engineering Metallurgy- Vol 1 : Applied Physical Metallurgy*. 6th edn. London: Edward Arnold.

Holleck, H. and Schier, V. (1995) 'Multilayer PVD coatings for wear protection', *Surface and Coatings Technology*. Elsevier Science S.A., 76–77(1995), pp. 328–336. doi: 10.1016/0257-8972(95)02555-3.

Hsu, H. J. *et al.* (2017) 'Shrinkage prediction using finite element analysis and experimental validation using three-dimension slurry printing system', *The International Journal of Advanced Manufacturing Technology*, 91(1–4), pp. 1289–1296. doi: 10.1007/s00170-016-9842-3.

- Hwang, T. W. and Malkin, S. (1999) 'Upper bound analysis for specific energy in grinding of ceramics', *Wear*, 231(2), pp. 161–171. doi: 10.1016/S0043-1648(98)00283-X.
- International Standard Organisation (1989) 'ISO 8688-2:1989 Tool life testing in milling -- Part 2: End milling.', *Geneva: ISO*.
- International Standard Organisation (1989) 'ISO 8688-1:1989 Tool life testing in milling -- Part 1: Face milling.', *Geneva: ISO*.
- International Standard Organisation (2007) 'ISO 14801:2007 Dentistry. Implants. Dynamic fatigue test for endosseous dental implants', *Geneva: ISO*. Geneva.
- Irvine, D. (2017) *The Tool Life of Machining Zirconia Crowns and the Relative Tool Wear Mechanism*. University of the West of England.
- Irvine, D. *et al.* (2019) 'The analysis of tool wear mechanisms in the machining of pre-sintered zirconia dental crowns', *Procedia Manufacturing*, 38, pp. 1026–1033. doi: 10.1016/j.promfg.2020.01.188.
- Jacobs, D. J., Steele, J. G. and Wassell, R. W. (2002) 'Crowns and extra-coronal restorations: Considerations when planning treatment', *British Dental Journal*, 192(5), pp. 257–267. doi: 10.1038/sj.bdj.4801350.
- Jia, K. and Fischer, T. E. (1997) 'Sliding wear of conventional and nanostructured cemented carbides', *Wear*, 203–204, pp. 310–318. doi: 10.1016/S0043-1648(96)07423-6.
- Johansson, D. *et al.* (2017) 'Assessment of Commonly used Tool Life Models in Metal Cutting', *Procedia Manufacturing*. The Author(s), 11(June), pp. 602–609. doi: 10.1016/j.promfg.2017.07.154.
- John, R. *et al.* (2021) 'Modified Taylor's equation including the effects of fiber characteristics on tool wear when machining natural fiber composites', *Wear*. Elsevier B.V., 468–469(December 2020), p. 203606. doi: 10.1016/j.wear.2020.203606.
- Kalpakjian, S., Schmid, S. Sekar, K. (2014) *Manufacturing engineering and technology*. 7th edn. Singapore: Pearson Education South Asia.
- Kalyanasundaram, D., Shrotriya, P. and Molian, P. (2010) 'Fracture mechanics-based analysis for hybrid laser/waterjet (LWJ) machining of yttria-partially stabilized zirconia (Y-PSZ)', *International Journal of Machine Tools and Manufacture*. Elsevier, 50(1), pp. 97–105. doi: 10.1016/j.ijmactools.2009.09.002.
- Katiyar, P. K. *et al.* (2016) 'Modes of failure of cemented tungsten carbide tool bits (WC/Co): A study of wear parts', *International Journal of Refractory Metals and Hard Materials*. Elsevier Ltd, 54, pp. 27–38. doi: 10.1016/j.ijrmhm.2015.06.018.
- Katsich, C. and Badisch, E. (2011) 'Effect of carbide degradation in a Ni-based hardfacing under abrasive and combined impact/abrasive conditions', *Surface and Coatings Technology*. Elsevier B.V., 206(6), pp. 1062–1068. doi: 10.1016/j.surfcoat.2011.07.064.
- Kaye, J. E. *et al.* (1995) 'Predicting tool flank wear using spindle speed change', *International Journal of Machine Tools and Manufacture*, 35(9), pp. 1309–1320. doi: 10.1016/0890-6955(94)E0031-D.
- Kim, S. W. *et al.* (2013) 'Sintering behavior and mechanical properties of HA-X% mol 3YSZ composites sintered by high frequency induction heated sintering', *Composites Part B: Engineering*. Elsevier Ltd, 45(1), pp. 1689–1693. doi: 10.1016/j.compositesb.2012.09.077.
- Kirmali, O., Akin, H. and Kapdan, A. (2014) 'Evaluation of the surface roughness of zirconia ceramics after different surface treatments', *Acta Odontologica Scandinavica*, 72(6), pp. 432–439. doi: 10.3109/00016357.2013.853320.

- Kirsch, C. *et al.* (2017) 'Trueness of four different milling procedures used in dental CAD/CAM systems', *Clinical Oral Investigations*. *Clinical Oral Investigations*, 21(2), pp. 551–558. doi: 10.1007/s00784-016-1916-y.
- Kizaki, T., Sugita, N. and Mitsuishi, M. (2016) 'Experimental analysis of the machinability in the thermally assisted milling process of zirconia ceramics', *Precision Engineering*. Elsevier Inc., 45, pp. 176–186. doi: 10.1016/j.precisioneng.2016.02.010.
- Kloypayan, J. and Lee, Y.-S. (2002) 'Material engagement analysis of different endmills for adaptive feedrate control in milling processes', *Computers in Industry*, 47(1), pp. 55–76. doi: 10.1016/S0166-3615(01)00136-1.
- Komanduri, R., Chandrasekaran, N. and Raff, L. M. (1998) 'Effect of tool geometry in nanometric cutting: a molecular dynamics simulation approach', *Wear*, 219(1), pp. 84–97. doi: 10.1016/S0043-1648(98)00229-4.
- Korsunsky, A. M. *et al.* (2011) 'Strain tomography of polycrystalline zirconia dental prostheses by synchrotron X-ray diffraction', *Acta Materialia*, 59(6), pp. 2501–2513. doi: 10.1016/j.actamat.2010.12.054.
- Kovalchenko, A. M. (2013) 'Studies of the ductile mode of cutting brittle materials (A review)', *Journal of Superhard Materials*, 35(5), pp. 259–276. doi: 10.3103/S1063457613050018.
- Kumar, V. *et al.* (2006) 'An analysis of grain boundaries and grain growth in cemented tungsten carbide using orientation imaging microscopy', *Metallurgical and Materials Transactions A*, 37(3), pp. 599–607. doi: 10.1007/s11661-006-0032-z.
- Kundrák, J. *et al.* (2017) 'Numerical examination of residual stresses developing during hard turning at different rake angles', *The International Journal of Advanced Manufacturing Technology*. *The International Journal of Advanced Manufacturing Technology*, 89(5–8), pp. 1989–1999. doi: 10.1007/s00170-016-9229-5.
- Kuppuswamy, R., Bower, D. and March, P. (2014) 'Blend of sharpness and strength on a ball nose endmill geometry for high speed machining of Ti6Al4V', *The International Journal of Advanced Manufacturing Technology*, 70(9–12), pp. 1827–1834. doi: 10.1007/s00170-013-5345-7.
- Kurtulmus-Yilmaz, S. and Aktore, H. (2018) 'Effect of the application of surface treatments before and after sintering on the flexural strength, phase transformation and surface topography of zirconia', *Journal of Dentistry*. Elsevier, 72(February), pp. 29–38. doi: 10.1016/j.jdent.2018.02.006.
- Lalwani, D. I., Mehta, N. K. and Jain, P. K. (2008) 'Experimental investigations of cutting parameters influence on cutting forces and surface roughness in finish hard turning of MDN250 steel', *Journal of Materials Processing Technology*, 206(1–3), pp. 167–179. doi: 10.1016/j.jmatprotec.2007.12.018.
- Lasemi, A., Xue, D. and Gu, P. (2010) 'Recent development in CNC machining of freeform surfaces: A state-of-the-art review', *Computer-Aided Design*, 42(7), pp. 641–654. doi: 10.1016/j.cad.2010.04.002.
- Le, M., Papia, E. and Larsson, C. (2015) 'The clinical success of tooth- and implant-supported zirconia-based fixed dental prostheses. A systematic review', *Journal of Oral Rehabilitation*, 42(6), pp. 467–480. doi: 10.1111/joor.12272.
- Lebon, N. *et al.* (2015) 'Influence of CAD/CAM tool and material on tool wear and roughness of dental prostheses after milling', *Journal of Prosthetic Dentistry*, 114(2), pp. 236–247. doi: 10.1016/j.prosdent.2014.12.021.

- Lee, H. U., Cho, D.-W. and Ehmann, K. F. (2008) 'A Mechanistic Model of Cutting Forces in Micro-End-Milling with Cutting-Condition-Independent Cutting Force Coefficients', *Journal of Manufacturing Science and Engineering*, 130(3), p. 031102. doi: 10.1115/1.2917300.
- Liao, Z. and Axinte, D. A. (2016) 'On chip formation mechanism in orthogonal cutting of bone', *International Journal of Machine Tools and Manufacture*. Elsevier, 102, pp. 41–55. doi: 10.1016/j.ijmachtools.2015.12.004.
- Lin, Y. C., Chen, X. and Liu, G. (2010) 'A modified Johnson – Cook model for tensile behaviors of typical high-strength alloy steel', *Materials Science & Engineering A*. Elsevier B.V., 527(26), pp. 6980–6986. doi: 10.1016/j.msea.2010.07.061.
- Liu, H. Y., Kou, S. Q. and Lindqvist, P. (2002) 'Numerical simulation of the fracture process in cutting heterogeneous brittle material', *INTERNATIONAL JOURNAL FOR NUMERICAL AND ANALYTICAL METHODS IN GEOMECHANICS*, 1278(January), pp. 1253–1278. doi: 10.1002/nag.243.
- Liu, H. T. *et al.* (2013) 'Experimental research of brittle-ductile transition conditions and tool wear for micromilling of glass material', *The International Journal of Advanced Manufacturing Technology*, 68(5–8), pp. 1901–1909. doi: 10.1007/s00170-013-4987-9.
- Llanes, L. *et al.* (2004) 'Surface Integrity Effects on the Fracture Resistance of Electrical-Discharge-Machined WC-Co Cemented Carbides', *Journal of the American Ceramic Society*, 87(9), pp. 1687–1693. doi: 10.1111/j.1551-2916.2004.01687.x.
- Lu, L. *et al.* (2011) 'An open CAM system for dentistry on the basis of China-made 5-axis simultaneous contouring CNC machine tool and industrial CAM software', *Journal of Huazhong University of Science and Technology - Medical Science*, 31(5), pp. 696–700. doi: 10.1007/s11596-011-0585-y.
- Ma, L. *et al.* (2017) 'Prediction model and simulation of cutting force in turning hard-brittle materials', *The International Journal of Advanced Manufacturing Technology*. The International Journal of Advanced Manufacturing Technology, 91(1–4), pp. 165–174. doi: 10.1007/s00170-016-9642-9.
- Maegawa, S. *et al.* (2016) 'International Journal of Machine Tools & Manufacture Mechanism for changes in cutting forces for down-milling of unidirectional carbon fiber reinforced polymer laminates : Modeling and experimentation', *International Journal of Machine Tools and Manufacture*. Elsevier, 100, pp. 7–13. doi: 10.1016/j.ijmachtools.2015.10.003.
- Malkin, S. and Hwang, T. W. (1996) 'Grinding Mechanisms for Ceramics', *CIRP Annals - Manufacturing Technology*, 45(2), pp. 569–580. doi: 10.1016/S0007-8506(07)60511-3.
- Marya, S. *et al.* (2008) 'Machinability of titanium alloys (Ti6Al4V and Ti555.3)', *Journal of Materials Processing Technology*, 209(5), pp. 2223–2230. doi: 10.1016/j.jmatprotec.2008.06.020.
- Matinlinna, J. P. (2011) 'What Do We Know About Zirconia as a Dental Biomaterial Today?', *Dental Medicine Research*, 31(3), pp. 266–278.
- Matsui, K. and Hojo, J. (2008) 'Sintering kinetics at constant rates of heating: Effect of GeO<sub>2</sub> addition on the initial sintering stage of 3 mol% Y<sub>2</sub>O<sub>3</sub>-doped zirconia powder', *Journal of Materials Science*, 43(3), pp. 852–859. doi: 10.1007/s10853-007-2179-4.
- Matsui, K. *et al.* (2005) 'Sintering kinetics at constant rates of heating: Effect of Al<sub>2</sub>O<sub>3</sub> on the initial sintering stage of fine zirconia powder', *Journal of the American Ceramic Society*, 88(12), pp. 3346–3352. doi: 10.1111/j.1551-2916.2005.00620.x.
- Miyazaki, T. and Hotta, Y. (2011) 'CAD/CAM systems available for the fabrication of crown and bridge restorations', *Australian Dental Journal*, 56, pp. 97–106. doi: 10.1111/j.1834-7819.2010.01300.x.

- Miyazaki, T. *et al.* (2009) 'A review of dental CAD/CAM: current status and future perspectives from 20 years of experience', *Dental Materials Journal*, 28(1), pp. 44–56. doi: 10.4012/dmj.28.44.
- Modi, O. P. (2001) 'Two-body abrasion of a cast Al–Cu (2014 Al) alloy–Al<sub>2</sub>O<sub>3</sub> particle composite: influence of heat treatment and abrasion test parameters', *Wear*, 248(1–2), pp. 100–111. doi: 10.1016/S0043-1648(00)00534-2.
- Montoya, M. *et al.* (2013) 'Evaluation of the performance of coated and uncoated carbide tools in drilling thick CFRP/aluminium alloy stacks', *The International Journal of Advanced Manufacturing Technology*, 68(9–12), pp. 2111–2120. doi: 10.1007/s00170-013-4817-0.
- Mormann, W. H. (2006) 'The evolution of the CEREC system', *The Journal of the American Dental Association*, 137(September), pp. 7S-13S. doi: 10.14219/jada.archive.2006.0398.
- Mormann, W. H. *et al.* (1990) 'CAD-CAM Ceramic Inlays and Onlays: A Case Report after 3 years in Place', *The Journal of the American Dental Association*, 120(5), pp. 517–520. doi: 10.14219/jada.archive.1990.0086.
- Mormann, W. H. *et al.* (2013) 'Wear characteristics of current aesthetic dental restorative CAD/CAM materials: Two-body wear, gloss retention, roughness and Martens hardness', *Journal of the Mechanical Behavior of Biomedical Materials*, 20, pp. 113–125. doi: 10.1016/j.jmbbm.2013.01.003.
- Muhamad Khairussaleh, N. K., Che Haron, C. H. and A. Ghani, J. (2016) 'Study on wear mechanism of solid carbide cutting tool in milling CFRP', *Journal of Materials Research*, 31(13), pp. 1893–1899. doi: 10.1557/jmr.2016.21.
- Muthuraja, A. and Senthilvelan, S. (2015) 'Abrasive wear performance of tungsten carbide based self-lubricant cutting tool material', *International Journal of Refractory Metals and Hard Materials*. Elsevier Ltd, 51, pp. 91–101. doi: 10.1016/j.ijrmhm.2015.03.007.
- Nasrin, S. *et al.* (2016) '3D statistical failure analysis of monolithic dental ceramic crowns', *Journal of Biomechanics*. Elsevier, 49(10), pp. 2038–2046. doi: 10.1016/j.jbiomech.2016.05.003.
- Niebel, B., Draper, A. and Wysk, R. (1989) *Modern manufacturing process engineering*. New York: McGraw-Hill.
- Occlusion, F. (2012) 'Book Reviews Dental Implant Restoration : Principles', 21, pp. 334–336.
- Oh, G.-J. *et al.* (2010) 'Sintering behavior and mechanical properties of zirconia compacts fabricated by uniaxial press forming', *The Journal of Advanced Prosthodontics*, 2(3), p. 81. doi: 10.4047/jap.2010.2.3.81.
- Ohbuchi, Y. and Obikawa, T. (2003) 'Finite Element Modeling of Chip Formation in the Domain of Negative Rake Angle Cutting', *Journal of Engineering Materials and Technology*, 125(3), p. 324. doi: 10.1115/1.1590999.
- Øilo, M. and Quinn, G. D. (2016) 'Fracture origins in twenty-two dental alumina crowns', *Journal of the Mechanical Behavior of Biomedical Materials*. Elsevier, 53(January), pp. 93–103. doi: 10.1016/j.jmbbm.2015.08.006.
- Oladijo, O. P. *et al.* (2012) 'Effect of substrate on the 3 body abrasion wear of HVOF WC-17wt.% Co coatings', *International Journal of Refractory Metals and Hard Materials*. Elsevier Ltd, 35, pp. 288–294. doi: 10.1016/j.ijrmhm.2012.06.011.
- PalDey, S. and Deevi, S. . (2003) 'Single layer and multilayer wear resistant coatings of (Ti,Al)N: a review', *Materials Science and Engineering: A*, 342(1–2), pp. 58–79. doi: 10.1016/S0921-5093(02)00259-9.



- Polishetty, A. *et al.* (2017) 'Cutting Force and Surface Finish Analysis of Machining Additive Manufactured Titanium Alloy Ti-6Al-4V', *Procedia Manufacturing*, 7, pp. 284–289. doi: 10.1016/j.promfg.2016.12.071.
- Ramesh, K. and Siong, L. B. (2011) 'Extraction of flank wear growth models that correlates cutting edge integrity of ball nose end mills while machining titanium', *The International Journal of Advanced Manufacturing Technology*, 52(5–8), pp. 443–450. doi: 10.1007/s00170-010-2753-9.
- Rao, C. J., Rao, D. N. and Srihari, P. (2013) 'Influence of Cutting Parameters on Cutting Force and Surface Finish in Turning Operation', *Procedia Engineering*, 64, pp. 1405–1415. doi: 10.1016/j.proeng.2013.09.222.
- Richardson, D. J., Keavey, M. A. and Dailami, F. (2006) 'Modelling of cutting induced workpiece temperatures for dry milling', *International Journal of Machine Tools and Manufacture*, 46(10), pp. 1139–1145. doi: 10.1016/j.ijmachtools.2005.08.008.
- Ritzberger, C. *et al.* (2010) 'Properties and Clinical Application of Three Types of Dental Glass-Ceramics and Ceramics for CAD-CAM Technologies', *Materials*, 3(6), pp. 3700–3713. doi: 10.3390/ma3063700.
- Rosa, P. A. R. *et al.* (2007) 'The transient beginning to machining and the transition to steady-state cutting', *International Journal of Machine Tools and Manufacture*, 47(12–13), pp. 1904–1915. doi: 10.1016/j.ijmachtools.2007.03.005.
- Rosentritt, M. *et al.* (2000) 'Comparison of in vitro fracture strength of metallic and tooth-coloured posts and cores', *Journal of Oral Rehabilitation*, 27(7), pp. 595–601. doi: 10.1046/j.1365-2842.2000.00548.x.
- Sawada, T. *et al.* (2016) 'Influence of Pre-Sintered Zirconia Surface Conditioning on Shear Bond Strength to Resin Cement', *Materials*, 9(7), p. 518. doi: 10.3390/ma9070518.
- Shen, Z. *et al.* (2015) 'Wear patterns and wear mechanisms of cutting tools used during the manufacturing of chopped carbon fiber', *International Journal of Machine Tools and Manufacture*. Elsevier, 97, pp. 1–10. doi: 10.1016/j.ijmachtools.2015.06.008.
- Shrot, A. and Bäker, M. (2012) 'Determination of Johnson–Cook parameters from machining simulations', *Computational Materials Science*. Elsevier B.V., 52(1), pp. 298–304. doi: 10.1016/j.commatsci.2011.07.035.
- Spintzyk, S. *et al.* (2016) 'Influence of the Conditioning Method for Pre-Sintered Zirconia on the Shear Bond Strength of Bilayered Porcelain/Zirconia', *Materials*, 9(9), p. 765. doi: 10.3390/ma9090765.
- Statement, P. (2018) 'CAD/CAM Dentistry', *International Dental Journal*, 68(1), pp. 18–19. doi: 10.1111/idj.12373.
- Suh, M.-S., Chae, Y.-H. and Kim, S.-S. (2008) 'Friction and wear behavior of structural ceramics sliding against zirconia', *Wear*, 264(9–10), pp. 800–806. doi: 10.1016/j.wear.2006.12.079.
- Sutharsini, U. *et al.* (2014) 'Low-temperature degradation and defect relationship in yttria-tetragonal zirconia polycrystal ceramic', *Materials Research Innovations*, 18(sup6), pp. S6-131-S6-134. doi: 10.1179/1432891714Z.000000000943.
- Suya Prem Anand, P., Arunachalam, N. and Vijayaraghavan, L. (2018) 'Effect of grinding on subsurface modifications of pre-sintered zirconia under different cooling and lubrication conditions', *Journal of the Mechanical Behavior of Biomedical Materials*, 86(June), pp. 122–130. doi: 10.1016/j.jmbbm.2018.06.026.

- Takagi, K. *et al.* (2011) 'Microstructural dependency of thermal expansion and sintering shrinkage in plasma-sprayed zirconia coatings', *Surface and Coatings Technology*. Elsevier B.V., 205(19), pp. 4411–4417. doi: 10.1016/j.surfcoat.2011.03.053.
- Tamizharasan, T., Selvaraj, T. and Noorul Haq, A. (2006) 'Analysis of tool wear and surface finish in hard turning', *The International Journal of Advanced Manufacturing Technology*, 28(7–8), pp. 671–679. doi: 10.1007/s00170-004-2411-1.
- Tapie, L. *et al.* (2016) 'Adaptation Measurement of CAD/CAM Dental Crowns with X-Ray Micro-CT: Metrological Chain Standardization and 3D Gap Size Distribution', *Advances in Materials Science and Engineering*, 2016, pp. 1–13. doi: 10.1155/2016/7963928.
- Taylor, F. W. (1907) *On the art of cutting metals*. New York: American society of mechanical engineers.
- Treatment, H. *et al.* (2019) 'Lithium Disilicate Bioactive glass / glass ceramics for dental applications Dental Glasses and Glass-ceramics', pp. 162–166.
- TSALOUCHOU, E. *et al.* (2008) 'Fatigue and fracture properties of yttria partially stabilized zirconia crown systems', *Dental Materials*, 24(3), pp. 308–318. doi: 10.1016/j.dental.2007.05.011.
- Tsanova, M., Manchorova-Veleva, N. and Tsanova, S. (2016) 'Application of 3d digital scanning and CAD/CAM systems for zirconia indirect restorations', *Journal of IMAB - Annual Proceeding (Scientific Papers)*, 22(3), pp. 1320–1323. doi: 10.5272/jimab.2016223.1320.
- Upadhyaya, G. S. (2001) 'Materials science of cemented carbides - an overview', *Material and Design*, 22, pp. 483–489.
- Upadhyaya, G. S. (1998) *Cemented tungsten carbides, Cemented Tungsten Carbides*. Westwood: Noyes Publications. doi: 10.1016/B978-081551417-6.50007-1.
- Uzun, G. (2008) 'An Overview of Dental CAD/CAM Systems', *Biotechnology & Biotechnological Equipment*, 22(1), pp. 530–535. doi: 10.1080/13102818.2008.10817506.
- Vera, V. *et al.* (2013) 'Applying soft computing techniques to optimise a dental milling process', *Neurocomputing*, 109, pp. 94–104. doi: 10.1016/j.neucom.2012.04.033.
- Wang, H., Aboushelib, M. N. and Feilzer, A. J. (2008) 'Strength influencing variables on CAD/CAM zirconia frameworks', *Dental Materials*, 24(5), pp. 633–638. doi: 10.1016/j.dental.2007.06.030.
- Wang, Q., Chen, Z. H. and Ding, Z. X. (2009) 'Performance of abrasive wear of WC-12Co coatings sprayed by HVOF', *Tribology International*, 42(7), pp. 1046–1051. doi: 10.1016/j.triboint.2009.02.011.
- Wang, S. *et al.* (2017) 'Simulation research on the anisotropic cutting mechanism of KDP crystal using a new constitutive model', *Machining Science and Technology*. Taylor & Francis, 21(2), pp. 202–222. doi: 10.1080/10910344.2017.1283960.
- Wang, W. *et al.* (2019) 'Trueness analysis of zirconia crowns fabricated with 3-dimensional printing', *Journal of Prosthetic Dentistry*. Editorial Council for the Journal of Prosthetic Dentistry, 121(2), pp. 285–291. doi: 10.1016/j.prosdent.2018.04.012.
- Wayne, S. F. and Buljan, S.-T. (1990) 'Wear of Ceramic Cutting Tools in Ni-Based Superalloy Machining', *Tribology Transactions*, 33(4), pp. 618–626. doi: 10.1080/10402009008981997.
- Xu, J. (2019) 'Orthogonal cutting mechanisms of CFRP / Ti6Al4V stacks', *International Journal of Advanced Manufacturing Technology*. The International Journal of Advanced Manufacturing Technology, pp. 1–21. doi: <https://doi.org/10.1007/s00170-019-03734-x>.

- Yin, L. *et al.* (2006) 'An overview of in vitro abrasive finishing & CAD/CAM of bioceramics in restorative dentistry', *International Journal of Machine Tools and Manufacture*, 46(9), pp. 1013–1026. doi: 10.1016/j.ijmachtools.2005.07.045.
- Yugeswaran, S. *et al.* (2012) 'Mechanical properties, electrochemical corrosion and in-vitro bioactivity of yttria stabilized zirconia reinforced hydroxyapatite coatings prepared by gas tunnel type plasma spraying', *Journal of the Mechanical Behavior of Biomedical Materials*. Elsevier Ltd, 9, pp. 22–33. doi: 10.1016/j.jmbbm.2011.11.002.
- Yussefian, N. Z. *et al.* (2010) 'Electro-erosion edge honing of cutting tools', *CIRP Annals - Manufacturing Technology*. CIRP, 59(1), pp. 215–218. doi: 10.1016/j.cirp.2010.03.009.
- Zheng, M. *et al.* (2015) 'Enhanced Biological Behavior of In Vitro Human Gingival Fibroblasts on Cold Plasma-Treated Zirconia', *PLOS ONE*. Edited by M. Yousfi, 10(10), p. e0140278. doi: 10.1371/journal.pone.0140278.
- Zhou, M. *et al.* (2006) 'Tool wear and surface finish in diamond cutting of optical glass', *Journal of Materials Processing Technology*, 174(1–3), pp. 29–33. doi: 10.1016/j.jmatprotec.2005.02.248.
- Zhu, L. *et al.* (2012) 'Experimental analyses to investigate the feasibility and effectiveness in using heat-pipe embedded end-mills', *The International Journal of Advanced Manufacturing Technology*, 60(5–8), pp. 497–504. doi: 10.1007/s00170-011-3629-3.
- Zucuni, C. P. *et al.* (2017) 'CAD/CAM machining Vs pre-sintering in-lab fabrication techniques of Y-TZP ceramic specimens: Effects on their mechanical fatigue behavior', *Journal of the Mechanical Behavior of Biomedical Materials*. Elsevier Ltd, 71(March), pp. 201–208. doi: 10.1016/j.jmbbm.2017.03.013.

The following Conference paper was presented in June 2019.

Irvine, D., Goh, M., Dailami, F., & Matthews, J. (2019). The analysis of tool wear mechanisms in the machining of pre-sintered zirconia dental crowns. *Procedia Manufacturing*, 38, 1026-1033. <https://doi.org/10.1016/j.promfg.2020.01.188>

29th International Conference on Flexible Automation and Intelligent Manufacturing (FAIM2019), June 24-28, 2019, Limerick, Ireland.

## The analysis of tool wear mechanisms in the machining of pre-sintered zirconia dental crowns

David Irvine<sup>a</sup>, Wan Tsin Goh<sup>b</sup>, Farid Dailami<sup>c</sup> & Jason Matthews<sup>a</sup>

<sup>a</sup> Department of Engineering, Design and Mathematics, University of the West of England, Bristol, United Kingdom.

<sup>b</sup> Prima Dental, Stephenson Drive, Waterwells Business Park, Gloucester, United Kingdom.

<sup>c</sup> Bristol Robotics Laboratory, Cold harbour Lane, Bristol, United Kingdom.

---

### Abstract

The growth of Digital Dentistry has opened new potentials in the dental restoration sector where personalised restorations could be made in a much shorter time than before. Zirconia has been widely used due to its excellent wear properties and biocompatibility. Zirconia is machined primarily in its pre-sintered state, using carbide tools. Even in its pre-sintered state, zirconia is abrasive and caused tool wear. Tool wear is affected by tool substrate used, cutting conditions used, machining method employed, etc. Tool substrates are such as tungsten carbide, steel, etc. Cutting conditions refer to speed, feed, depth of cut, etc. Machining methods refer to milling wet or dry. Understanding tool wear helps in better tool design. Tools that lasted longer would mean the end users i.e. dental technicians would have less unproductive downtime changing tools. Also, worn tool would produce broken restorations which is undesirable. With this in mind, the aim of this paper was to study tool wear by identifying the wear mechanism that occurred when carbide tools machined pre-sintered zirconia. Test was constructed using recommendations from ISO 8688:1989. Cutting conditions used were adapted from those used in desktop dental milling machines. Pre-defined stopping criterion was set, and flank wear of tool was measured every 15 minutes using an optical microscope. When tools reached the stopping criterion, Scanning Electron Microscope (SEM) and Quadrant Backscatter Diffraction (QBSD) were used to analyse worn tool in detail. Findings showed transgranular and intergranular fractures were the wear mechanisms on carbide tools when machining pre-sintered zirconia.

© 2019 The Authors, Published by Elsevier B.V.

Peer review under the responsibility of the scientific committee of the Flexible Automation and Intelligent Manufacturing 2019

*Keywords:* Digital dentistry; Tool Wear; Carbide; Pre-Sintered Zirconia

---

## **1. Introduction**

For decades dental prosthesis has been a common method of restoration, but like many other medical sectors the method, material and technology used to create these restorations has evolved throughout the application of these procedures. The most recent of these evolutions is the shift in material to using zirconia for structural parts of these restorations, such as crowns and copings, due to its high strength, excellent wear properties and biocompatibility. To create these the generally implemented method is Computer Numerically Controlled (CNC) milling of zirconia in a pre-sintered state as it allows for access to this material and other along with the repeatable accuracy precision and high quality control[1]. This happens in the dental laboratories or in milling centres and has become known as dental CAD CAM. Pre-sintered zirconia is machined instead of its sintered counterpart as the latter is high in hardness and poor in thermal conductivity giving it low machinability. Pre-sintered zirconia has a hardness around 66 Vickers hardness. Once the same block is fully sintered the hardness value increases to be above 1600 Vickers hardness. This increased hardness comes from the consolidation of grains. The pre-sintered zirconia also could sustain greater amounts of mechanical damage and absorb more energy [2]. This allows it to resist cracking induced damage during machining.

Dental restorations, such as copings and crowns, have the main purpose of repairing damaged teeth to a state where they can again be used for mastication. The ability for restorations to resist wear and impact comes from the material. The need for an aesthetic matching of the surrounding teeth leads to other parts of material selection. The dental material should be able to blend in with the natural colour of teeth or be semi-translucent. This has caused the shift to zirconia with the development of yttria-stabilized zirconia. The speed of generating restorations as well as the accuracy required on final restorations has led to the shift away from the classic hand tooling towards Computer-Aided-Design (CAD) and Computer-Aided-Manufacturing (CAM) in dentistry. The machining process in dental labs typically uses a small desktop 5-axis Computer Numerical Control (CNC) machines. These machines are usually set up for machining disc of pre-sintered zirconia (cf. Figure 10). Geometry and dimensions of the restoration are taken directly from the patient mouth using impression moulding or laser scanning this give a highly accurate model to work with that the CAM package can build straight from.

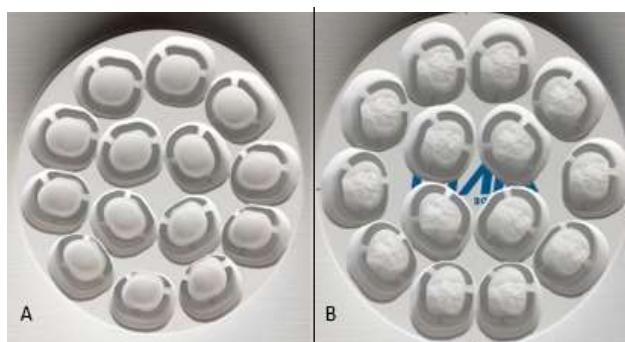


*Figure 10: Machined zirconia dental crowns A) underside or fitting edge B) top side or visible surface*

The process also uses extraction and air blasts to control the waste material for dry milling and coolant or water for wet milling. The pre-sintered zirconia discs that are used in the manufacture of restorations are formed by cold isostatically pressing powdered, or what is referred to as green state zirconia. From the dentists perspective, the actual process of machining is not a main priority in their working function, beyond the points that the process must be simple to operate and accurate in the final output. Tools wearing, changing the surface geometry of the crowns or even damaging the material are certainly unwanted and would be unwanted effects for both the dentist and the tooling manufacturer. To build an understanding of the tool wear that occurs during the prosthesis production, the remainder of the paper presents a modified ISO 8688:1989 test method for investigating tool wear in machining pre-sintered zirconia using carbide tools.

## **2. Tool life**

Tool life is the measure of how long a tool can be used until it can no longer achieve its specified purpose. Much works has shown the direct effect that tool wear has on the surface finish of the machined surface and the stresses induced during the machining process [3, 4]. Both of these affect the end product of dental restorations especially at the high tolerance areas such as the marginal fitting edge, which is where failures occurs the most [5]. It is therefore important to understand the propagation of wear and the affect it has on both the tool and work surface. Tool wear has many specific classifications that have been set in stone by ISO 8688:1989 [6] these are: Flank wear, Face Wear, Chipping, Cracking and catastrophic failure. Flank Wear is the gradual loss of tool material from the tools flank or edge during cutting which leads to the progressive development of flank wear land. This flank wear land is a newly formed surface created from the worn away edge. Face wear is a gradual loss of material from the cutting tools leading face, or rake face, during cutting. This can result in one of two differing forms known as Crater wear and Stair Formed Wear, which form craters or a sloping land respectively on the face. Wear occurs due to friction and heat generated during cutting and of course the properties of material being machined. Zirconia, which is to be studied in the paper is abrasive in nature [7].

## **3. Test Method**

In order to analyse wear, three carbide grades with different properties as summarised in Table 1 were used to make tools. The aim was to identify which carbide grades wear out the least when machining pre-sintered zirconia and what was the wear mechanism. Test was conducted on a 3-axis router. The cutting conditions used are summarised in Table 2. These conditions were adapted from those used in desktop milling machines in dental labs. Ø2mm ball nose end mills made from three different carbide grades were tested. These tools were uncoated. Each tool milled a circular pocket until it worn out. The stopping criterion used was when the flank wear of a tool reached 3.5% of the tool diameter. For a Ø2mm tool, this was 70 microns. Flank wear on the tool was checked at 15 minutes interval until the stopping criterion was reached. However, when tools broke halfway through the test or it caused margin of the milled pocket to crack, the tool would be considered as worn and no measurement would be taken on this tool for comparison purpose. Figure 2 shows pre-sintered zirconia discs in the CNC router that had a bed large to accommodate multiple discs at once. Vacuum extraction and air blasts were to control dusts that were formed from machining.

*Table 1: The material properties of carbide grades*

Carbide grade	CARBIDE A	CARBIDE B	CARBIDE C
<b>Transverse Rupture Toughness (MPa)</b>	3700	4000	4200
<b>Fracture Toughness (MPa)</b>	10	10.4	9
<b>General Grain Size (µm)</b>	0.8	0.5-0.8	0.5
<b>Hardness (Hv 30)</b>	1590	1600	1920

Table 2: Cutting Conditions

Process	X,Y Feed (mm/min)	Z Feed (mm/min)	Spindle Speed (rpm)	Step over (mm)
Roughing	2100	1200	25,000	0.8



Figure 11: Pre-sintered zirconia disc inside the CNC router

Figure 3 show the flank wear of tools which the left image showing flank wear after 15 minutes and the right showing flank wear after 310 minutes. The width of wear was measured using an Optical Microscope coupled with Stream, a measurement software from Olympus.

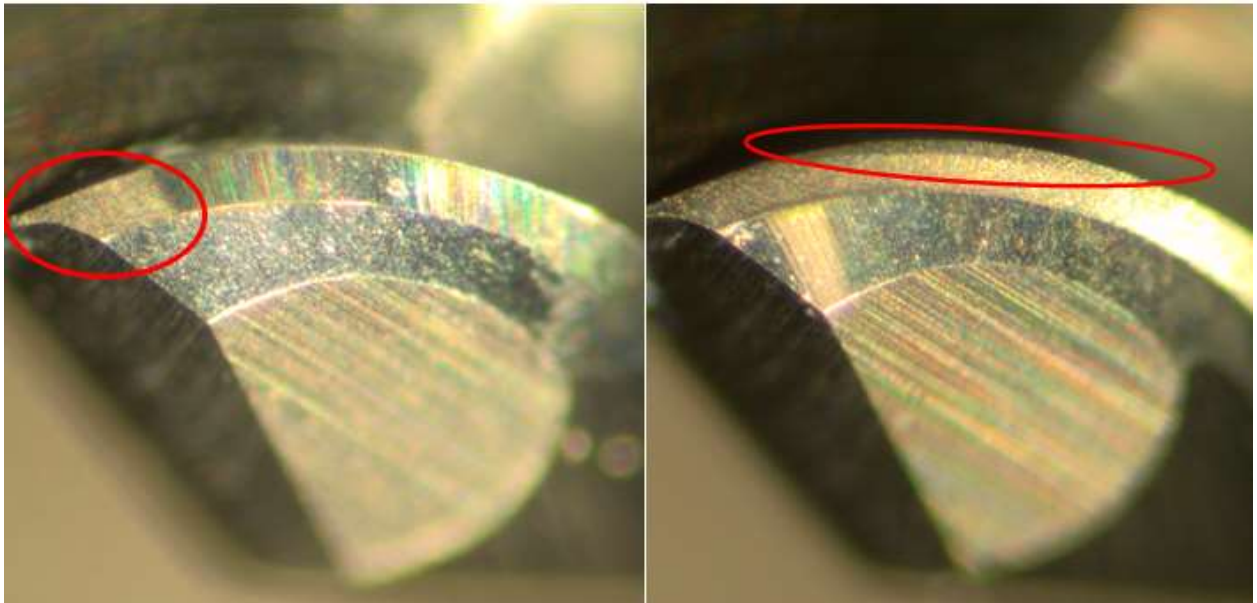


*Figure 12: Tool wear progression on a ball nose end mill after 15 minute (left) and 310 minutes (right) at X8 magnification*

#### **4. Results and Analysis**

The flank wear measured at the 15 minutes interval was plotted as shown in Figure 4, with the red line indicated as Tool End Life was the stopping criterion of 70 microns used in the test. The final tool life in minutes is summarised in Table 3.



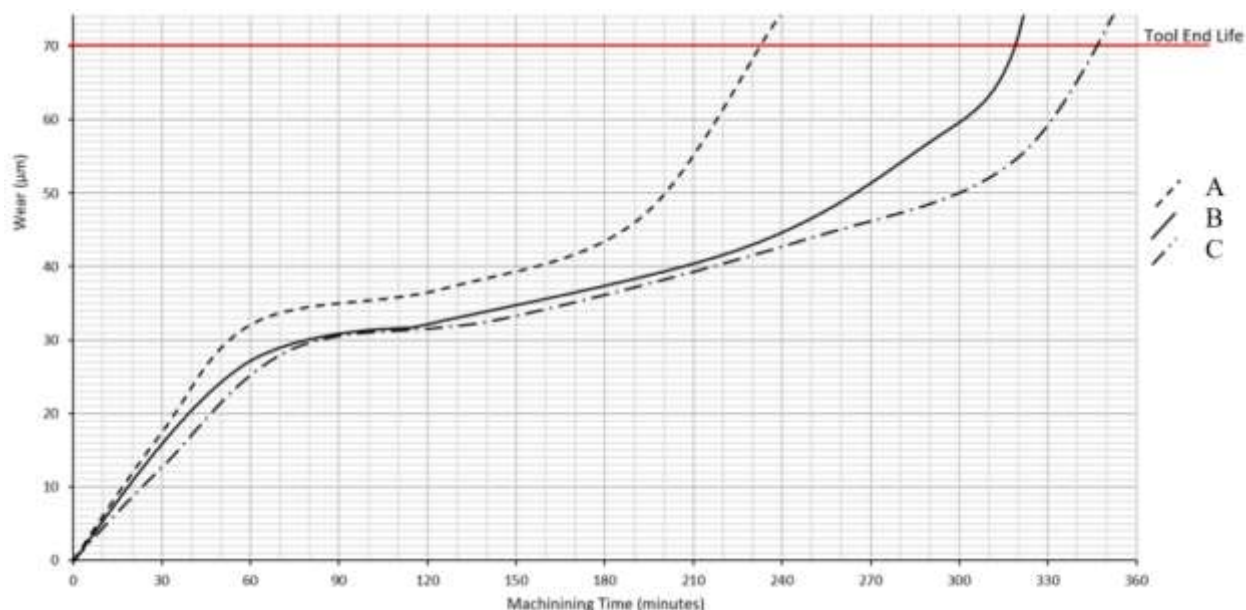


Figure 13: Tool wear curve

Table 3: Average tool life for Carbide grades and material properties of Carbide grades

Carbide grade	CARBIDE A	CARBIDE B	CARBIDE C
Average Tool Life (minutes)	240	315	350

After testing was completed, the tools were prepped for observation under SEM and more specifically Electron Backscatter Diffraction (EBSD). The purpose of this was to observe the affect the three body abrasive wear has on the microstructure of the cemented carbide to determine which properties might be causing the failure of the tool. This was done by mounting the tested tools in the resin and polishing and etching the worn area the samples so that a decent image can be taken of the grain structure around the worn faces and tool tips. These samples were then observed under the SEM in the clean rooms at the optical research centre (ORC) in Southampton. From these images observations of how the grain has deformed after the tool life has been reached. Figure 5 shows the images taken of the three carbide grades when unworn by the machining process. These images were used as a reference point to make observation and a series of initial observations, such as the gran density and grain size. As can be seen in Figure 5C, carbide C has a very fine grain structure that is fairly tightly packed were as the other two are medium and mixed grain carbide for A and B respectively.

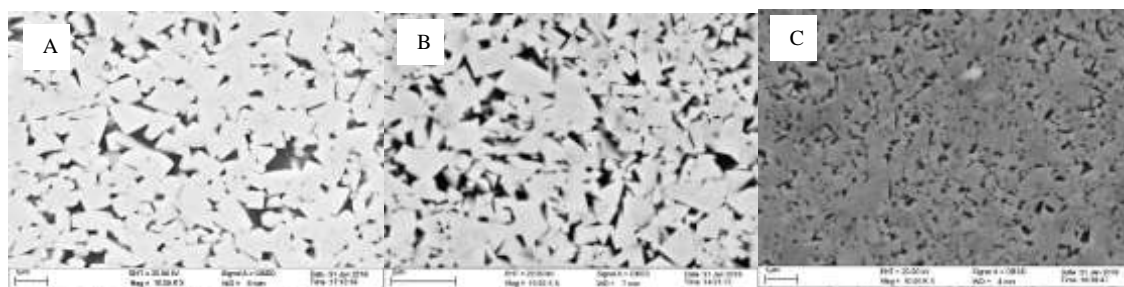
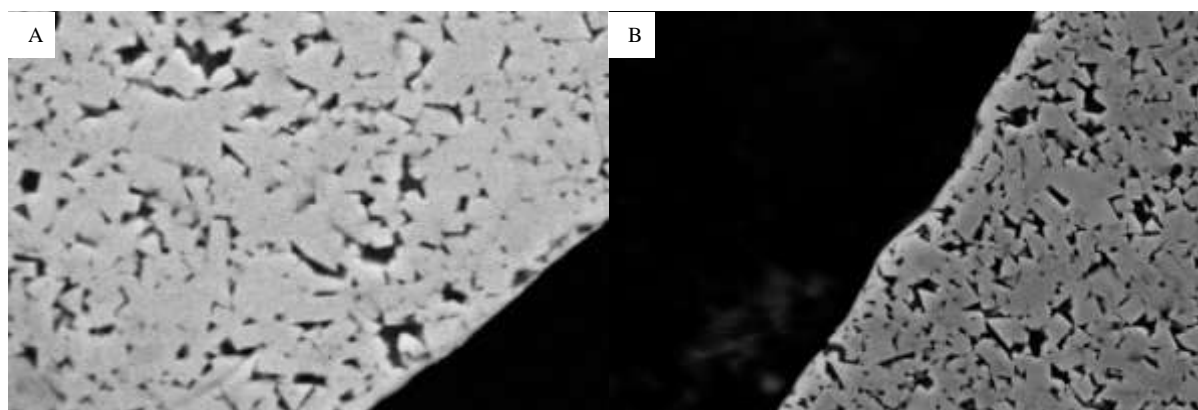


Figure 14: Unworn Carbide grades left to right A, B & C

This disparity in grain size is very common for cemented carbide due to the sintering forming process which allows for it to be such a tailorable tool material. The crystal structure of cemented is also very variable, however this due more the nature of material. This inconsistent structure is what leads to poor grain tessellation especially at larger grain sizes; which in turn causes the brittle nature of the material. The images Figure 6 shows how the first grade of carbide resisted the tool wear. This tool shows the most transgranular fracturing having entire rows of crystals sheared in a straight line ignoring the grain boundaries. This can be seen especial well in Figure 6B toward the top of the image.



*Figure 15: QBSD images of Carbide A worn edges at 10 kX magnification*

This grade of Carbide also had the shortest tool life by more than an hour. This form of fracturing happens in place of intergranular fracturing were the fracture follows roughly the grain boundaries of each crystal. This can be seen to be happening in some cases in both Figure 6 and Figure 7. This tends to happen more in materials where the grains align or the intergranular interactions are much weaker than the grains themselves, or when the material removal mechanism provokes such a reaction such as hard particle abrasion. The images of the tool edges reveal how the edge deteriorates and resist the forces of the machining process such as in carbide B shown in Figure 7. This deformation is fairly typical of abrasive wear causing the grain to round in some places. It also causes grains to break away but where the grain breaks. Some of the grains break through their own boundaries. This again is transgranular fracturing and can be seen in the highlighted in Figure 7A.

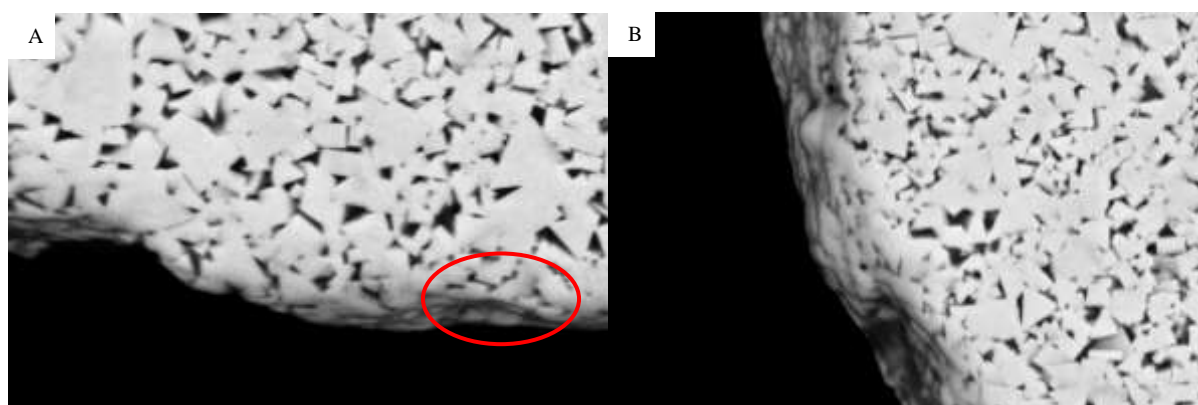


*Figure 16: QBSD images of Carbide B worn tool edges at 10 kX magnification*

This is a product of poor transgranular fracture toughness. However most of the fracturing happens around the some of the grains unlike the wear that occurs in carbide C. As can be seen in Figure 8B the grains are compressed at the tool edge increasing the crystal density drastically. This is part of the forming process of the tool to harden the tool. This tool did also have the longest tool life and highest transgranular fracture toughness. This is more than likely due to the hardened surface grain. In the area where the tool wear is more concentrated the edge looks like Figure 8A. this show much more intergranular fracturing along the edge than previously. The tools made from this grade Carbide failed due to localised chipping quite rapidly toward the end of its tool life were as the other tools gradually developed a flank land slowly.

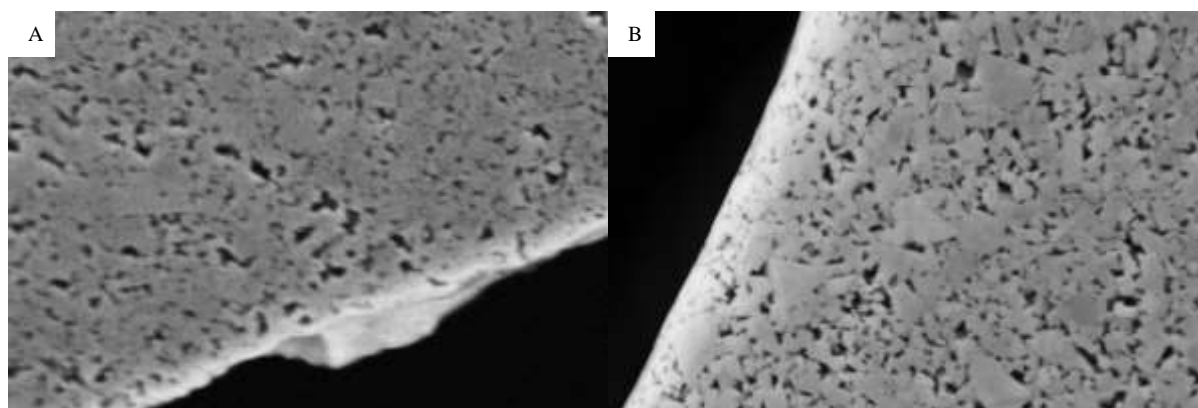


*Figure 17: QBSD images of carbide C worn edges 10 kX magnification*

This shows that transgranular fracture toughness key to resisting the three body abrasion that occurs during the machining of pre-sintered zirconia. This is more than likely due to the individual crystals of zirconia still be hard especially in comparison to the hardness of a whole disc of pre-sintered zirconia.

## **5. Discussion**

The three carbide grades show less and less signs of transgranular fracturing from carbide A to carbide B to carbide C (left to right of Table 3). This points toward transgranular fracturing being the leading cause of tool failure. This further highlights that when machining pre-sintered zirconia three body abrasion is the primary wear mechanism as these go hand in hand. Oddly enough zirconia has a very high transgranular fracture toughness allowing it to resist three body abrasion itself [8]. This resistance comes from the fine grain size of the carbide C grade carbide. As Carbide is a brittle failure material with in consistent grain structure is minimalizes the amount of material that is removed with each removal of the tool edge. Carbide C grade tools failed in a slightly different way to the other tools. Most of the tools had a progressive increase in flank wear land growth to point of failure like shown in Figure 12. Carbide C tools did this but much slower, then a small chip formed that rapidly propagated to point of failure as shown in Figure 9. This rapid propagation pointed towards this occurring due to the upper surface of this grade of carbide being harder, therefore once a chink had been made in this layer the abrasion had two things going for it the increase surface area and the softer material.

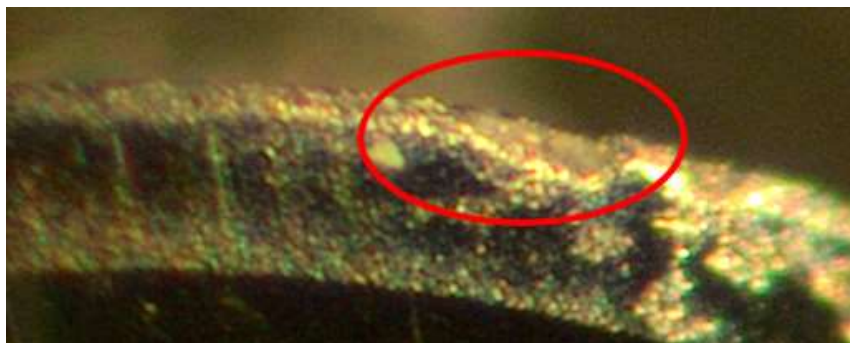


*Figure 18: Chipping on tool edge of carbide C*

This information will be especially useful to tool manufacturers when selecting carbide for creating tools to machine pre-sintered zirconia and materials that cause the same wear mechanism. Also in many dental labs technicians are typically not from an engineering background meaning that tool wear is not something greatly understood in the sector. This has led to many parts failing inspection as the worn tool fails to create an accurate fitting edge.

During machining, zirconia dusts could get entrapped between the tool and the zirconia surface to create a three-body abrasion effect. Such effect had caused two types of material fracture on carbide, namely transgranular and intergranular fractures. Carbide A and B with submicron grain exhibited higher transgranular fracture as compared to the ultrafine grain, Carbide C. While Carbide C exhibited lower transgranular fracture, it also experienced intergranular fracture. Carbide C which had finer grains had a higher hardness value. Hence, it was able to withstand abrasion caused by machining longer than any other carbide grades.

## **6. Conclusion and future work**

With the increased application of zirconia in digital dentistry, there is a need to have an in-depth understanding of the mechanisms of wear that are likely to happen as crowns etc. are manufactured. This is important from two perspectives, the manufacturer of the cutting tools needs to provide a product that does not fail in operation. The other player in this process is the dentist, they need to have confidence that the tools will remain intact and that the final crown is to the geometry they expect. Through SEM analysis and pattern of tool wear it was observed that the wear is three body abrasion as theorised by other works. Potentially problematic as only tooling with diamond coatings is likely to have the abrasive properties to withstand hard particle three body abrasion. However, further analysis of fracture including mean free path between grains need to be studied to make the analysis complete.

### *6.1 Future works*

Now the groundwork of tool wear is understood, other parts of tooling need to be investigated so that the process can be more automated, or tools can be put in place so that technician know when to change tools before parts start failing inspection. Further research should start with the reducing the sudden chipping that was shown to occur in carbide C.

## **Acknowledgements**

The work reported in this paper arose from a research project sponsored by the Prima Dental group and UWE, the authors gratefully thanks both parties for their financial support. The authors also thank UPCERA for the manufacture and supply of the pre-sintered zirconia discs used in the testing.

## **References**

1. Buhner-Samra, A., Morais, E., Mazur, R., Vieira, S. and Rached, R. (2016). CAD/CAM in dentistry – a critical review. *Revista Odonto Ciência*, 31(3), p.140.
2. Alao, A. and Yin, L. (2014) Prediction of the resistance to machining-induced cracking in zirconia by Nano indentation. *Recent Advances in Structural Integrity Analysis - Proceedings of the International Congress (APCF/SIF-2014)*. pp. 580-584.
3. Tamizharasan, T., Selvaraj, T. and Noorul Haq, A. (2005) Analysis of tool wear and surface finish in hard turning. *The International Journal of Advanced Manufacturing Technology*. 28 (7-8), pp. 671-679.
4. Diniz, A. and Filho, J. (1999) Influence of the relative positions of tool and workpiece on tool life, tool wear and surface finish in the face milling process. *Wear*. 232 (1), pp. 67-75.
5. Nasrin, S., Katsube, N., Seghi, R. and Rokhlin, S. (2016) 3D statistical failure analysis of monolithic dental ceramic crowns. *Journal of Biomechanics*. 49 (10), pp. 2038-2046
6. ISO 8688-2-1989" Tool life testing in end milling"
7. Suh, M., Chae, Y. and Kim, S. (2008) Friction and wear behaviour of structural ceramics sliding against zirconia. *Wear*. 264 (9-10), pp. 800-806. Antonov, M., Hussainova, I., Veinthal, R. and Pirso, J. (2012). Effect of temperature and load on three-body abrasion of cermets and steel. *Tribology International*, 46(1), pp.261-268.